Aalto University
School of Engineering

Lassi Heikari

System modeling and pre-feasibility analysis of local low temperature hybrid energy system

Master's thesis
Aalto University
School of Engineering
Department of Energy Technology

Thesis submitted as a partial fulfillment of the requirements for the degree of Master of Science in Technology

Espoo, 04.07.2019
Supervisor: Professor Markku J. Virtanen
Advisor: D.Sc. (Tech.) Janne P. Hirvonen

Aalto University
School of Engineering

Aalto University, P.O. BOX 11000, 00076
AALTO
www.aalto.fi

Abstract of master's thesis

Author Lassi Heikari

Title of thesis System modeling and pre-feasibility analysis of local low temperature hybrid energy system

Master programme Advanced Energy Solutions **Code** ENG3068

Major Sustainable Energy in Buildings and Built Environment

Thesis supervisor Professor Markku J. Virtanen

Thesis advisor D.Sc. (Tech.) Janne P. Hirvonen

Date 04.07.2019 **Number of pages** 94+13 **Language** English

Abstract

Due to the climate change, CO_2 emissions has to be lowered also in building sector as buildings cover a large share of total final energy consumption. Sun is a significant and emission free energy source and thus it is appropriate solution to replace CO_2-intensive fossil fuels in heating energy production. In Nordic countries such as Finland the seasonal mismatch between solar energy availability and heating energy demand is drastic and thus seasonal thermal energy storage is needed to utilize solar energy to heat the buildings in winter time.

The main objective of this study was to find a feasible and cost-optimal low temperature local heating solution based on solar energy for a residential district. The aim of the local hybrid energy system was to cover a part of total heating demand, and the rest of the load was covered with district heat. Solar energy utilization was based on electricity generation with photovoltaic panels and running heat pumps using that electricity. Thermal energy was stored to the borehole thermal energy storage and discharged in winter to heat the residential buildings. Research method was combined simulation and optimization. First the local hybrid energy system was modeled, and then simulated and optimized to maximize the system performance and minimize costs using genetic algorithm.

Rooftop area for photovoltaic panels was noticed to be most limiting issue to achieve high renewable energy fraction in residential area consisting of apartment buildings. In optimal solutions, 37 % - 54 % of total heating energy demand of the buildings can be covered with on-site produced energy with LCOE 110 – 184 €/MWh. Increasing utilization rate of the heat pumps using grid electricity in addition to solar electricity, 41 % - 88 % share of on-site energy of total heating demand can be achieved with LCOE 108 – 201 €/MWh. District heat demand can be decreased by 200 – 600 kWh (25 % - 75 %) during peak demand by using on-site energy. CO_2 emissions can be lowered 100 – 215 tons annually with studied system in comparison to situation where 100 % of heating demand is covered with district heat.

Cost of on-site produced energy is higher than district heat prices, but if the aim is to lower CO_2 emissions and decentralize heating energy production, this local hybrid energy system is potential solution to develop further. Increasing share of on-site energy by running heat pumps with electricity imported from the grid might be feasible but it depends on electricity costs, CO_2 emissions of grid electricity and operation principle of the system.

Keywords Borehole thermal energy storage, Heat pump, Pre-feasibility analysis, Seasonal thermal energy storage, Solar district heating, System modeling

Aalto-yliopisto
Insinööritieteiden korkeakoulu

Aalto-yliopisto, PL 11000, 00076 AALTO
www.aalto.fi

Diplomityön tiivistelmä

Tekijä Lassi Heikari

Työn nimi Alueellisen matalalämpötilaisen hybridienergiajärjestelmän mallinnus ja kannattavuustarkastelu

Maisteriohjelma Advanced Energy Solutions **Koodi** ENG3068

Pääaine Sustainable Energy in Buildings and Built Environment

Työn valvoja Professori Markku J. Virtanen

Työn ohjaaja TkT Janne P. Hirvonen

Päivämäärä 04.07.2019 **Sivumäärä** 94+13 **Kieli** Englanti

Tiivistelmä

Rakennusten hiilidioksidipäästöjä on vähennettävä ilmastonmuutoksen hillitsemiseksi, sillä rakennusten osuus energian loppukulutuksesta on huomattava. Aurinko on merkittävä ja päästövapaa energianlähde, joten aurinkoenergia on hyvä vaihtoehto korvaamaan fossiilisia polttoaineita lämmöntuotannossa. Pohjoisissa olosuhteissa aurinkoenergian saatavuuden ja rakennusten lämmitystarpeen välillä on erittäin suuri ero, joten lämpöenergian kausivarastointi on tärkeässä asemassa, kun aurinkoenergiaa halutaan hyödyntää rakennusten lämmitykseen talvella.

Tutkimuksen tavoitteena oli löytää kerrostaloalueelle toteuttamiskelpoinen ja kustannusoptimaalinen aurinkoenergiaan perustuva toimiva hybridienergiajärjestelmä. Alueellisen energiajärjestelmän tarkoituksena oli tuottaa osa asuinrakennusten tarvitsemasta lämmitysenergiasta, ja loppuosa katettiin kaukolämmöllä. Aurinkoenergian hyödyntäminen perustui aurinkopaneeleilla tuotettuun sähköenergiaan, jolla käytettiin lämpöpumppuja. Tuotettu lämpöenergia varastoitiin porareikävarastoon, josta sitä purettiin lämmityskaudella asuinrakennusten lämmitykseen. Tutkimus toteutettiin simuloimalla ja optimoimalla.

Aurinkopaneeleiden asennukseen käytettävissä oleva kattopinta-ala huomattiin merkittävimmäksi rajoittavaksi tekijäksi saavuttaa korkea omavaraisuusaste kerrostaloalueen lämmöntuotannossa. Optimaalisilla ratkaisuilla 37 % - 54 % alueen lämmitysenergiantarpeesta voitiin kattaa alueella tuotetulla energialla. Alueella tuotetun energian hinta (LCOE) oli 110 – 184 €/MWh. Huipputehontarpeiden aikana ostetun kaukolämmön tarvetta on mahdollista vähentää 200 – 600 kWh (25 % - 75 %) käyttämällä mahdollisimman paljon alueella tuotettua energiaa. Vuosittaisia hiilidioksidipäästöjä on mahdollista vähentää tutkitulla järjestelmällä 100 – 215 tonnia.

Alueella tuotetun energian hinta on korkeampi verrattuna kaukolämmön hintaan, mutta mikäli tarkoituksena on vähentää hiilidioksidipäästöjä ja hajauttaa lämmitysenergiantuotantoa, tällainen alueellinen hybridienergiajärjestelmä on potentiaalinen ratkaisu jatkokehitykseen. Alueella tuotetun energian määrää on mahdollista nostaa käyttämällä verkkosähköä lämpöpumpuille, sillä lämpöenergian omavaraisuusasteeksi saatiin 41 – 88 % LCOE:n ollessa 108 – 201 €/MWh. Tällaisen ratkaisun kannattavuus ja järkevyys riippuu sähkön hinnasta, hiilidioksidipäästöistä ja järjestelmän toimintaperiaatteesta.

Avainsanat Aurinkokaukolämpö, järjestelmämallinnus, kannattavuustarkastelu, lämmön kausivarastointi, lämpöpumppu, porareikävarasto

Preface

Building energy systems, renewable energy and optimization have been one of the most interesting fields during my studies. For that reason I was really excited when I heard from Professor of Practice Markku J. Virtanen about this master's thesis topic in December 2018. The aim of the thesis was to study a solar energy based hybrid energy system for residential area to lower carbon dioxide emissions and therefore to restrict the climate change. During this thesis process I have learned lots of new about hybrid energy systems and seasonal energy storages, and interested in this topic even more.

This thesis was carried out for Fortum, and I would like to thank all the people who participated into this project there. It has been a pleasure to discuss the possibilities and targets of this thesis with strong experts and receive good advices.

I would like to thank my thesis supervisor, Professor of Practice Markku J. Virtanen, for inspiring, supportive and positive attitude. This thesis would have been much more challenging to accomplish without my professional advisor Janne P. Hirvonen. All support and advices as well as constructive feedback during thesis process have been invaluable. I would also like to thank the entire staff of HVAC team in Sähkömiehentie 4 building for interesting conversations as well as technical support during spring 2019. Special thanks to other master's thesis writers and my fellow students Tiia and Ville for numerous relaxing lunchbreaks and conversations. I would also like to thank my employer RE Group for giving me time to fully concentrate on this thesis.

These years in Aalto have been great and unforgettable and I am grateful all the friends I have met during my studies. In addition to that I would like to thank all my friends for the good time that we have spent together. Last but not least I would like to thank my family for always supporting me and giving good advices.

Espoo 04.07.2019

Lassi Heikari

Lassi Heikari

Table of Contents

Abbreviations

AW-HP	Air-to-water heat pump
BHE	Borehole heat exchanger
BTES	Borehole thermal energy storage
CHP	Combined heat and power
CO_2	Carbon dioxide
COP	Coefficient of performance
DH	District heat
DHW	Domestic hot water
GA	Genetic algorithm
LCC	Life cycle cost
LCOE	Levelized cost of energy
LTN	Low temperature network
MOBO	Multi-objective building optimizer
MOO	Multi-objective optimization
NSGA-II	Non-dominated sorting genetic algorithm II
PV	Photovoltaic
REF	Renewable energy fraction
RES	Renewable energy source
SC	Space cooling
SH	Space heating
TRY	Test reference year
VH	Ventilation heating
WW-HP	Water-to-water heat pump

1 Introduction

1.1 Background

Global warming and the climate change is one of the biggest challenges in human history. To restrain the global warming, greenhouse gas emissions, such as carbon dioxide has to be decreased which denotes that fossil energy sources has to be replaced with renewable energy. Buildings and building construction sector consume globally 36 % of total final energy and produce almost 40 % of direct and indirect carbon dioxide (CO_2) emissions (International Energy Agency 2019). In European Union the building sector energy consumption share is nearly 40 % of total final energy consumption. Roughly 55 % share of energy used in buildings consists of thermal energy demand which includes space heating, domestic hot water heating and space cooling. (Rohde et al. 2018). In Finland, in the year 2018 buildings covered 25 % of final energy consumption (Statistics Finland 2019a) and the share of fossil fuels of total primary energy was 35 % (Statistics Finland 2019b). Improving energy efficiency of buildings and using renewable energy sources (RES) in heat and electricity production, there is a significant potential to reduce greenhouse gas emissions.

Energy sources and their shares of district heat production in Finland in year 2018 are presented in Figure 1. As can be noticed, the coal is still having the largest share of fuels in district heating supply. CO_2-neutral energy sources do not cover even 50 % of DH supply, and the share of renewable energy sources is totally 36 %. (Finnish Energy 2019). From the figure it can be also seen that almost all energy sources are based on combustion. Only non-combustion based energy sources are heat recovery and possibly "Others", which means that non-combustion based energy sources cover only 10 - 13 % of district heat supply. Thus it can be stated that there is a significant necessity to increase the share of CO_2-neutral energy sources to decrease CO_2 emissions of Finnish district heat production.

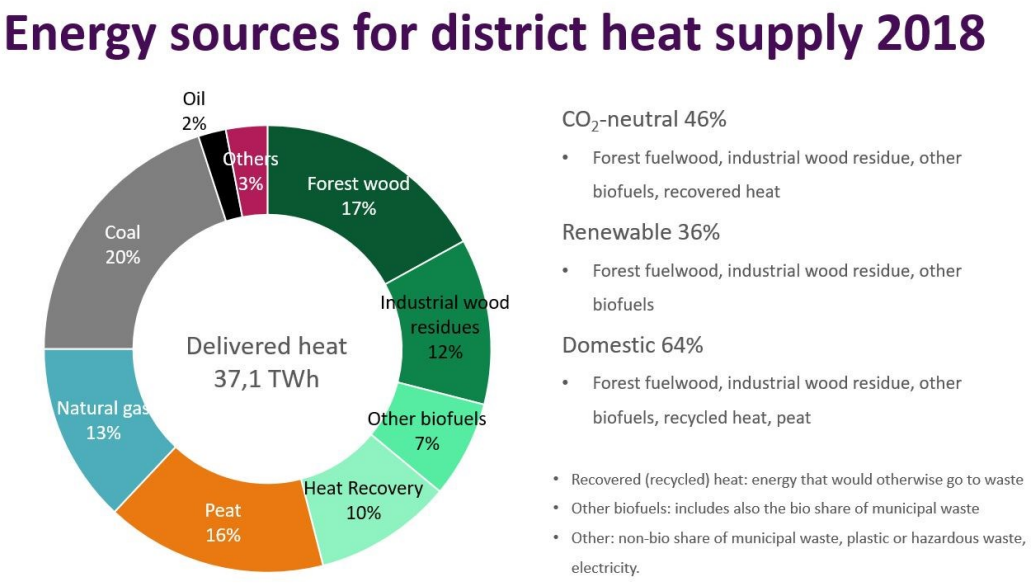

One carbon-free renewable energy source is solar energy. Technology to utilize solar energy for heating and electricity purposes has been developed significantly during past decades and cost level has been lowered as the technologies and solutions have become more common and advanced. For those reasons, the solar energy is an interesting option for heating energy production and has lots of potential also from economical point-of-view. The challenge utilizing solar energy for heating in high latitude area is that there is a remarkable seasonal mismatch between the solar radiation and heating energy demand. Solar radiation is at highest level in summer time when the heating energy need is much lower than in winter time, when the situation is upside down. In Figure 2 is shown the seasonal mismatch between solar radiation and heat demand in high latitude areas.

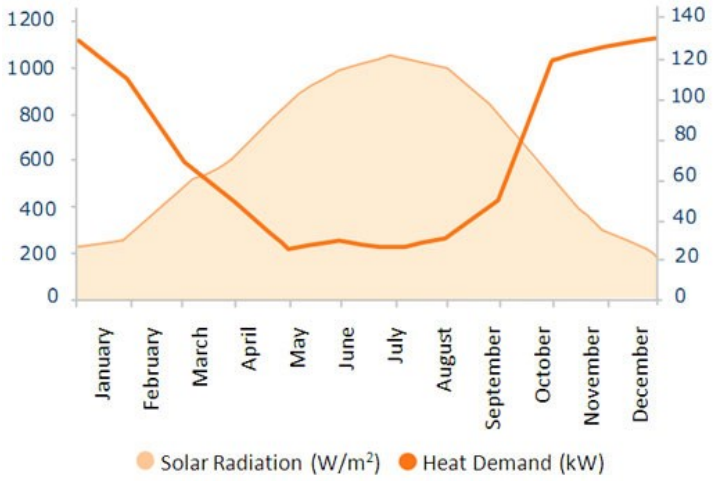

Figure 2. Seasonal mismatch of solar radiation and heat demand (E-hub 2018).

To make supply and demand meet each other, the solar energy has to be collected in summer time and stored somehow so it can be used for heating purposes in winter time. It is possible by utilizing different kind of seasonal thermal energy storages. Designing solar energy based heating system at neighborhood level instead of each building having their own, it is possible to achieve better energy efficiency and cost-optimality. Seasonal thermal energy storages are not possible to utilize in smaller scale solutions as the smaller storage sizes are not functional and losses are relatively high, but with larger community level solutions they become more potential and feasible.

1.2 Objective of the thesis

In this study the main objective is to find a feasible and optimal low temperature local heating solution based on solar energy for a residential district located in Espoo, Southern Finland. In addition to local energy, all buildings are also connected to traditional, larger scale district heating and electricity networks. Another objective is to find out the cost level of that kind of hybrid energy system by calculating the levelized cost of energy (LCOE) for each solution. The aim is to find out the cost-optimal size of components for the local hybrid energy system using multi-objective optimization (MOO). Some optimal solutions are studied in more detail to find out differences between them.

1.3 Novelty of research

The aim of this thesis is to produce new information related to local hybrid energy system based on solar energy in apartment block neighborhood in high latitude area. In earlier studies on this research area it has been considered single-family house solar communities but there are no studies relating to apartment buildings with that kind of system. The target of this study is to find out the size and cost level of the local hybrid energy system so that it can be evaluated if it is feasible to improve that kind of hybrid energy solutions further.

1.4 Structure of the thesis

The thesis is divided into this introduction, literature review, methodology description, results, discussion and conclusions. Chapter 2 contains literature review on solar energy, thermal energy storage technologies, heat pumps, district heating and previous studies of seasonal heat energy storing and solar heating systems. Chapter 3 explain the methodology and limitations of the study. In chapter 4 is presented the results and analysis. In chapter 5 the main findings of study are discussed. Chapter 6 summarizes the main conclusions of the study and suggests avenues for future research. In appendices is presented annual energy flows of analyzed cases.

2 Review of literature

2.1 Solar energy

Solar energy is a significant energy source. Based on some estimates, in annual level the solar energy potential that can be utilized is approximately 1 575 – 79 837 EJ. Annual total primary energy supply of the world was 573 EJ in year 2014, so by utilizing solar energy, it would be possible to cover all primary energy demand in the world. (Alva et al. 2018). In the solar fusion reaction occurring in the sun, energy is released at a total power of about $3.8 \cdot 10^{23}$ kW, of which roughly $1.7 \cdot 10^{14}$ kW is emitted to the Earth. This amount of energy is about 20 000 times the energy used by industry and heating on the planet. (Erat 2008). In high latitude areas, such as Finland, building heating energy has a notable share of total energy consumption. Annual solar radiation and solar energy potential in Southern Finland are similar than in Northern Germany. In Northern Germany, annual solar radiation to optimally oriented and tilted surface is annually between 1100 – 1300 kWh/m² and in Southern Finland, where Helsinki area is also located, 1000 – 1200 kWh/m². (European Commission 2012b). Thus it can be stated that there is a remarkable potential to utilize solar energy also in Finland.

In Figure 3 is presented annual solar radiation in Finland. The numerical values above the color bar are annual amount of total solar radiation in kWh that is radiated to optimally tilted surface with area of 1 m². The numerical values below the color bar are annual PV generation potential of 1 kW_p PV system where panels are optimally tilted. From the figure it can be seen that in Helsinki area annual PV generation potential is 825 – 900 kWh with 1 kW_p optimally tilted PV system. The performance ratio is 0.75 i.e. the solar panel achieves 75 % of its theoretical efficiency. (Motiva 2018).

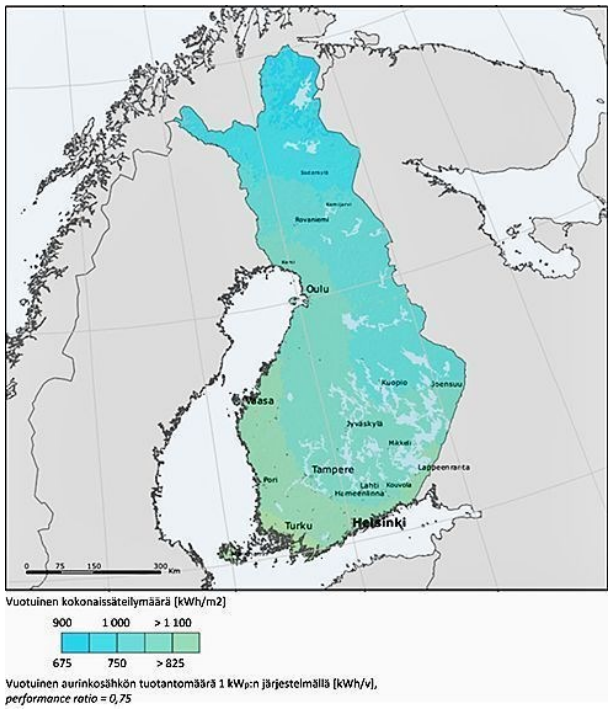

Figure 3. Annual solar radiation in Finland to surface with optimal angle (Motiva 2018).

Solar energy utilization can be divided into passive and active utilization. Passive utilization of solar energy refers to the use of energy without additional equipment. An example of passive utilization is a situation where the sun shines and heats the building. At least a small amount of solar energy is temporarily stored in each building, but for efficient use, appropriate solutions for building, environment, and structural design are needed. Active utilization of solar energy denotes utilization of solar energy by using technical equipment i.e. solar thermal collectors (STC) or photovoltaic (PV) panels. Active utilization is the conversion of solar radiation into electrical energy by solar panels and thermal energy through solar collectors. In the same building, solar energy can be simultaneously used both passively and actively by various methods to achieve maximum gain from solar energy. (Erat 2008).

The solar radiation consists of direct radiation, diffuse radiation and ground reflected radiation. In Figure 4 is presented different types of solar radiation that affect the total solar radiation on a tilted surface. Direct radiation is the radiation that is coming straight from the sun. Diffuse radiation is reflecting from clouds and atmosphere. In Finland, share of diffuse radiation is typically roughly half of total annual solar radiation, but the daily and monthly shares are depending on weather conditions. On a cloudy weather, the share of diffuse radiation can be even 80 % of total radiation. Due to relatively high share of diffuse radiation, concentrating and tracking systems are not as economically profitable as they can be in countries where direct solar radiation has a larger share of total solar radiation. (Motiva 2018). Ground reflected radiation is solar radiation that is reflected from the ground, buildings and so on. For example snow, water, ground and glossy roof material can increase the total solar radiation momentarily even 20 % but in an annual level the share of ground reflected radiation is only few percent of total solar radiation. In total, ground reflected radiation has significantly smaller impact to total solar radiation than diffuse radiation. (Motiva 2018, PVeducation 2019).

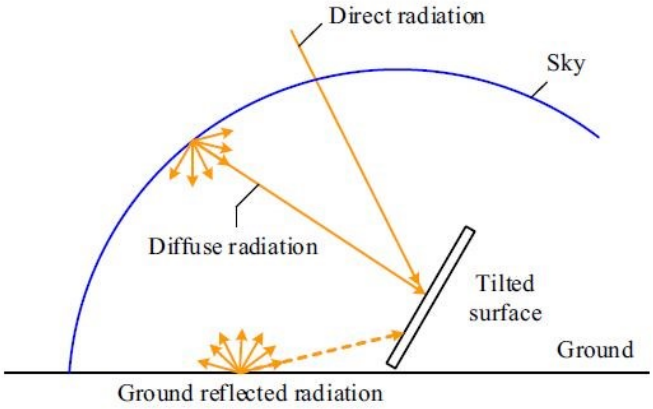

Power production of PV panel does not depend only on solar radiation of sun. The main factors affecting to the power production of PV panels are the tilt angle and the orientation angle of PV panel. The tilt angle is the angle that PV panel is inclined from the horizontal plane. The orientation angle is the angle in vertical axis i.e. the compass point which the PV panel is oriented. In northern latitudes the proper orientation angle for PV panels achieve the highest electricity generation is south. However, always it is not possible to face the panels directly to the south as there might be structural or architectural challenges. When PV panels are installed on flat roof, it is important to avoid panels shading each other. Thus minimum distance between PV panel rows depends on the tilt angle of PV panels. The optimal tilt angle of PV panels to reach maximum possible PV power generation is depending on, in which time of the year the PV electricity is needed the most. When absorbing plane is perpendicular to sunlight, the maximum power output of PV panel can be achieved. Due to the fact that the angle of solar radiation to the PV panel is varying all the time, it is not possible to reach maximum possible power production continuously if the tilt angle is fixed. In Figure 5 is shown solar radiation to the tilted surface and affecting angles. Angle α is the angle at which the sun is radiating on horizontal plane and β is the tilt angle of PV panel from horizontal plane. (PVeducation 2019).

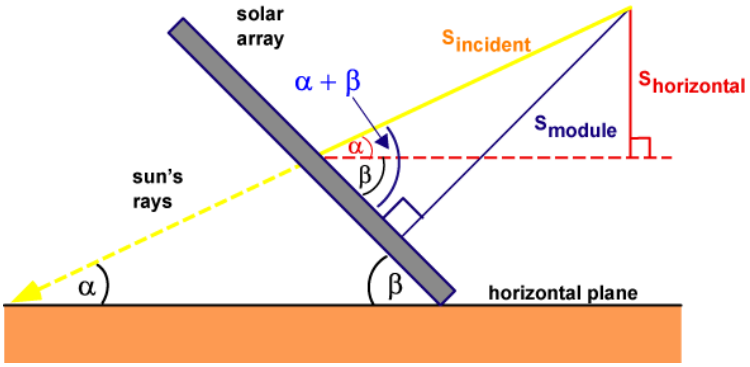

Because solar radiation on a tilted surface depends on angles, the amount of solar radiation on a tilted surface is lower than total solar radiation. Solar radiation on tilted surface can be defined as

$$S_{tilted\ surface} = S_{incident} \cdot \sin(\alpha + \beta) \quad (1)$$

where

$S_{tilted\ surface}$	Solar radiation to the tilted surface (kWh/m²)
$S_{incident}$	Solar radiation to the surface located in incident angle (kWh/m²)
α	Elevation angle (°)
β	Tilt angle of PV module measured from horizontal plane (°).

Elevation angle depends on two separate angles that are latitude angle i.e. the location from the equator and declination angle which depends on the day of the year. Elevation angle is shown in equation 2 and declination angle in equation 3, respectively.

$$\alpha = 90 - \Phi + \delta \tag{2}$$

where

α	Elevation angle (°)
Φ	Latitude angle (°)
δ	Declination angle (°).

$$\delta = 23.45° \, sin\left[\frac{360}{365}(284 + d)\right] \tag{3}$$

where

δ	Declination angle (°)
d	Day of the year (-).

Depending on several factors, the optimal installation angle of PV array can be defined. If the aim is to maximize PV electricity production in summer time, the optimal angle is different than in situation where PV electricity is needed more in spring or autumn time. More steep tilt angles maximize PV electricity production in winter time when the elevation angle of solar radiation is low. In summer time, when the elevation angle is higher, maximum electricity production is achieved with more gently sloping tilt angles. (PVeducation 2019).

Solar insolation to the surface with two different tilt angles are presented in two figures below. In Figure 6 the tilt angle is 30° and in Figure 7 it is 70°, respectively. In both figures the latitude angle is 60° which is the latitude of Espoo. The blue curve is incident power curve and it describes the solar radiation that can be received if the PV panel is perfectly oriented to the sun. The red curve is the solar radiation that is received to the horizontal plane i.e. the PV panel having tilt angle 0°. These two curves depend only on latitude and time of the year and thus they are similar in both figures. The only deviating curve is the green curve which describes the solar radiation to plane having tilt angle 30° in Figure 6 and 70° in Figure 7. When the tilt angle is lower, the received power is almost as high as possible i.e. very close to the incident power in middle of summer. In other seasons, the received power is slightly lower than incident power, but actually the difference is small. When the tilt angle is steeper, in summer time the received power is significantly lower than incident power. On the other hand during other seasons, the received power is very close to incident power. Therefore it is necessary to define, when the PV electricity is mostly needed that the optimal angle of PV system can be selected. (PVeducation 2019).

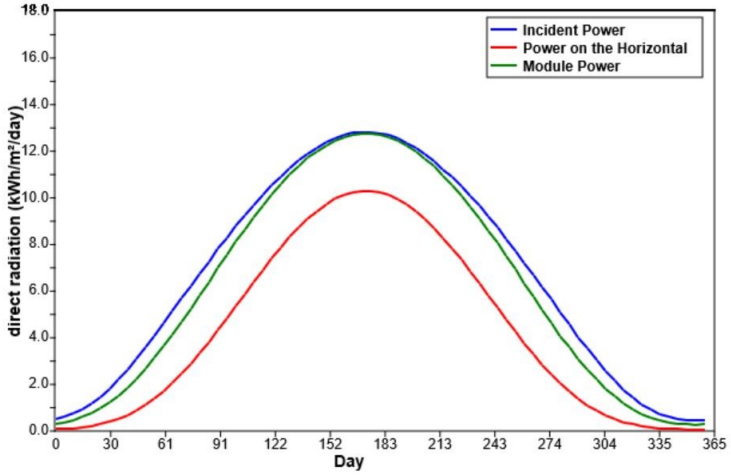

Figure 6. Solar insolation to the surface when tilt angle is 30° and latitude is 60° (PVeducation 2019).

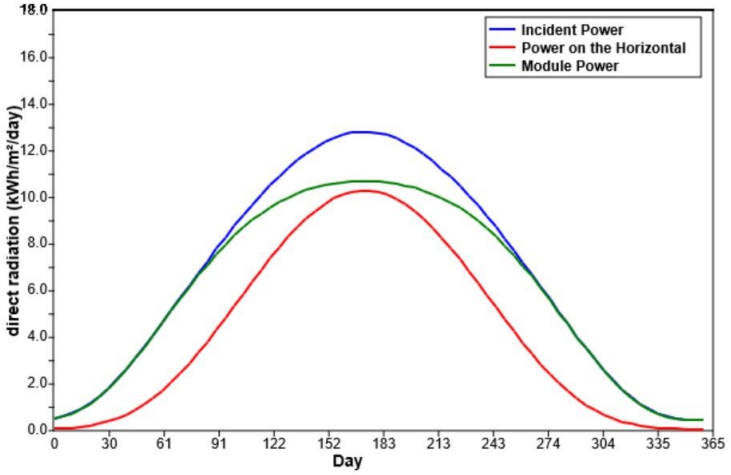

Figure 7. Solar insolation to the surface when tilt angle is 70° and latitude is 60° (PVeducation 2019).

2.2 Thermal energy storage technologies

To store thermal energy produced in one season and utilize stored energy in another season, thermal energy storage is essential component of energy system. In this chapter, some common thermal energy storages are introduced to understand the diverse of thermal energy storages and to realize the differences between them. Storage technologies based on latent or chemical heat have been researched and developed, but still all existing storage technologies at the moment are based on sensible heat i.e. the temperature change in storage material. (Rad, Fung 2016). Thermal energy storage technologies are e.g. aquifer thermal energy storage (ATES), pit thermal energy storage (PTES), tank thermal energy storage (TTES) and borehole thermal energy storage (BTES). In Figure 8 is presented sections of the mentioned seasonal storage technologies.

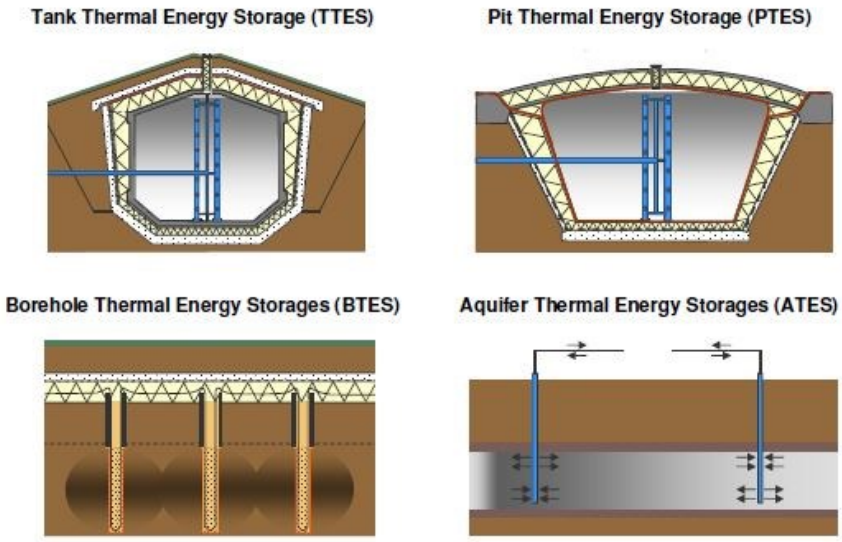

Figure 8. Seasonal storage technologies (Schmidt, Miedaner 2012).

2.2.1 Aquifer thermal energy storage

Aquifer thermal energy storage (ATES) is based on storing heat energy in confined aquifers that are having very low water flow or no water flow at all. If there is too high water flow i.e. the aquifer is unconfined, the aquifer cannot be used as a thermal energy storage due to heat losses that are caused by high water flows. However, even if the water flow is low in aquifer, the heat losses can be remarkable at least when the temperature level of the storage is high. Thus surface-to-volume ratio of the storage should be as low as possible. The basic principle of ATES is that there is at least two drilled wells, and the heat energy is injected to and extracted from the aquifer via the wells. The notable thing is that ATES systems are open-loop solutions i.e. the groundwater itself is the heat transfer fluid. When ATES is charged, the groundwater is pumped from one well and heated in heat exchanger. After that the water is pumped into another well and from there it goes back to the aquifer. It is important that injection and extraction wells are located at some distance from each other to achieve better heat transfer to the aquifer. To achieve the best system performance, it is necessary to examine the physical and chemical properties of the aquifer. (Rad, Fung 2016, Underground Energy 2018a).

Practical example of ATES system can be found in Sweden's largest airport, Arlanda, which is located in Stockholm region. The airport is geologically situated on a large boulder ridge and under its surface there is a large aquifer with approximately volume of 600 000 m³. The first idea to utilize the aquifer for seasonal storage in Arlanda was given in 2005, and after feasibility studies, hydro-geological investigations and permit applications the construction work began in autumn 2008. Operation of ATES started in summer 2009. ATES system was designed to cover both heating and cooling demands approximately 8 MW and having maximum ground water flow 720 m³/h. There are 5 cold wells and 6 warm wells and they are located so that the cold wells are drilled in the northern part of the aquifer and warm wells in the southern part, respectively. In winter time the heat discharged from the ATES is utilized to pre-heat supply air that is ventilating airport terminals and to heat ground and thus melting ice near the gates. Temperature of ATES is between 3 – 5 °C in winter time. In summer time, the ATES is utilized to deliver cooling energy to the terminals. Temperature

of the warm water returning from the terminals to the ATES is approximately 15 °C, but if the ground heating pipes that were melting ice in winter are utilized as a solar thermal collectors, temperature of water injected to the ATES can be 25 °C in sunny days. Up to 19 GWh imported heating and cooling energy is saved annually which equals to average annual energy consumption of 2000 Swedish detached houses. (SPECIAL Project 2015).

2.2.2 Pit thermal energy storage

Pit thermal energy storage, also known as PTES, is a large pit that is excavated into the ground and filled with water which is the storage media. Finally a floating cover is installed on the top of the storage. PTES is suitable seasonal storage type in areas where the ground is easy to excavate. Ground in the PTES has to be covered with tight liner to avoid water leakages to the ground and thus increasing heat losses and decreasing the storage capacity. For example liners made of polymer or elastomer can be used as well as metals such as stainless steel and aluminium. The good thing with metal liners is that they can resist higher temperatures than polymer and elastomer. In addition to that, they are vapor-proof. On the other hand the material costs and installation costs of metal liners are significantly higher. When using metal liners, corrosion issues have to be considered detailed as they are installed to the ground and there is water on the other side of the liner.

PTES can be constructed in different shapes but the most common and simplest shape is an upside down placed truncated pyramid i.e. the edges are widening when moving from base to upwards. To minimize the heat losses from the top of the PTES, a floating cover is needed. Usually the floating cover is the most expensive component of PTES as the area is large and materials are expensive. There are different solutions to make the floating cover. Flexible insulations mats with water-proof floating liner can be used. A benefit of that alternative is flexibility, as the mat can be installed at the edges and it can move up and down when the water level varies due to thermal expansion. Another method is to use floating stiff elements. Bulk insulation, where the insulation material is installed between water-proof floating liner and top liner, can be also used. Charging and discharging can be implemented by direct water exchange or indirectly using pipes that are installed into the storage. (Jensen 2014, Schmidt, Miedaner 2012).

One example where PTES is implemented is Dronninglund, Denmark. There is a 35 000 m² solar thermal collector plant, 60 000 m³ PTES and 3 MW heat pumps. The heat energy from solar thermal collectors is charged to the PTES. Heat pumps are using PTES as a heat source. The aim of the system is to supply approximately 50 % of Dronninglund's heating demand which is annually 20 GWh. The rest of the heating demand is covered using heat energy produced in natural gas fired combined heat and power plant. The PTES was excavated in an old gravel pit. Due to soil in the area is consisting of gravel and sand and ground water level is approximately 3 m below, implementation of the storage was easy. The construction work of the system started in spring 2013 and the operation of the system began in spring 2014. In first operation year, maximum storage temperature was 86 °C and minimum 12 °C and the storage efficiency was 78 %. (Sunstore 3 Project 2015).

A variant of water-filled pit thermal energy storage is gravel-water thermal energy storage, also term GWTES can be used. The idea is the same as in PTES, but instead of water, a combination of water and gravel, sand or soil mixture is used as a storage media. GWTES is also insulated on the edges and top. Due to lower heat capacity of the ground, volume of

GWTES has to be approximately 50 % larger to achieve the same storing capacity than water-filled PTES. The benefit of GWTES is that covering is simpler and thus covering costs are lower than in water-filled PTES. In GWTES, charging and discharging is done indirectly using plastic pipes that are installed into the storage. (Rad, Fung 2016, Schmidt, Miedaner 2012).

2.2.3 Tank thermal energy storage

Tank thermal energy storage (TTES) is thermal energy storage that is built of concrete, steel or glass fiber reinforced plastic i.e. sandwich elements. Additional liner is usually required on inner surface of the edges to ensure the vapor and water tightness of the storage. Main difference of TTES in comparison to PTES is that in PTES the outer edges are natural material like soil or hard rock instead of concrete or other construction material. Usually the outer edges of the TTES are insulated to minimize the heat losses to the environment. TTES can be either fully or partly excavated into the ground or it can be located above the ground. Piping can be installed in such a way that water can be injected and extracted from different heights to increase the performance of the storage. (Schmidt, Miedaner 2012). A practical example of tank thermal energy storage is in waste incineration plant operated by Vantaan Energia. There is a 10 000 m³ storage tank for storing heated water before it is supplied to the district heating network.

2.2.4 Borehole thermal energy storage

Borehole thermal energy storage (BTES) is thermal energy storage where the ground itself is working as a storage material. BTES is a borehole field consisting on a large amount of vertical boreholes with typical length from 30 m to 100 m that are drilled to the ground. The distance between boreholes is typically between 3 m and 4 m. Heat transfer fluid consisting of water or water-glycol mixture to avoid freezing, is circulated in single or double U-pips that are installed in boreholes. Depending on the temperature difference between fluid and fill material of borehole, the heat is injected to the storage or extracted from the storage. BTES is a flexible thermal energy storage solution as it can be implemented in various ground materials. The ground, that can be unconsolidated material or rock or something between them, is the actually the storage media, and boreholes are the heat exchangers through which the heat is injected and extracted. Benefit of BTES is that it is quite easy to enlarge afterwards by simply drilling more boreholes and connecting the pipes together with existing heat transfer pipes. (Reuss 2015, Rad, Fung 2016). In Figure 9 is shown a vertical section of a single borehole.

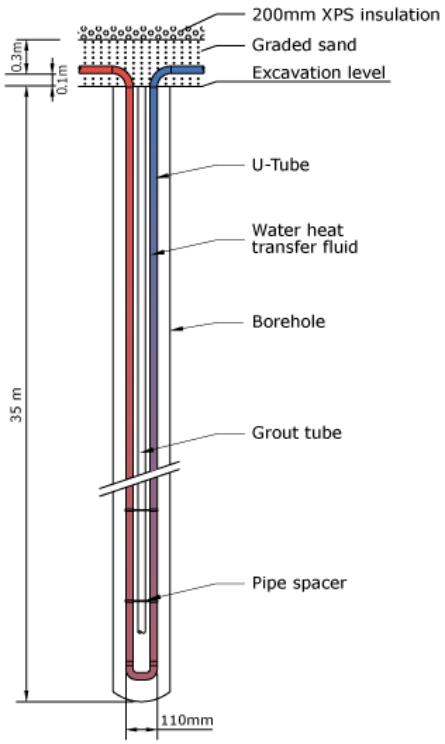

Figure 9. Vertical section of single borehole (Drake Landing Solar Community 2019a).

Geological conditions affect significantly to the implementation and effectiveness or borehole heat exchangers and therefore the whole BTES. To achieve a high heat transfer into the ground and from the ground respectively, a high thermal conductivity of storage material is preferred. On the other hand, when considering on avoiding of heat losses, the thermal conductivity of ground surrounding the storage should be lowest as possible. In Scandinavia area and Finland, where there are large areas of hard rock, the boreholes are filled typically with water. With this kind of combination the performance of BTES is very high, as the thermal conductivity of hard rock is high in comparison to other ground materials and as the water has a great volumetric heat capacity. In such areas where ground material is unconsolidated, like large areas of Europe, boreholes are filled with grout material. The weakness of this solution is that heat exchange potential is lower.

When considering on BTES efficiency, the size of storage is important. Heat losses of the storage are proportional to the outer surface area of BTES and the larger the area is, the larger the heat losses are. On the other hand, the storage capacity is proportional to the storage volume. Based on these, the term surface-to-volume ratio can be introduced. It describes how large the outer surface area is in comparison to storage volume. The lower the ratio is, the smaller the heat losses are and thus better efficiency of storage is achieved. (Reuss 2015). If the BTES has a cylindrical shape, doubling the BTES volume increases the area of the outer surface only by half. Thus smaller solutions are not very effective, and larger storages are more preferable. Ground water flows affect also to the efficiency of BTES. Heat losses can be significantly higher if there exists ground water flows in BTES area as the heat is transferred to the ground water and the flow transfers the heat away from the storage. (Rad, Fung 2016). All in all it can be stated that geological and hydrological research of area where BTES is planned to be implemented is very important to find out if it is feasible or not.

In charging mode, the heat collecting fluid is pumped into the center of BTES and then towards the edges to maximize the heat in center of BTES to avoid heat losses to the outside of the BTES. In discharge mode, the fluid flows opposite direction i.e. the cold heat collector fluid is pumped into edges of the BTES and from there towards the center to increase the temperature gradient of the fluid and therefore maximize the discharge power. In Figure 10 is presented the principle of boreholes connected in series. Cooler fluid is always on the edges and warmer on the center of BTES. Figure 11 describes the main principle of BTES in charge mode. Warm or hot heat transfer fluid is flowing from energy center to BTES. The fluid is injected in center of BTES and after cooling down in BTES and transferring heat energy to the storage the fluid is extracted from the edges of the BTES and then it returns back to the energy center. In Figure 12 is shown a BTES in discharge mode. Cold heat transfer fluid is flowing to BTES from the energy center and the cold fluid is injected to the BTES in the edges of BTES. While flowing in BTES, the fluid is heating up i.e. transferring heat from the ground. Then the fluid is extracted from the center of BTES and after that it returns back to the energy center. (Drake Landing Solar Community 2019a, Underground Energy 2018b).

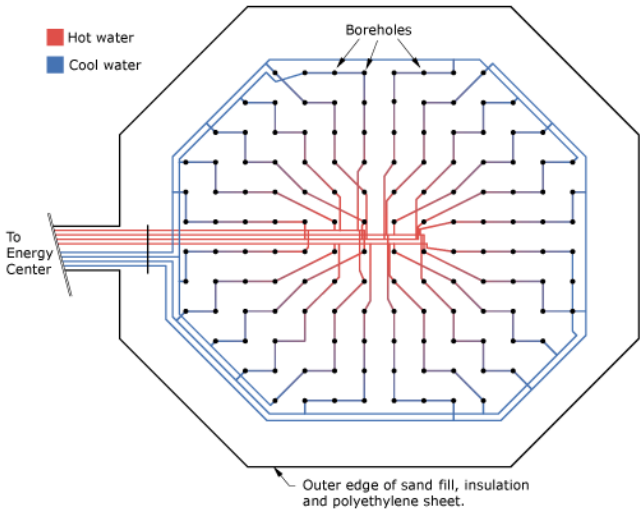

Figure 10 Principle of boreholes connected in series (Drake Landing Solar Community 2019a).

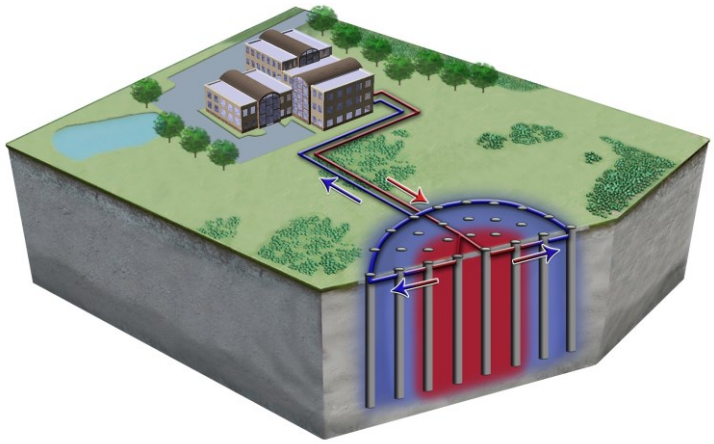

Figure 11. BTES in charge mode (Underground Energy 2018b).

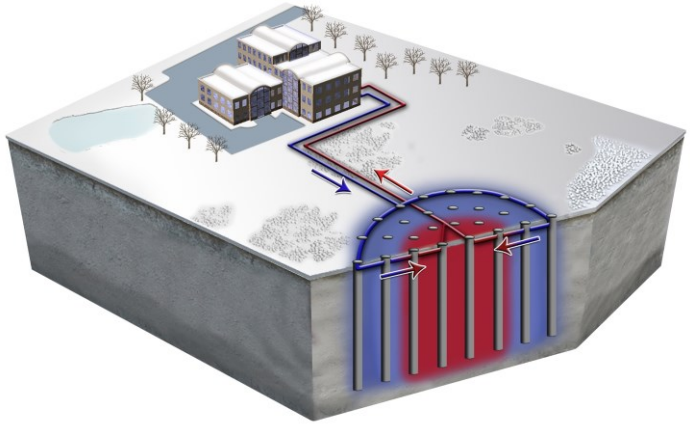

Figure 12. BTES in discharge mode (Underground Energy 2018b).

Borehole thermal energy storages can be categorized in low temperature BTES and high temperature BTES, depending on operating temperatures. Low temperature BTES is operating between 0-40 °C and high temperature BTES systems between 40-80 °C. (Rad, Fung 2016). Thus the temperature of the heat source from where the heat is injected to the storage defines if the BTES is low-temperature or high-temperature solution. If the heat energy is utilized for heating straightly from the BTES, the storage temperature has to be higher than in solution where heat pump is used between the storage and final destination. Due to temperature decrease in the storage because of heat losses, the charging temperature of the storage should be higher, respectively. In addition to that, the higher the storage temperature is, the higher are the heat losses from the storage as the temperature difference between the storage and surrounding ground is also higher. Thus the low-temperature BTES might be more feasible alternative to building heating purposes where heating network temperatures are relatively low. If a heat pump is utilized in discharging of BTES, the lower temperature of BTES is not restricting issue as the heat pump can increase the temperature level suitable for heating purposes. (Reuss 2015).

Heat transfer from the boreholes to the surrounding ground is based on change of internal energy of the ground material. Change of internal energy can be solved from following equation

$$\Delta U = mc_p(T_f - T_i) \tag{4}$$

where

ΔU	Change of internal energy (kJ)
m	Mass of storage material (kg)
c_p	Specific heat capacity of storage material (kJ/kgK)
T_f	Final temperature of storage material (K)
T_i	Initial temperature of storage material (K).

As the heat losses to the ground surrounding the BTES reduce the efficiency of BTES, the losses of BTES has to be considered. In principle, if the energy balance of BTES is in equilibrium, the heat loss of BTES is the reminder of energy that is charged to the BTES and energy that is discharged from the BTES. Therefore the efficiency of BTES can be defined

as a ratio of energy discharged from the BTES and energy charged to the BTES. (Flynn, Sirén 2015). Based on that the BTES efficiency can be calculated using following equation

$$\eta_{BTES} = \frac{E_{DC}}{E_C} \cdot 100 \quad (5)$$

where

η_{BTES} Efficiency of BTES (%)
E_{DC} Thermal energy discharged from the BTES (MWh)
E_C Thermal energy charged to the BTES (MWh).

One implemented BTES system is Drake Landing Solar Community (DLSC) which is located in Okotoks, Alberta province, Canada. DLSC is the first neighborhood in North America which is utilizing borehole thermal energy storage as a seasonal thermal energy storage. It is also the first large community in the world that is utilizing large seasonal storage. The neighborhood consist of 52 detached houses and over 90 % of annual heating demand of the neighborhood can be covered with solar energy. The heating energy production of the community is based on solar thermal collectors that are installed rooftops of garages. Heat energy is either charged to the BTES or distributed to the buildings depending on heating demand. When the heating demand in the neighborhood is higher than solar thermal collectors can produce heating energy, the BTES is discharged and heat is supplied to the buildings. The BTES consists of 144 boreholes which are connected so that there are 24 parallel loops where 6 boreholes are connected to the series. Depth of the boreholes is 37 m and distance between each borehole is 2.25 m. Shape of the BTES is octagonal and width is 35 m. DLSC proved that using seasonal storage there is a potential for solar energy utilization also in high latitude areas. (Drake Landing Solar Community 2019b, Xu, J. et al. 2014).

2.3 Heat pump

A heat pump is a system designed to transfer heat energy from one side to another. The operation of the heat pump is based on the process of circulating the refrigerant, in which the compressor compresses the refrigerant from low pressure and temperature to a higher pressure, thereby increasing its temperature. Source side is the side from where the heat energy is transferred to the refrigerant circuit, and load side is the side from where the heat energy is transferred from the refrigerant circuit, respectively. Heat pump technology can be utilized for both heating and cooling purposes depending on location of source and load sides. (Juvonen, Lapinlampi 2013).

Utilizing different kind of heat pump solutions, heat can be transferred from air to air, air to liquid or liquid to liquid. The most common application of an air-to-air heat pump is a solution for heating and cooling in households. Outdoor air is lead to evaporator unit in which the heat energy of outdoor air is transferred into the refrigerant circuit. Pressure and temperature of the refrigerant is increased in compressor and after that the refrigerant is lead to condenser unit from where the heat energy is transferred to the indoor air. (SULPU - Finnish heat pump association 2019). In air-to-water heat pump solution, the heat energy of ambient air is transferred to the refrigerant cycle in same way as in the air-to-air heat pump solution. After increasing the pressure and temperature of the refrigerant in compressor, the refrigerant is circulated to the condenser. In air-to-water heat pump the condenser is actually a heat exchanger where also in secondary side there is a liquid instead of air as in air-to-air heat

pump. In a liquid to liquid heat pump, heat energy is first transferred to the source side heat transfer fluid from the heat source which can be e.g. ground water filled borehole. From the source side heat transfer fluid the heat is transferred into the refrigerant cycle using a heat exchanger, which is an evaporator. After the pressure and temperature of the refrigerant is increased in compressor, the heat energy is transferred from the refrigerant to the load side heat transfer fluid using another heat exchanger which is condenser. (SULPU - Finnish heat pump association 2019).

In Figure 13 is shown the process of circulation process of the refrigerant in the heat pump. The process of refrigerant circulation begins from evaporator (1), which can also be a heat exchanger, depending on whether the heat transfer is from the air to the refrigerant or from the liquid to the refrigerant. In the evaporator, the heat in the state of the liquid or gas is transferred to the vaporized refrigerant that is in lower temperature. The compressor (2) absorbs the refrigerant in the form of steam and increases its pressure to achieve a sufficiently high temperature. Thereafter, the refrigerant at high pressure and temperature flows to the condenser (3). The condenser may be a condenser radiator or a heat exchanger, depending on whether the heat is transferred from the refrigerant to the air or to the liquid. In the condenser, the heat bound to the refrigerant is transferred to the air or liquid at a lower temperature than the refrigerant. From the condenser, the condensed refrigerant which is now in the liquid state, flows to the expansion valve (4), where its pressure decreases. After the expansion valve, the refrigerant in the mixture of liquid and vapor goes back to the evaporator, and the circulation process starts from the beginning. (Juvonen, Lapinlampi 2013).

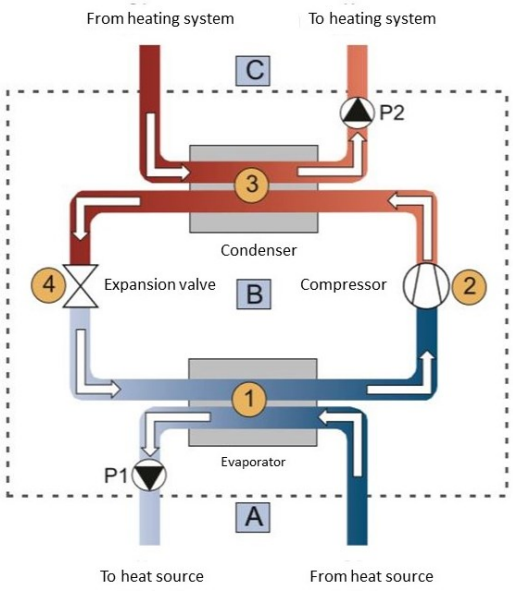

Figure 13. Heat pump process (Juvonen, Lapinlampi 2013).

An important indicator of heat pumps and other refrigeration systems efficiency and performance is coefficient of performance, also known as COP. The COP is defined as a ratio of amount of useful heating energy that can be extracted from condenser and consumed electricity by compressor. When the heat pump is utilized for cooling purposes, the COP is a ratio of amount of cooling energy that can be utilized from evaporator and the amount of electricity that is used by compressor and accessory equipment like pumps and control valves. In other words, the COP denotes how the amount of heating or cooling energy can be produced by using one unit electricity. For example, if the COP of heat pump is 3, it

means that 1 kW of electricity is required to produce 3 kW of thermal power. The COP can be calculated using equation

$$COP = \frac{Q_{heat}}{Q_{electric}} \quad (6)$$

where

COP	Coefficient of performance (-)
Q_{heat}	Thermal power extracted from condenser (kW)
$Q_{electric}$	Electrical power needed by compressor and accessory equipment (kW).

The theoretical maximum value of the COP of the heat pump is the Carnot thermal coefficient also known as Carnot efficiency. The Carnot's thermal coefficient depends only on the condensation temperature and the evaporation temperature of the refrigerant. Temperatures are given as absolute temperatures. Carnot efficiency is presented in equation 7.

$$COP_{Carnot} = \frac{T_{condensing}}{T_{condensing} - T_{evaporation}} \quad (7)$$

where

COP_{Carnot}	Carnot efficiency (-)
$T_{condensing}$	Condensing temperature (K)
$T_{evaporation}$	Evaporation temperature (K).

Due to the fact that the heat pump process is not lossless and it does not operate exactly like Carnot heat pump, the actual COP of heat pump is always lower than Carnot efficiency.

2.4 District heating

District heating (DH) is a common solution to supply heating energy to the buildings in Finland. Almost 50 % of people in Finland live in buildings that are heated using district heat. District heating is a system, that is usually operating in communal or at least in district level. Heating energy is produced in centralized power plants and is distributed to the customers using distribution network. In earlier times the heat was distributed to the customers using steam, but current systems are operated using hot water for heat transfer. In general, the operation principle of DH system is, that first DH water is heated up to the required temperature in heat exchanger in power plant. Then the DH water is pumped to the DH network which supplies the hot water to the buildings. In the building there is a heat exchanger where the heat is transferred from DH water to the building networks for space heating, ventilation heating and domestic hot water heating. The DH water that is cooled down in the heat exchanger is then returning back to the power plant to be heated up again. In Finland a large share of district heating is produced in CHP plants. CHP process is based on combined production of heat and electricity, and the aim is to maximize the energy efficiency. Usually in CHP production, the electricity generation is prioritized and optimized based on electricity markets, and sometimes there might be a situation that need for CHP production is low due low imported electricity prices but there is still a need for district heat. In those situations, additional heat production plants might be used instead of CHP plants. (Mäkelä, Tuunanen 2015).

The cost of DH is based on amount of supplied energy in MWh. In addition to that there is also power cost which depends on supplied peak power. Lowering the peak demand of the building, it is possible to lower DH costs. Because the share of power cost is significantly lower than supplied energy cost, it is not considered in detail in this study. Pricing of district heat depends on the contract between the energy company and customer. Price per unit can be either fixed i.e. it stays the same during the whole year, or it can vary depending on the month. In Figure 14 is presented monthly DH prices of Fortum energy company. In general the price trend is that in summer time when the heat demand is lower, the prices are also lower, and in winter time the prices are higher as the heat demand is higher.

Figure 14. Fortum Aktiivilämpö monthly district heat prices (€/MWh, VAT not included)

District heating will be an important part of heating systems also in the future energy systems. However the present district heating networks operate at quite high temperature level and there has to be implemented transition to lower operating temperatures to integrate with sustainable energy systems, smart and low-energy buildings and other smart energy systems. Fourth generation district heating networks (4DH) operate at low temperatures, between 30 – 70 °C. Integration of fourth generation networks is possible when using low temperature heating systems in buildings which can be either floor heating or low-temperature radiators. (Lund et al. 2014). The challenge of integrating 4DH systems in Finland is the regulations of DHW temperatures by Ministry of the Environment because to avoid legionella in DHW networks, the temperature of DHW has to be at least 55 °C (Ministry of the Environment 2019). Due to that regulation, the supply temperature of 4DH has to be relatively high also in summer time even though the DHW heating might be the only heat demand. Another solution might be that DHW is pre-heated using heat from 4DH and there is another back-up heater for increasing the DHW temperature to required level.

Fortum has recently opened their district heating grid for other operators, which allows consumers to be producers also i.e. term prosumer can be used (Fortum 2019b). In near future the utilizing of excess heat will become more important. Instead of producing more heat in centralized power plants, buying excess heat helps reducing emissions and primary energy use. (Energiateollisuus ry 2019). The excess heat can be originated e.g. in apartment buildings, commercial buildings or industrial processes. The buying of excess heat is based on hourly metering and buying tariffs vary as an operation of long term monthly outdoor temperatures and company's own production costs. The buying price depends also on whether the excess heat is sold to the supply or return pipe of the district heating network i.e. the temperature of the supplied heat. The heat that is sold to the supply pipe has higher monetary value because the district heating network operates better when the excess heat is transferred

to the supply pipe instead of return pipe. This is based on fact that if the temperature of fluid returning to the district heating plant is too high, the efficiency of production will decrease. (Fortum 2019b).

2.5 Earlier studies on hybrid energy systems with BTES

2.5.1 Integrated heating and cooling system with BTES

Rohde et al researched integrated heating and cooling for a building complex, where also long-term thermal storage has been utilized. In the study a neighborhood-level integrated heating and cooling system (IHCS) was modeled and system performance and annual heat balance of thermal energy storages were analyzed. The studied neighborhood was located in Norway, having total floor area of 38 500 m² that the IHCS was serving, and consisted of apartments, hotels, offices, shops, food court and event location. The IHCS is supplying thermal energy to space heating, domestic hot water heating, snow melting, space cooling and product cooling. The main components of the IHCS system were heat pumps, solar thermal collectors, storage tanks and two kind of thermal energy storages: ice thermal energy storage (ITES) and borehole thermal energy storage (BTES). There were traditional communal district heat connection as a backup in case of that the local energy system does not work. The simulation was performed using Modelica software. (Rohde et al. 2018).

As a result it was found out that due to cold climate conditions in Norway, the heating demand were significantly higher than cooling demand. That caused the situation that there was not enough waste heat in summer time to charge to the BTES which led to negative annual heat balance of BTES. If BTES is discharged continuously more than energy is charged there, the BTES will cool down. There were to recommended improvements to fix the energy balance of the BTES. By increasing number of solar thermal collectors it is possible to increase the on-site energy production and therefore BTES can be charged more in summer time. Another recommendation was that energy amount discharged from the BTES must be lower. (Rohde et al. 2018).

2.5.2 Solar community with solar thermal collectors and BTES

Hirvonen et al. researched a solar community in high latitude residential area in a study, where the heat production was based mainly on solar thermal collectors (STC). As the seasonal mismatch between solar energy availability and heating demand is drastic in the higher the latitude is from the equator, a borehole thermal energy storage was utilized to store heat energy between seasons. The solar community was located in Finland and consisted of 100 m² detached houses. To find out better understanding of technical and economical affects, the simulation and optimization was done for different size of communities consisting of 50, 100, 200 and 500 detached houses, depending on case. Modeling was performed by using commercial dynamic modeling and simulation software TRNSYS. Optimization of the system was done using MOBO optimization tool which uses genetic algorithm for optimization. (Hirvonen, ur Rehman et al. 2018)

The energy system consisted of solar thermal collectors, photovoltaic panels, two centralized short-term storage tanks for lower and higher temperatures, heat pumps, borehole thermal energy storage and local heating network. STC located on the rooftop of each building were connected in parallel to both tanks to optimize the charge potential. Lower temperature tank was used for heating space heating water and pre-heating domestic hot water, which was boosted to required temperature in the hot tank. When the temperature in the tank was high

enough, the energy was charged to the BTES. In heating season, heat energy from the BTES was discharged to the tank. Flow from BTES was used directly to heat the tank always when it was possible, but if the temperature of fluid coming from BTES was not high enough, the fluid flow from the BTES was used as a source side of heat pumps to reach suitable temperature to heat the tank up. As a backup there were direct electric heaters. Building energy performance was also considered i.e. there were different options for insulation, windows and heat recovery efficiency. The optimization was done based on life cycle costs and amount of imported electricity with aim to minimize both of them. (Hirvonen, ur Rehman et al. 2018).

As a result several things were noticed. Firstly, reducing the heating demand by investing in more efficient windows, insulation and heat recovery was found out very cost-effective instead of increasing energy generation. When considering on BTES, better efficiency was achieved with larger community (and BTES) sizes. In addition to that, in larger communities a higher share of heat energy was possible to supply without using heat pump. Also the number of boreholes connected in series was lower than expected, but it was concluded that the reason might be the solar community size as in larger communities only 1-3 boreholes were connected in series. With larger solar communities a lower LCC per floor area was reached, but system performance was not varying significantly. (Hirvonen, ur Rehman et al. 2018).

2.5.3 Fully electrified solar community with BTES

Hirvonen and Sirén have studied fully electrified solar community in a high latitude residential area. The main difference to study introduced in previous chapter based on STC system was that in this study only PV panels were utilized. The idea was that excess PV electricity was utilized to operate air-to-water heat pumps in summer time to charge BTES instead of selling the surplus PV electricity to the grid. The system modeling and simulation was performed using commercial dynamic simulation software TRNSYS, and the optimization was done using MOBO optimization tool. Solar community was located in Finland and was consisting of 100 m² detached houses. Two different community size was examined so that there were either 100 or 500 houses depending on simulation case. (Hirvonen, Sirén 2018).

The main components of the energy system were PV panels, two centralized short-term storage tanks for lower and higher temperatures, water-to-water heat pumps, air-to-water heat pumps, BTES and local heating network. AW-HP was used to charge the warm tank which was used for heating space heating water and pre-heating domestic hot water. WW-HP was connected between warm and hot tanks in such a way, that WW-HP used warm tank as a source to increase the temperature in hot tank high enough to heat the domestic hot water to a required temperature. PV electricity was prioritized so that first it was used to cover the appliance load in the buildings, and if there was surplus electricity after that, it was utilized to run the heat pumps. BTES was charged from the warm tank when the temperature in the tank was high enough. In heating season, energy was discharged from the BTES to the warm tank. If the heating demand was not totally covered with on-site energy, direct electric heaters were used as a backup. The optimization was done based on LCC and imported electricity with aim to minimize both of them. (Hirvonen, Sirén 2018).

From the results it can be noticed several things. LCC was lower in larger solar community, mainly due to higher BTES efficiency and lower PV unit cost. When results were compared to the STC case referred earlier, the better system performance and lower LCC were

achieved with this fully electrified system. The same observation related to boreholes connected in series was done also in this study as in 100 building case 4-9 boreholes were connected in series, but in 500 building case there were 2-4 boreholes in series. This is related to the fact that when the width of BTES was large enough, it was not so necessary to increase the temperature gradient between center and edges of the storage. The flow per borehole loop was kept constant, but increasing the number of boreholes connected in series reduced the number of loops and thus total flow in the BTES. This affected system performance as well. In most of optimal cases the BTES flow per loop was 1200 kg/h. In optimal results of 100 buildings, the renewable energy fraction varied from 69 % to 98 % and LCC varied roughly from 220 €/m² to 370 €/m², respectively. In 500 building case, REF varied from 84 % to 98 % and LCC varied roughly from 220 €/m² to 340 €/m². (Hirvonen, Sirén 2018).

2.5.4 Reviews of BTES

Xu et al. investigated and reviewed properties of borehole thermal energy storages. Even though it has been proved that BTES has potential for large scale seasonal energy storing, there are several issues that are important to take into account. In comparison to seasonal storage where water is the storage media, 3-5 times higher volume is needed for BTES to store the same amount of heat. This is due to the fact that the energy density of ground is lower than energy density of water. Usually an auxiliary buffer tank is needed to stabilize the heat distribution from the storage to buildings. One disadvantage of BTES is high investment cost. Borehole drilling as well as soil excavation and refilling cost are usually the largest part of total cost of BTES. Due to borehole drilling is expensive, the investment cost of the BTES is high. Another downside is the complexity of underground conditions. Thermal conductivity of the ground as well as heat capacity affect significantly to the heat transfer between heat transfer fluid and the ground. Thus soil and ground has to be investigated carefully to find out the suitability of the ground for BTES. Third disadvantage is that it takes long time to reach the appropriate performance of BTES. It has been noticed that usually 3-4 years of operation is required until BTES have reached the typical performance. This is related to the fact that it takes quite long time that the ground surrounding the BTES warms up because heat transfer in the ground is slower than in water. (Xu, J. et al. 2014).

Lanahan and Tabares-Velasco argue in their article that even though there are many challenges related to BTES, it is feasible storage method in many cases due to its flexibility. BTES is flexible solution that can be implemented in different kind of areas because no special conditions are required unlike e.g. in ATES systems. The most important thing for implementing BTES is that geological conditions are suitable. Disadvantages of BTES are mentioned relatively high heat losses and expensive drilling costs. The heat losses of BTES are usually larger than in insulated water tanks or gravel storage systems. In addition to that, the climate conditions may affect to the efficiency of BTES. (Lanahan, Tabares-Velasco 2017).

The hybrid energy system studied by Hirvonen and Sirén would be interesting to examine also in residential area that consists of apartment blocks as one key finding of the study was that utilizing PV panels to run heat pumps was more feasible than collecting heating energy using solar thermal collectors. However, studies related to solar heating systems based on PV electricity driven heat pumps in residential area consisting of apartment buildings was not found. The main difference implementing that kind of hybrid energy system to neighborhood consisting of apartment blocks instead of detached houses is, that rooftop area for photovoltaic panels is limited. In detached houses, the rooftop area is higher in comparison

to heated floor area i.e. possible PV capacity per heated floor area is higher. On the other hand, when comparing solar energy heating systems based on either solar thermal collectors or PV panels, PV panels might be more feasible for de-centralized installation. This is due to the fact that there are no any thermal losses and piping needed for PV panels.

2.6 Implemented BTES systems

In addition to Drake Landing Solar Community, also other local heating systems where BTES is utilized as a seasonal storage have been implemented in practice, even in Nordic countries. Finnspring soft drink factory in Toholampi, Finland and Anneberg residential area in Danderyd, Sweden are two examples of real life solutions.

2.6.1 Finnspring Toholampi

A Finnish soft drink company Finnspring has started a pilot project in Toholampi, Central Ostrobothnia, where solar energy and waste heat from the factory are stored to the borehole thermal energy storage. The project is a part of larger EVAKOT project where year-round solar energy storing and utilization of stored energy as an additional heat source of buildings are investigated. The waste heat, of which temperature is 60 - 70 °C, is coming from compressors that are blowing plastic bottles to their final shape. In addition to waste heat, there are also solar thermal collectors installed to the rooftop of the factory. Heat energy from both sources is injected to the BTES. The heat energy discharged from the BTES is utilized for heating office spaces of the factory and a swimming hall that is located near the factory, which is actually also a fire water storage of the factory. The BTES is located in a field near the factory buildings. There are total 61 boreholes drilled into the ground with depth of 50 m. Total volume of BTES is 15 000 m³. Heat transfer pipes of the BTES are installed in four nested circles and the control system can route the water flow to the most optimal circle. The aim is that the heat energy can be always injected optimally to the BTES to widen the charging and discharging temperature zone. The system has been planned to start operation in summer 2019 and the stored heat energy will be utilized first time in winter 2019-2020. So there are no practical results related to system performance and function available yet. (Geofoorumi 2018, Keskipohjanmaa 2018, Yle 2018).

2.6.2 Anneberg residential area

Anneberg residential area is located in Sweden, near Stockholm. The area consists of 50 buildings which are two-family houses, row houses and a nursing home. Total floor area of the buildings is roughly 9 000 m². The energy system of the residential area consists of solar thermal collectors, borehole thermal energy storage and low-temperature underfloor heating system. For back-up heating there are electrical heaters. Totally 2 400 m² solar thermal collectors (STC) are installed on the rooftops of the buildings. STC array size per building varies between 80 m² and 240 m². BTES consists of 100 boreholes that are 65 m deep. The boreholes are drilled so that they are forming 10x10 quadratic pattern with 3 m distance between the boreholes. The boreholes are connected in such a way that 5 boreholes are connected in series. Thus there are 20 parallel loops. Total volume of the BTES is 60 000 m³. Preliminary design of the system was started 1998 and the construction work began 2000. At the beginning of 2002 the area was ready and most of the residents moved to the buildings. Though there were problems with solar thermal collectors due to wrong pipe material, the operation of system could be started fully in spring 2002. After some fixing, the operation of system started in autumn 2002. (Dalenbäck et al. 2000, Lundh, Dalenbäck 2008).

After few years operation, performance of the energy system was evaluated by comparing measured data and the expected performance which was based on calculations. Total energy production of the energy system was lower than expected, which indicated that solar thermal collectors do not produce energy as much as it was expected. It was noticed that measured energy outputs of some STC sub-units was corresponding rather good to calculated energy outputs, even though the measured values were slightly lower than calculated. In some other sub-units the difference between measured and calculated data was more significant. Because all the sub-units was not studied, there may be also malfunctions in some of those sub-units which might be the reason for lower energy output of the system. (Lundh, Dalenbäck 2008).

3 Methodology

The aim of the local hybrid energy system of this study was to cover a part of heating demand of residential district. Basic assumption of the whole study was that district heat was available in each building to cover the remaining share of heating demand. Another aim of DH connection in each building was to be as a backup if there would be malfunctions or other problems with local energy production.

Study of the local hybrid energy system was based on combined dynamic simulation and optimization. There are numerous separate things that affect the operation of the local hybrid energy system. By simulating models and changing parameters, it would be a long and difficult process to find out reasonable solutions, as there can be thousands or tens of thousands of different solutions. Thus optimization is necessary method to find out the most feasible solutions. Modeling and simulation were done using commercial dynamic modeling software TRNSYS. In the first phase, the building systems, such as the heating networks in the buildings and hourly energy demand profiles were modeled. Second task was to model the local heat distribution network. Then the BTES and heat pumps were modeled. When all components were in the model, the models were combined and checked that the whole local energy system model was working properly and the output results were reasonable. After that the simulation model was combined with multi-objective optimization tool (MOBO) using Matlab as interface platform. Based on selected optimization decision variables, the optimization was performed.

To clarify the focus of the study, limitations were imposed. Solar thermal collectors are not considered on at all in this study as in previous studies it was found out that solar community with PV electricity-based heat energy production had more potential than solar community equipped with solar thermal collectors. In this study, building quality is not considered at all. The energy demand profiles are based on IDA ICE simulations of apartment buildings that are fulfilling the latest Finnish Building Code regulations. Electrical energy storages are not discussed in this study. In case that there would be excess electricity after heat pump operation, the excess electricity is sold to the grid. Demand response and optimal control system of local hybrid energy system is not considered because the aim of this study is to find out a feasible energy system and demand response is different research area. However, that kind of optimization of system operation is an interesting topic and thus the next phase of developing this kind of local hybrid energy system would be a separate study to find out the most suitable control algorithms to operate the local hybrid energy system in optimal way.

3.1 Introduction of residential district

The residential district which was considered in this study was located in Espoo, Finland. There were planned to build 14 totally new eight storey apartment buildings, with total floor area of 31 100 m² and total annual heating demand of 2 005 MWh. To utilize solar energy to heat the buildings in winter, seasonal thermal energy storage was needed. The ground material in the residential district was bedrock and there was only thin, less than 5 m layer of soil covering the bedrock (City of Espoo 2019). Comparing the storage technologies discussed in chapter 2.2, it was noticed that to implement PTES or TTES to the site, lots of excavation would have been required which was not feasible at all as the ground material was hard rock. Moreover, the number of buildings was that high that TTES would have been very large if located above the ground and that was not feasible due to high land costs. Thus

the most preferable seasonal storage type for this residential area was borehole thermal energy storage as the boreholes can be drilled to the hard rock.

Heat distribution method in buildings was underfloor heating which has relatively low operating temperatures. To keep indoor climate at comfortable level also in summer time, high temperature space cooling network was also assumed to be in the buildings. Cooling distribution method was not defined or modeled exactly but underfloor cooling or cooling panels installed to the ceiling were suitable distribution methods for high temperature cooling. In this study the main focus was on local hybrid energy system for heating. For that reason the cooling system is not discussed in detailed way. Moreover, cooling energy production is different business and has to be considered separately. Therefore the main purpose to model the cooling system was, that the condensate from the heat pumps generating needed cooling energy, was utilized for local energy system as an excess heat. For the same reason, the costs of cooling system was not considered on at all.

3.2 Weather data

Weather data was needed in the simulation to define PV electricity generation and outdoor temperature conditions. Weather data used in this study was Test Reference Year 2012 (TRY2012) which was developed in year 2011 to correspond current climate conditions. In the data, Finland was divided in three different zones I-II (Vantaa), III (Jyväskylä) and (IV) Sodankylä due to the fact that weather conditions vary between those zones because of geographical issues (Ministry of the Environment 2011). Because the residential area of this study was located in Espoo, Southern Finland, I-II Vantaa weather data was utilized. In TRY2012 data, the leap day that takes place every fourth year was not taken into account. Based on this, in simulations performed in this study the leap day was not taken into account at all. The effect of absent leap day is relatively small so it can be assumed that it has not significant influence to the final results.

3.3 Heating energy demand profile

The buildings are new, so they must fulfill current regulations of The National Building Code of Finland (Ministry of the Environment 2019). The hourly heating energy demand profile of the buildings was based on simulations performed in previous study where cost-optimal energy renovation of Finnish apartment buildings were examined and for which the building energy model was created. (Hirvonen, Heljo et al. 2018). The building energy model was created using IDA ICE software. Weather data utilized in the building energy model was Test Reference Year 2012. Main parameters of modeled building are shown in Table 1.

Table 1. Building parameters.

U-values			Other		
External wall	0.17	W/m²K	Indoor temperature	21	°C
Floor	0.16	W/m²K	DHW use	56	l/person/day
Ceiling	0.09	W/m²K	**Energy demands**		
Doors	1.00	W/m²K	Space heating energy	17	kWh/m²a
Windows	1.00	W/m²K	Ventilation heating energy	6	kWh/m²a
Air tightness			Domestic hot water heating energy	41	kWh/m²a
n50	0.7	1/h	Cooling energy	6	kWh/m²a
q50	1.54	m³/(h, m²)	Electricity	35	kWh/m²a
Ventilation					
HR temperature efficiency	0.65				
Air exchange rate	0.5	1/h			
SFP	2.0	kW/(m³/s)			

The hourly energy demand profile was modified to this project based on total floor area of the buildings. Although there are variations in energy consumption between each building in real life, for simplicity the energy demand is assumed to be exactly the same in every building in this study. Monthly heating energy demand of the residential district of this study is shown in Figure 15. From the figure it can be noticed that heating of domestic hot water has a largest share of total heating energy demand on annual level, and during the peak demand months it is still almost half of total demand even the space heating and ventilation heating are at highest level of the year. In summer time, the DHW heating is actually the only heating demand as there is no need to heat spaces or ventilation in summer. Modern buildings are well insulated, U-values of windows and doors have been improving and heat recovery efficiencies of air handling units are so high, that space heating and ventilation heating demands are significantly lower and therefore having a smaller share of total heating energy demand than in older buildings. Total annual heating energy demand of the residential area is 2 005 MWh which consists of 535 MWh of space heating (SH) energy, 191 MWh of ventilation heating (VH) energy and 1279 MWh of DHW energy.

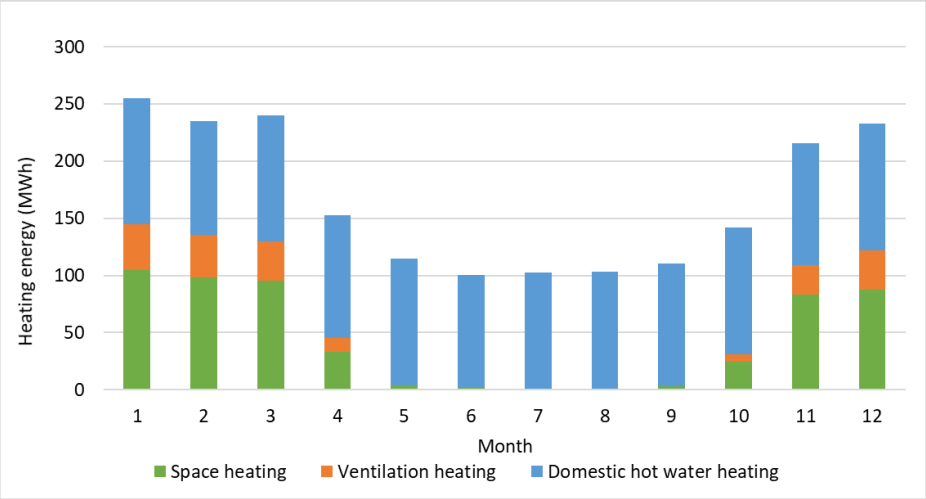

Figure 15. Monthly heating energy demand of the residential district.

Cooling system is becoming more common in new residential buildings. Although the cooling demand in residential buildings is relatively low when comparing to heating demand of residential building, it is an important actor to maintain comfortable indoor environment in summer time. Moreover, the excess heat that is removed from the buildings with cooling system can be utilized for local hybrid energy system. Thus cooling system was assumed to be in all buildings and modeled as a part of local hybrid energy system. In Figure 16 is presented monthly cooling demand of residential area of this study. Annual total cooling demand of the neighborhood was 179 MWh. The cooling energy demand profile was based on the same IDA ICE model as in heating case, because heating and cooling profiles were calculated simultaneously.

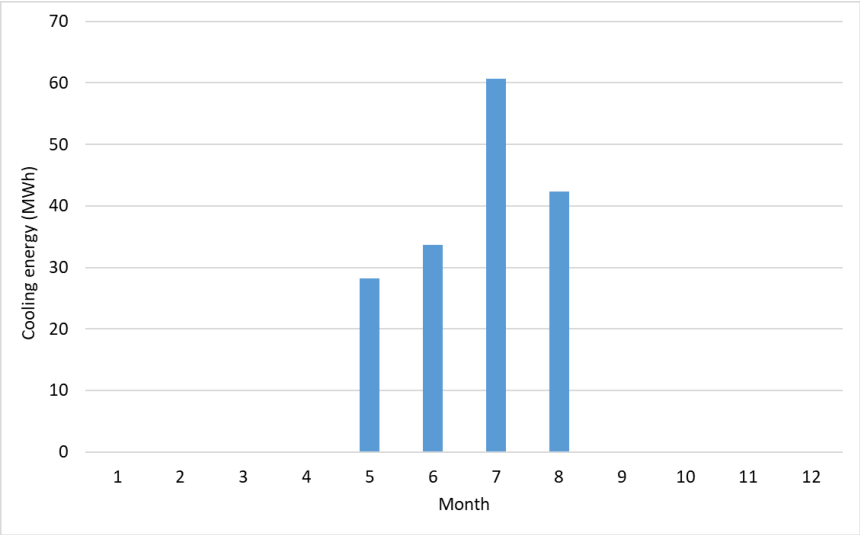

Figure 16. Monthly cooling demand of residential district.

3.4 Dynamic modeling of local hybrid energy system

The hybrid energy system of this study was a combination of solar energy, heat pumps and district heat. The main components of the system were photovoltaic (PV) panels, air-to-water heat pumps (AW-HP), water-to-water heat pumps (WW-HP), buffer tank for short time heat energy storing and borehole thermal energy storage (BTES) for seasonal heat energy storing.

The operating principle of the local hybrid energy system was that AW-HPs were operated utilizing PV electricity and producing heat energy to the buffer tank. When the temperature in the tank was high enough, the heat energy was discharged from the tank into the seasonal storage. Also the condensate heat from the space cooling energy production was charged into tank and further to the seasonal storage. In discharging mode, mainly in wintertime, the heat energy was discharged from the seasonal storage to the buffer tank and further to the local heating network. WW-HPs were connected between BTES and buffer tank in such a way that WW-HPs were operated always when BTES was discharged to reach the high enough temperature level for heat energy distribution to the buildings.

One key issue related to PV electricity generation was, whether the centralized or decentralized installation was more preferable. Usually, the centralized installation of solar thermal collectors or PV panels is more cost-efficient than decentralized installation to the rooftop of the buildings. However, the cost of land can affect strongly to the final cost. (Hirvonen,

Sirén 2018). Energy system evaluated in this study was located in Espoo where the cost of land is one of the highest in Finland. Thus it was more feasible to prefer decentralized solar energy production and place the photovoltaic panels to the rooftop of the buildings.

Because the simulation model was complex and 25 years life cycle was assumed for the local hybrid energy system, simulation time had to be decided based on few different factors. As the BTES requires few years to heat up and achieve final temperature level and performance, one year simulation was not a feasible method. However it was not reasonable to run the simulation through the whole life cycle of the local hybrid energy system due to very long simulation time. After running the simulation several times and observing the results it was noticed that after four years there were no significant changes in BTES temperature levels. So as a compromise, the simulation was run four years and the rest of the years were assumed to be similar to the fourth year. The simulation was started from the beginning of the year. Time step used in the simulations was 0.125 hours.

The local hybrid energy system modeled in this study is described in Figure 17. Changing flow directions are marked with different colors. The temperatures given in the figure are only directive to clarify in which temperature level each part of the system operate. Exact temperatures depend on the case.

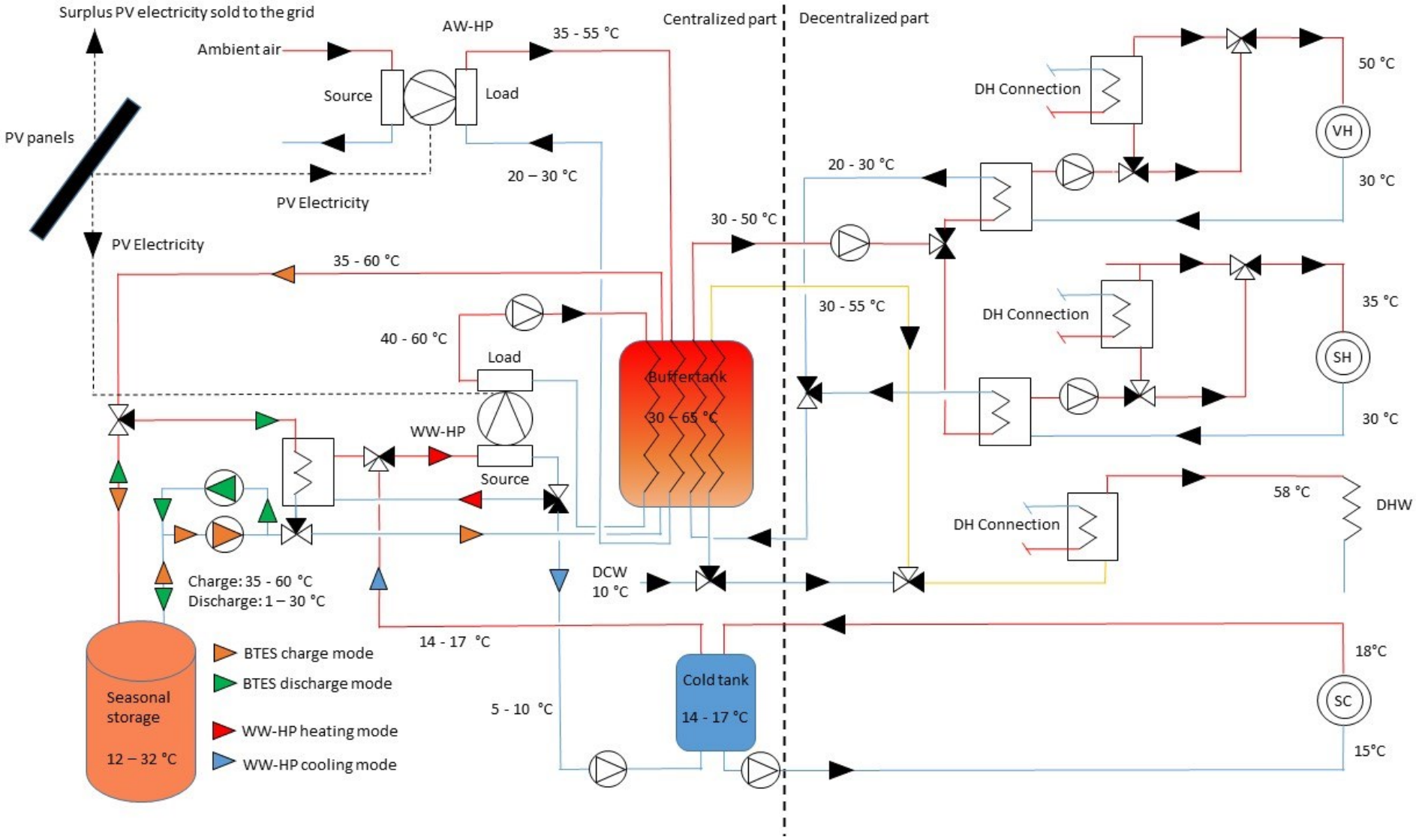

Figure 17. Local hybrid energy system of this study.

3.4.1 Heating networks in the buildings

As the heating energy was distributed to the apartments using underfloor heating, the space heating network operation temperatures were relatively low. Maximum inlet temperature of the SH network was 35 °C and maximum outlet temperature was 30 °C. Network inlet and outlet temperatures were dependent on outdoor air temperature which was based on the fact that the lower the outdoor air temperature is, the higher heat demand is. To control inlet temperature of the network based on outdoor air temperature, control curves were needed. (Ouman Oy 2017). In this study, a linear control curve for underfloor heating was implemented and it is presented in Figure 18. Though the shape of control curve can have different shapes in real life and has an important role maintaining comfortable indoor temperature conditions and energy efficiency of building, the effect of control curve for the whole energy system is not so significant that it would have been feasible to consider in more detailed. The residential district was located in Espoo so the design outdoor air temperature was - 26 °C. Design outdoor air temperature defines the lowest temperature when heating system must operate normally and at that temperature the maximum network inlet temperature is in use. (Ministry of the Environment 2017).

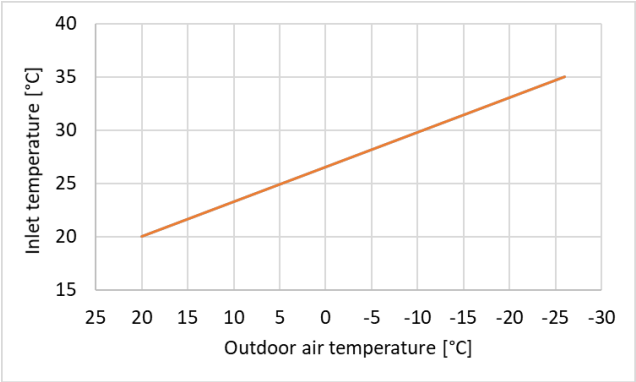

Figure 18. Space heating network inlet temperature.

It was assumed that there was a centralized ventilation system in each building. In other words, there were air handling units in technical rooms located inside the building serving all apartments in the building. The efficiencies of heat recovery units in air handling units have been evolved significantly, but as the effectiveness of heat recovery cannot be 100 %, there was a need for heating coils that heated supply air to final temperature before distributing it to the apartments. Thus separate ventilation heating network (VH) was needed as the operation temperatures air handling unit heating coils are higher than underfloor heating network. In general there are several design temperatures for VH network, for example with maximum inlet temperature 60 °C and maximum outlet temperature 30 °C (Finnish Energy 2014). Actually those temperatures are not absolutely the operating temperatures of the heating coil as there is usually mixing connection so that the supplying network operates 60 °C / 30 °C temperatures and heating coil with 50 °C / 30 °C temperatures. Some air handling unit manufacturers provide heating coils with lower operating temperatures, e.g. 40 °C / 20 °C so as a compromise in this study, the VH network was operated with maximum inlet temperature 50 °C and maximum outlet temperature 30 °C. Similarly as in SH network, also in VH network inlet and outlet temperatures depend on the outdoor air temperature. (Laihian Nuuka Lämpö Oy 2015). Control curve of VH network of this study is linear to simplify modeling and it is presented in Figure 19.

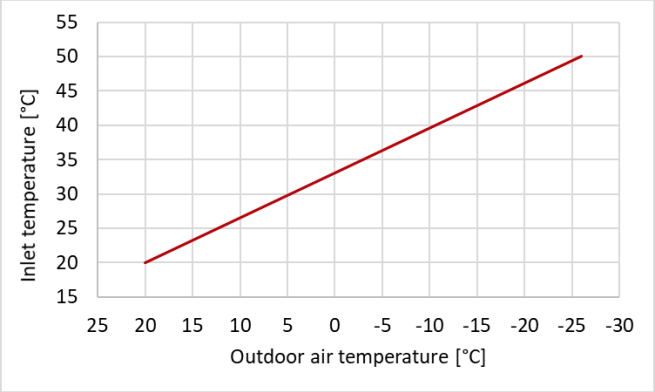

Figure 19. Ventilation heating network inlet temperature.

3.4.2 Photovoltaic system

It was assumed, that photovoltaic panels can be installed on the rooftop of each building. Rooftop was assumed to be flat roof, and the tilt angle of PV panels was adjusted using racks. Each building had rooftop area roughly 290 m². As there were 14 buildings in the residential district, the total rooftop area was approximately 4100 m². It was assumed, that half of the rooftop area could be utilized for PV panels as there might be also other structural and technical components in rooftop area, like roof-installed extraction fans, rain-water wells and chimneys. Even if the PV panels were not installed on a fully horizontal plane, each PV panel was assumed to need space of same amount that the area of PV panels was. The reason for that was to avoid them shading to each other and thus decreasing the PV electricity generation significantly.

PV panels used in modeling were Axitec AC-270P/60S having nominal output power 270 W and area of 1.627 m² (Axitec 2018). Based on technical data of panels, a maximum of 1260 PV panels (90 per building) with total nominal output power of 340 kW were modeled. Inverter is required to convert the DC electricity to AC electricity. As there are conversion losses in the inverter, inverter efficiency was taken into account in calculations. Efficiency of inverter was used 90 % (Pearsall 2017). It is also known, that power productivity of PV panels is decreasing slightly every year. Based on analytical review of photovoltaic degradation rates, 0.7 % annual degradation was used in this study. (Jordan, Kurtz 2012). However, as the simulation was performed only for 4 years, the annual degradation would have been taken into account only for 4 years period and after 4 years the degradation would have been the same as in 4th year. On the other hand, it was not possible to calculate the degradation rate and decreasing PV electricity generation for each year of the life cycle separately due to simulation time. Thus an average value $(1\text{-}0.007)^{12.5}$ for degradation of whole life cycle was used to achieve proper amount of PV electricity generation. The average value was based on the fact that if the annual degradation is 0.7 %, at the end of the life cycle PV panels can generate only $(1\text{-}0.007)^{25}$ i.e. 84 % of initial electricity generation at the beginning of the life cycle. When using average value for degradation in PV electricity generation calculations, the total amount of generated electricity during life cycle was almost the same as if the degradation rate would have been calculated for each year separately. The main difference when using the average degradation rate was, that PV electricity generation stayed same each year. In real life it is higher at the beginning of the life cycle and lower at the end of the life cycle.

Storing electricity was not considered in this study. Usually it is more cost-effective to utilize all PV electricity on the site because the selling prices to the grid are lower than electricity prices when importing electricity from the grid. However, there were difficulties to define the value of PV electricity in the case that the PV electricity produced by the owner of the local hybrid energy system would have been sold to the residents of the apartments. Moreover, the proper electricity consumption profile of electricity consumed in common spaces of apartment buildings i.e. elevators, common saunas, clubrooms, lighting in staircases and so on was not available. Thus, if there was excess PV electricity, it was sold to the grid.

3.4.3 Heat pumps

Heat pumps that were utilized in this local energy system were AW-HPs and WW-HPs. AW-HP was modeled based on properties of NIBE F2120-20 with nominal heat output 20 kW per heat pump. The actual heat output of the AW-HP was limited to 16 kW due to manufacturer's technical reasons so each AW-HP in the model had maximum output power of 16 kW. In Figure 20 is presented the heating capacity of NIBE F2120-20 as a function of ambient air temperature. It can be noticed from the figure that the full heating capacity can be achieved starting from -5 °C - +5 °C ambient air temperature depending on final temperature of the fluid that is heated up. (NIBE 2018a).

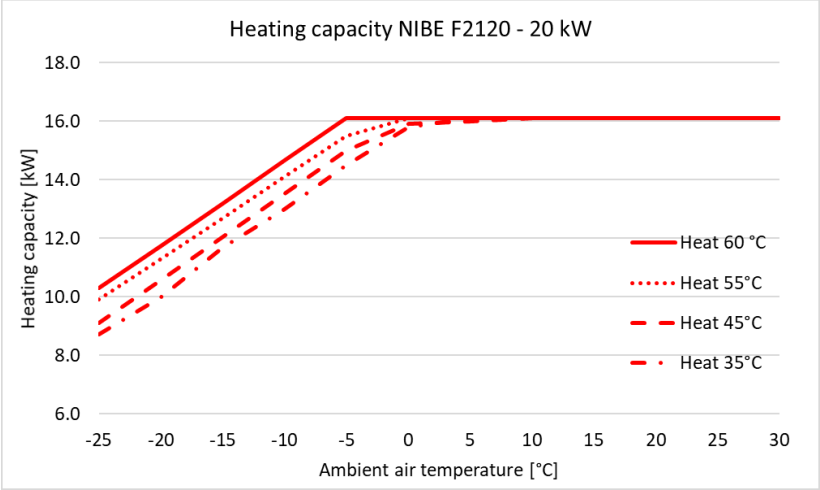

Figure 20. Heating capacity of NIBE F2120 (NIBE 2018a).

In Figure 21 is presented COP of AW-HP NIBE F2120-20. The higher the outdoor air temperature is, the higher COP can be achieved. As the PV electricity was used to run the AW-HPs in this study and PV electricity is mostly available in summer time when the outdoor air temperature is on highest level in annual period, the average COP of AW-HPs was expected to be quite high.

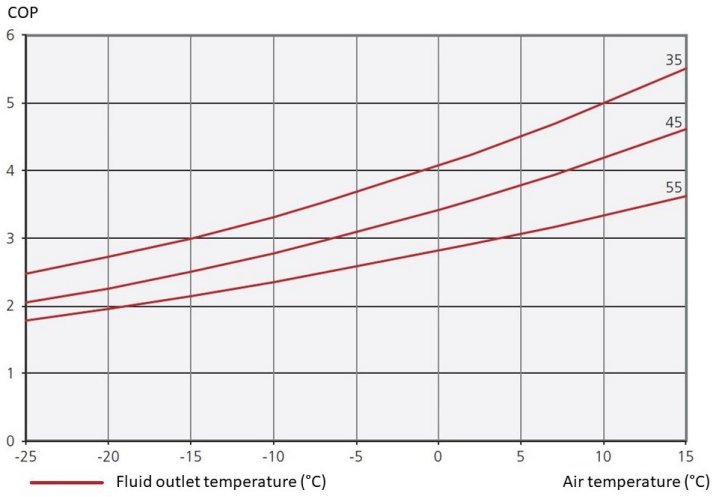

Figure 21. COP of NIBE F2120 in different load side temperatures (NIBE 2018a).

WW-HP was utilized to heat up the water in buffer tank during heating period using heat energy discharged from BTES as source side heat energy. In summer time when there was a need for cooling in the buildings, the same heat pumps were utilized for producing cooling energy for space cooling. WW-HP was modeled based on properties of NIBE F1345-60. In Figure 22 is shown the heating capacities and cooling capacities of NIBE F1345-60 as a function of source side inlet fluid temperature. (NIBE 2018c, NIBE 2018b).

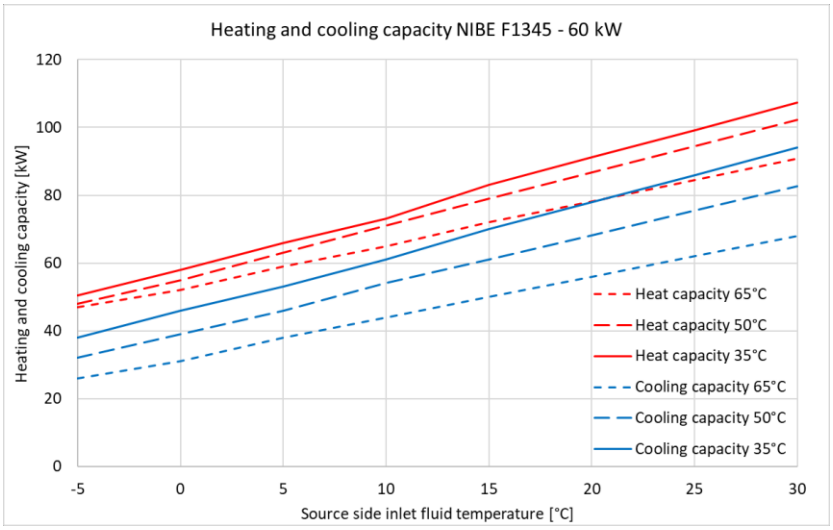

Figure 22. Heating and cooling capacity of NIBE F1345 – 60 kW.

As there were no suitable heat pump components for AW-HP or WW-HP in TRNSYS, both heat pumps were modeled as a calculators where all input values, output values and variables were taken into account. Based on a basic principle of heat pump and the material supplied by manufacturer, heating capacities, cooling capacities and power consumptions as well as COPs were calculated for different source side and load side temperatures. Necessary equations were programmed into the calculators and they were set to interpolate the exact heating outputs, cooling outputs, power consumptions, source side outlet temperatures and load side outlet temperatures based on source and load side flows and source side inlet temperature and load side inlet temperature. As most of the heat pump properties were based on technical

data of heat pumps, the most important values to calculate for each time step were outlet temperatures of source and load sides as they have significant affect to heating capacity, electricity consumption and COP. Outlet temperature of source side was based on equation

$$T_{source,outlet} = T_{source,inlet} - \frac{P_{cooling}}{q_{m,source} \cdot c_{p,source} \cdot \rho_{source}} \quad (8)$$

where

$T_{source,outlet}$	Outlet temperature of the source side fluid (°C)
$T_{source,inlet}$	Inlet temperature of source side fluid (°C)
$P_{cooling}$	Cooling power of the source side (W)
$q_{m,source}$	Flow rate of the source side fluid (kg/s)
$c_{p,source}$	Specific heat capacity of source side fluid (J/kg°C)
ρ_{source}	Density of source side fluid (kg/m³).

Respectively, the outlet temperature of load side was based on equation

$$T_{load,outlet} = T_{load,inlet} + \frac{P_{heating}}{q_{m,load} \cdot c_{p,load} \cdot \rho_{load}} \quad (9)$$

where

$T_{load,outlet}$	Outlet temperature of the load side fluid (°C)
$T_{load,inlet}$	Inlet temperature of load side fluid (°C)
$P_{heating}$	Heating power of the load side (W)
$q_{m,load}$	Flow rate of the load side fluid (kg/s)
$c_{p,load}$	Specific heat capacity of load side fluid (J/kg°C)
ρ_{load}	Density of load side fluid (kg/m³).

3.4.4 Borehole thermal energy storage

Borehole thermal energy storage was modeled using vertical U-Tube ground heat exchanger Type557 in TRNSYS. Parameters of BTES, soil and bedrock are presented in Table 2. Header depth was the height of the soil layer between the top of the ground and the bedrock. It was assumed to be 5 meters based on the fact that the soil layer covering the bedrock is typically thin in large share of Espoo land area (City of Espoo 2019). Radius of borehole was based on typical larger borehole radius. Heat capacity of the soil layer outside the storage volume was assumed to be water saturated gravel which has volumetric heat capacity 2200 kJ/m³/K (Smoltczyk 2003). The thermal conductivity of the storage was assumed to be the average thermal conductivity of rock types in Finland which is 3.24 W/mK (Hakala et al. 2015). The boreholes were assumed to be filled with water with a thermal conductivity of 0.6 W/mK (Engineering Toolbox 2018). U-tube pipes in boreholes were assumed to be plastic pipes made of polyethylene and having thermal conductivity 0.375 W/mK (Engineering Toolbox 2018). Heat transfer fluid circulating in U-tube pipes was assumed to be 30 % mixture of ethylene glycol and water with specific heat capacity of 3660 J/kgK and density of 936 kg/m³ (Engineering Toolbox 2019). An insulating cover could be used to reduce heat

losses on the top of the storage. Insulation was assumed to be polystyrene boards with thermal conductivity of 0.03 W/mK (Engineering Toolbox 2018). In Southern Finland, the average ground temperature may vary between 6-8 °C (Geological Survey of Finland 2019). To ensure the reliability of the results, the lowest value was used as an initial surface temperature of the storage volume.

Table 2. BTES parameters used in the simulation model.

Parameter	Unit	Value
Header depth	m	5
Borehole radius	m	0.08
Storage heat capacity	kJ/m³/K	2200
Storage thermal conductivity	W/mK	3.24
Fill thermal conductivity	W/mK	0.6
Pipe thermal conductivity	W/mK	0.375
Fluid specific heat	J/kgK	3660
Fluid density	kg/m³	936
Insulation thermal conductivity	W/mK	0.03
Initial surface temperature of storage volume	°C	6.0

Flow rate of each loop was kept constant. In a study made by Hirvonen and Sirén it was noticed that in similar type of solar community energy system, constant 1200 kg/h flow per loop was the most favorable in optimal solutions, so it was reasonable to use the same value also in this study. (Hirvonen, Sirén 2018). In addition to these values presented in above, there are several values that were used as an optimization parameters and thus they are presented later in chapter 3.8.

3.4.5 Buffer tank

Buffer tank was modeled using cylindrical storage tank Type534. Stratification of water in the tank was taken into account in modeling by dividing the tank into 5 temperature layers. The idea of stratification was to increase the temperature gradient between water in the tank and heat transfer fluids flowing through tank in pipes and therefore to improve the system performance. Thus pipe nodes were connected to the tank so that the inlet of hot fluid flows coming from AW-HP and WW-HP were on the top side of the tank and outlets were on the bottom side of the tank. The inlet flows of cold fluid flows from SH, VH, DHW networks as well as from the BTES charge loop were on the bottom side of the tank and outlets were on the top side of the tank. As the tank volume was estimated to be relatively high, it was not feasible to assume that tank could be installed inside the building. Moreover, due to cold climate conditions it was not feasible to assume that tank is located in outside on the site as the heat losses would have been increased significantly. Thus it was assumed that the tank was excavated to the ground. That increased investment cost of the tank, but on the other hand the investment cost would have been high also if it would have been installed into the building somehow. Tank was modeled so that there was 10 cm layer of mineral wool wrapped around the tank. The heat losses of the tank installed into the ground are calculated based on the same average ground temperature 6.0 °C as used also in BTES. The shape of the tank was defined in such a way that height-to-width ratio was kept constant 1.5.

3.4.6 Local heating pipes

Local heating network was modeled using buried pipe Type951 in TRNSYS. Distribution network from the energy center to the buildings was assumed to be star topology to simplify modeling i.e. there were separate distribution pipes from energy center to each building. The pipes were plastic pipes. There were separate pipes for domestic hot water (DHW) and combined space heating (SH) and ventilation heating (VH). Insulation material of local heating pipes were assumed to be plastic foam with thermal conductivity of 0.03 W/mK (Engineering Toolbox 2018). Pipes were installed into the gravel and the average ground temperature was 6.0 °C.

3.4.7 Cooling system

Cooling system was not considered in detail, but to understand the consequence for local hybrid energy system, it is necessary to define the method how it was modeled in the study. The core of the cooling system was a 20 m³ cold buffer tank which was kept in such temperature that water entering to the cooling network was almost constant 15 °C. Maximum outlet temperature from the network was 18 °C and the flow was based on cooling demand and the temperature difference. Cooling energy was produced utilizing same WW-HPs that were discharging BTES in winter. This solution needs additional connections and control valves for WW-HPs. However it is feasible solution as there was no need to use WW-HPs for heating purposes in summer time. WW-HPs used cold buffer tank as a source side and they were operating always, when there was cooling need in the cold tank. Load side of the WW-HPs were connected to the warm buffer tank which was charged, and the heat energy was charged further to the BTES. Electricity consumption or COP of cooling system was not considered, it was only checked that they were at reasonable level. Moreover, any cooling system components were not optimized at all, they were just checked that temperature levels were reasonable and system was operating as desired. Location or space need of cooling system components was not considered either.

3.4.8 Back-up heat

The energy system was not planned to be totally self-sufficient, so additional heat energy was imported from traditional district heating network. The purpose of district heat was also to be as a back-up if the local energy system would have malfunctions or other problems. As the district heating network and connections to the buildings was not considered in more detailed in this study, the modeling of DH connections in TRNSYS model were implemented by using auxiliary heaters Type659. Each network (SH, VH and DHW) had their own back-up heater. The back-up heater measured the temperature of incoming fluid which was coming from local heating network. If the temperature did not meet the set point temperature of network as discussed in chapter 1.1.1, the back-up heater increased the temperature up to the set point and calculated the needed amount of energy. That was the amount of DH energy. In real life that kind of solution would not work properly due to the reason that DH heat exchanger have operating temperatures which depend on the temperature level of supplied DH water. If the total flow of SH/VH/DHW water would be routed through DH heat exchanger, the temperature of the SH/VH/DHW water may increase too high. Therefore flow diverters. mixing valves and temperature indicators are needed to divide some share of SH/VH/DHW water to flow through DH heat exchanger to the mixing valve and some other share straight to mixing valve so, that the desired set point temperature is reached at after mixing valve. In Figure 23 is presented a simplified chart of control logic that is needed for back-up heating.

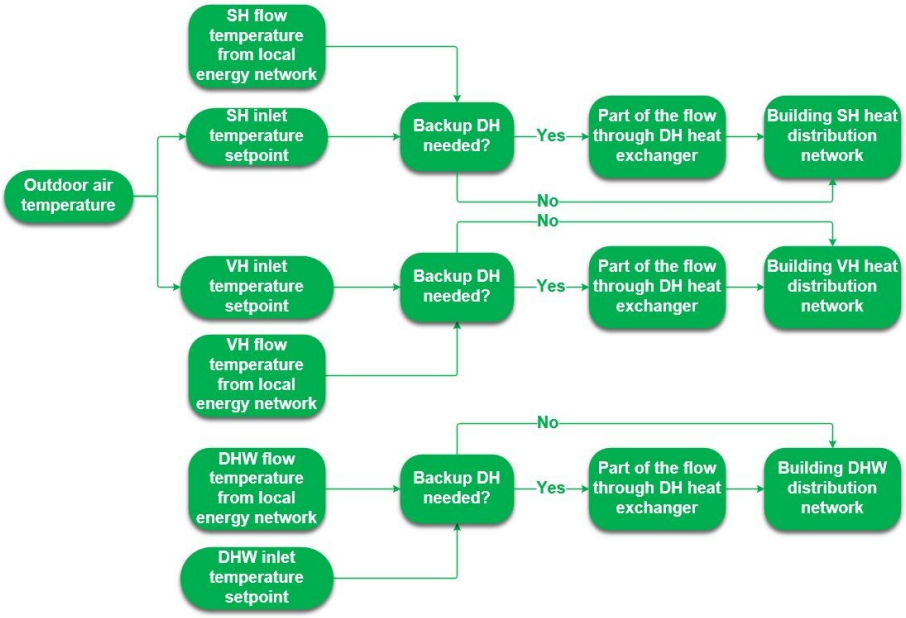

Figure 23. Control logic of back-up heating.

3.4.9 Control logic

PV electricity distribution was prioritized such a way that first AW-HPs were operated. If there was no need for AW-HP operation or there was more PV electricity available than the AW-HPs consumed, WW-HP was operated with PV when they were utilized for heating. Due to cooling system electricity consumption was not considered, PV electricity was not used for WW-HPs when they were in cooling mode. If there was still surplus PV electricity, it was sold to the grid as argued in chapter 3.4.2. Both AW-HP and WW-HP were assumed to be able to operate with part-load in such a way that minimum part-load state was 10 %. Control logic of the local hybrid energy system was mainly dependent on temperature of buffer tank and thus the most important temperatures affecting the operation of different components are described in Figure 24.

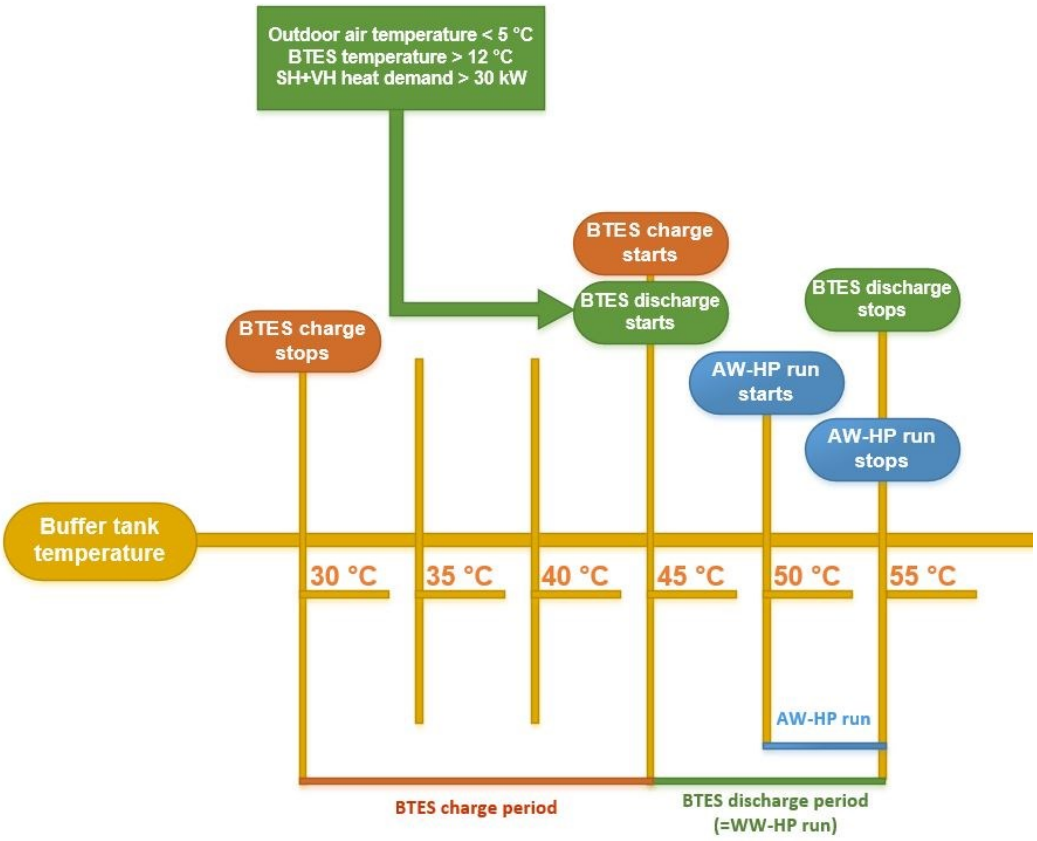

Figure 24. Buffer tank temperatures and operation of different components.

Air-to-water heat pumps were operated by utilizing PV electricity generated in residential district. Air-to-water heat pumps were controlled so that if there was PV electricity available and there was a need for heat in the buffer tank, AW-HPs were run. The heat need in the tank was based on tank temperature so that if the temperature in the tank was decreased below 50 °C, there was a heat need. When the temperature in the tank reached 55°C, there was no heat need anymore and the run of AW-HPs was stopped. Water-to-water heat pumps were utilized in summertime for space cooling. As discussed earlier, the cooling system was not considered in a detailed way, but the condensate from the SC production was fed into the buffer tank. The heat energy from the buffer tank was started to transfer into the seasonal storage whenever the temperature in the tank exceeded 45 °C. Charging of the BTES continued until the tank temperature dropped to 30 °C. In charging mode, the hot water from the tank was fed to the center of the BTES and proceeded to the edges through linked boreholes allowing a radial temperature distribution.

To maximize the utilization of the energy charged to the seasonal storage, the BTES discharge was allowed only when the total heat demand without DHW i.e. the sum of SH and VH demand in the neighborhood exceeded 30 kW. Heat demands below 30 kW were covered using district heat. That size of heat demands occur mainly in late spring or early autumn time when there is a high potential to run AW-HPs and charge BTES, and on the other hand the DH prices are lower than in winter time. As the local energy system was originally decided to cover only some share of annual heat demand of the neighborhood and the capacity

of the system was restricted, it was feasible to allocate the on-site energy utilization to highest heat demand period to decrease the amount of imported DH. Thus BTES discharge was allowed when the outdoor air temperature decreased below 5 °C.

When the conditions mentioned above were fulfilled, the BTES discharge was based on tank temperature. If the tank temperature decreased below 45 °C, the BTES was discharged. After the tank temperature reached 55 °C, BTES discharge was stopped. As the WW-HPs were connected to the BTES with heat exchanger, WW-HPs were operated always when the BTES was discharged. Number of operating WW-HPs was based on total heat demand. To retain the energy balance and avoid BTES cooling down too much, the BTES discharge was stopped if temperature of the BTES decreased below 12 °C. Discharging was restricted until the temperature of BTES increased 14 °C. There was also time limit between charge and discharge modes so that there is always two hours break when changing from charge mode to discharge mode or vice versa. So as a conclusion BTES was discharged when the tank temperature decreased to 45 °C, total heat demand were higher than 30 kW, outdoor air temperature were below 5 °C and the temperature of BTES were higher than 14 °C.

In this local hybrid energy system district heat was supplied in each building in addition to on-site produced heat, which us why it was not feasible to heat the DHW to the final temperature required by Ministry of the Environment as expressed in chapter 2.4. This was because the tank temperature should have been higher and the efficiency of the system would have been lowered. However, the local energy was utilized to pre-heat the DHW in the tank and the final heating was done in each buildings' district heat heat exchanger. Moreover, as the local hybrid energy system was decided not to cover 100 % of total heating energy demand, it was reasonable to allocate utilization of local energy to winter time when heating demand is higher and district heat prices are higher. As introduced in Figure 15 in chapter 3.3, DHW heating demand is almost same during the year. If DHW would have been pre-heated also in summer using local heating energy, BTES could not have been charged as much, and therefore there would have been less local heating energy to utilize in winter. To maximize the local energy utilization in winter and on the other hand to utilize the low DH prices in summer, DHW was pre-heated in buffer tank when the outdoor air temperature was 5 °C or lower. When outdoor air temperature exceeded 5 °C, DHW was heated totally using only DH.

3.5 Cost data

To evaluate economic feasibility of the energy system, all costs during life cycle were taken into account. The life cycle cost consists of investment costs and operation costs. All investments were assumed to be done in year 0. Operation costs included electricity costs and maintenance costs. Profit of surplus electricity that was sold to the grid was subtracted from sum of operation costs i.e. profit from sold energy lowered the operation costs of local hybrid energy system. Real interest used in calculations was 3 % according to EU recommendations for long-term investments, as higher interest rates discourage long-term investments (European Commission 2012a). Escalation rate for electricity price was conservative 1 % as it is difficult to predict the price trends in future. Life cycle of the system was assumed to be 25 years. It was assumed that additional investments were not needed during the life cycle.

3.5.1 Investment costs

Costs of energy system components were retrieved from manufacturers, internet sources, and other studies they are presented in Table 3. VAT 24 % is included in all costs. PV system cost was based on the average of several offerings that professional companies have released. The cost estimate of PV panels are in form €/kW_p where the kW_p means the nominal power that panel can generate in optimal conditions. The cost of PV system included installation costs and inverter cost. Cost of heat pumps were collected from retailer's website and scaled so that the cost is depending on total heating capacity of heat pumps. Cost of buffer tank was 785 €/m³ and it was based on cost level introduced in report by International Energy Agency. As the volume of buffer tank seem to be relatively high in this study based on some test simulations, the cost was based on larger scale buffer tank cost structure. Due to high land cost and on the other hand practical difficulties to locate large scale buffer tank into the building, it was assumed that the tank has to be integrated to the ground. As the cost of that kind of integration was challenging to evaluate, rough estimation was done by assuming that cost of the integration was equal to tank cost. Thus total cost of the tank was 1570 €/m³.

Cost of BTES consists of several main components. Borehole drilling cost was based on estimation of typical drilling costs of large-scale ground source heat field. Drilling cost included also cost of connecting the boreholes to each other. Because the soil has to be excavated off when insulating the BTES and after that it has to be put back, the excavation cost was needed to take into account. Excavation cost was based on average excavation cost used in previous, similar kind of study. The cost was retrieved from retailer website and scaled so that it was based on insulation volume.

Space heating and ventilation heating energy was assumed to be distributed to the buildings in the same pipes, but for domestic hot water distribution separate pipes were required. Pipes were assumed to be typical plastic, insulated local heating pipes. Distance from the energy center to each building was assumed to be 60 m. As the distances and number of buildings did not changed in optimization process, the needed length of local heating pipes remained the same. Thus the pipe cost was a constant value. The heating pipe price was higher than DHW pipe price because the heating pipes must be larger size. In addition to the costs discussed already, the pump cost was also taken into account. One pump was needed for circulating BTES heat transfer fluid, and another for local heating network to supply heating energy to the buildings. Constant cost of 10 000 € was estimated for pumps which was based on typical larger scale pump costs.

Table 3. Prices for components of local energy system.

Component	Cost	Unit	Reference
PV system	1000	€/kW_p	(Photovoltaic electricity home 2019)
AW-HP	410	€/kW	(Finnish ground source heat wholesale 2019b)
WW-HP	280	€/kW	(Finnish ground source heat wholesale 2019a)
Tank	1570	€/m³	(International Energy Agency 2016)
Borehole drilling	38	€/m	(Techeat 2018)
BTES excavation	6	€/m³	(Hirvonen, Sirén 2018)
BTES insulation	75	€/m³	(K-rauta 2019)
Local heating pipes for heating	108	€/m	(Rauheat 2019)
Local heating pipes for DHW	48	€/m	(Rauheat 2019)

3.5.2 Operation costs

The electricity cost consisted of three main components that were energy price, distribution price and taxes. In this study, hourly NordPool Elspot prices were used so electricity price for each hour was calculated separately. To get variation to the electricity prices in this study, NordPool prices of five different years, 2014-2018, were utilized in sequence to make the price profile for 25 year life cycle calculation period. First five years were calculated straight based on 2014-2018 cost data, and after the end of the year 2018 was reached, the cost data was started again from beginning of year 2014. Annual average prices of electricity as well as standard deviations of prices are presented in Table 4.

Table 4. Annual averages of Elspot electricity prices and standard deviations (VAT not included).

Year	Annual average price (€/MWh)	Standard deviation (€/MWh)
2014	36.02	± 11.50
2015	29.66	± 14.46
2016	32.45	± 13.15
2017	33.19	± 9.61
2018	46.80	± 15.12

As spot electricity prices was used, 0.3 c/kWh commission fee was added to the Elspot price (Fortum 2019c). Value added tax 24 % was added to the energy price also. Electricity distribution in Espoo area is operated by Caruna Espoo Oy and the price for distribution was 3.14 c/kWh. Electricity tax was 2.79372 c/kWh and it was added to the total price. (Caruna Espoo Oy 2018). Equation for electricity buying price is

$$P_{Electricity,buying} = (P_{Elspot} + P_{CF,buying} + P_{distribution} + P_{Electricity\ tax}) \cdot \left(1 + \frac{VAT}{100}\right) \quad (10)$$

where

$P_{Electricity,buying}$ Hourly electricity buying price (c/kWh)
P_{Elspot} Hourly Nordpool Elspot price (c/kWh)
$P_{CF,buying}$ Commission fee (c/kWh)
VAT Value added tax (%)
$P_{distribution}$ Electricity distribution price (c/kWh)
$P_{Electricity\ tax}$ Electricity tax (c/kWh).

Hourly electricity cost can be calculated using equation

$$C_{electricity,import} = \frac{P_{Electricity,buying}}{100} \cdot E_{Electricity,import} \quad (11)$$

where

$C_{electricity,import}$ Hourly electricity cost (€)
$P_{Electricity,buying}$ Hourly electricity buying price (c/kWh)
$E_{Electricity,import}$ Hourly imported electricity (kWh).

Because there was an option to sell surplus electricity to the grid, selling price of electricity has to be considered as well. Selling price of surplus electricity was NordPool Elspot price

from where 0.24 c/kWh commission fee is subtracted (Fortum 2019a). If annual sales of electricity exceed 8500 €, value added tax has to be paid which lowers profits by 24 %. The equation for electricity selling price is

$$P_{Electricity,selling} = P_{Elspot} - P_{CF,selling} \quad (12)$$

where

$P_{Electricity,selling}$	Electricity selling value (c/kWh)
P_{Elspot}	Hourly Nordpool Elspot price (c/kWh)
$P_{CF,selling}$	Commission fee (c/kWh).

Hourly surplus electricity selling profit can be calculated using equation

$$C_{electricity,export} = \frac{P_{Electricity,selling}}{100} \cdot E_{Electricity,export} \quad (13)$$

where

$C_{electricity,export}$	Hourly electricity surplus selling profit (€)
$P_{Electricity,selling}$	Hourly electricity selling price (c/kWh)
$E_{Electricity,export}$	Hourly exported electricity (kWh).

Annual maintenance cost was assumed to be five percent of total investment costs, divided by the life cycle i.e. the equation for annual maintenance costs is

$$C_{Maintenance} = \frac{0.05 \cdot P_{investment}}{LC} \quad (14)$$

where

$P_{Maintenance}$	Annual maintenance cost of local hybrid energy system (€)
$P_{investment}$	Total investment cost of local hybrid energy system (€)
LC	Life cycle of the local hybrid energy system (a).

Based on components of operation costs described above, annual operation costs can be defined using equation

$$C_{Operation} = \sum C_{electricity,import} - \sum C_{electricity,export} + C_{Maintenance} \quad (15)$$

where

$C_{Operation}$	Annual operation cost (€)
$\sum C_{electricity,import}$	Annual electricity cost (€)
$\sum C_{electricity,export}$	Annual surplus electricity selling profit (€)
$C_{Maintenance}$	Annual maintenance cost (€).

3.6 System performance indicators

To evaluate the performance of the modeled system, some indicators have to be introduced. From economical point of view the life cycle cost (LCC) of the system is important information to find out if the system is feasible to develop further. However, even more reasonable is to examine what is actually the cost of one unit of on-site produced heating energy. For that purpose levelized cost of energy (LCOE) is a suitable method. To evaluate the economical profitability of the local hybrid energy system, LCOE can be compared to district heat prices. Production prices of district heat were not available due to confidentiality issues, and thus the LCOE of on-site produced energy were compared to district heat consumer prices to find out a rough estimation of profitability of this kind of hybrid energy system.
Renewable energy fraction (REF) presents what kind of proportion of total energy demand can be covered with on-site produced energy taking into account also the imported electricity that is needed to produce on-site energy. Carbon dioxide emissions have to be considered also as the aim of the local hybrid energy system was to reduce CO_2 emissions. Emission reduction achieved by utilizing hybrid energy system can be computed by calculating carbon dioxide emissions of local hybrid energy system and comparing the result to the situation where all heating demand of the residential district is covered using district heat.

3.6.1 Life cycle cost

In life cycle cost calculation, investment costs and operation costs in each year has to be taken into account. Sum of annual costs has to be discounted. Life cycle cost for each year can be calculated using following equation

$$LCC = \sum\left[(C_{I,t} + C_{O,t} + C_{M,t}) * (1+r)^{-t}\right] \tag{16}$$

where

C_t Investment costs in year t (€)
$C_{O,t}$ Operation costs in year t (€)
$(1+r)^{-t}$ The discount factor for year t (-).

3.6.2 Levelized cost of energy

To evaluate the system performance and compare feasibility to traditional district heat, the price of produced energy has to be calculated. Levelized cost of energy (LCOE) is a suitable method for that purpose thus it takes into account all life cycle costs as well as economical discount rates. In principle, total costs and produced energy amount are calculated for every year, they are discounted, summed up during whole life cycle and finally total discounted life cycle costs are divided by total discounted produced energy amount. (Syri 2018).

$$LCOE = P_{MWh} = \frac{\sum\left[(C_t + O\&M_t + Fuel_t + Carbon_t + D_t)\cdot(1+r)^{-t}\right]}{\sum[E_t \cdot (1+r)^{-t}]} \tag{17}$$

where

P_{MWh} The constant life cycle remuneration of produced energy (€/MWh)
C_t Investment costs in year t (€)
$O\&M_t$ Operation and maintenance costs in year t (€)

$Fuel_t$	Fuel costs in year t (€)
$Carbon_t$	Carbon costs in year t (€)
D_t	Decommissioning and waste management costs in year t (€)
E_t	The amount of energy produced (MWh)
$(1+r)^{-t}$	The discount factor for year t (-).

In this energy system there were neither no fuel costs thus electricity costs were included in operation costs, nor carbon costs as they were actually included in electricity and district heat prices. Decommissioning and waste management costs did also not exist, so the simplified LCOE equation gets the form

$$LCOE = \frac{\sum[(C_{I,t}+C_{O,t}+C_{M,t})*(1+r)^{-t}]}{\sum[E_t*(1+r)^{-t}]} \quad (18)$$

where

$LCOE$	The constant life cycle remuneration of produced energy (€/MWh)
C_t	Investment costs in year t (€)
$C_{O,t}$	Operation costs in year t (€)
E_t	The amount of heat energy produced (MWh)
$(1+r)^{-t}$	The discount factor for year t (-).

3.6.3 Renewable energy fraction

Renewable energy fraction (REF) indicates how large proportion of total energy demand can be covered using on-site energy. REF in this study is similar to on-site energy fraction (OEF) which is introduced by Cao et al but the difference is that instead of dividing on-site produced energy by total energy demand, REF is calculated indirectly (Cao et al. 2013).
The reason for that is, that producing on-site energy also grid electricity is needed to operate WW-HPs, because in wintertime there is not enough solar electricity available. Moreover, calculating only amount of on-site produced energy is not feasible due to relatively high losses of seasonal storage i.e. it is not sensible to compare energy production values. So dividing on-site produced energy by total energy demand does not give correct value. In this study, REF is defined as

$$REF = 1 - \frac{E_{import}+DH_{import}}{Heat\ demand_{total}} \quad (19)$$

where

REF	Renewable energy fraction (-)
E_{import}	Electricity imported from the grid for heat pumps (MWh)
DH_{import}	Imported district heat (MWh)
$Heat\ demand_{total}$	Total heat demand (MWh)

The idea is to sum up imported district heat and grid electricity that is needed to produce on-site energy and divide the sum by total heat demand. That gives the fraction of off-site energy so one minus the result gives fraction of on-site energy of which all is renewable energy because the electricity consumption of heat pumps is now taken into account in calculations.

3.6.4 Carbon dioxide emissions and costs of emission allowances

On-site energy production reduces consumption of district heat which lowers CO_2 emissions of district heat production. However in on-site energy production electricity was needed to operate heat pumps which increases CO_2 emissions of electricity production. Thus it is necessary to find out the total CO_2 emissions of local hybrid energy system to evaluate the system performance. In CO_2 emission calculations, emission factor for district heat produced in CHP plants was used 164 g CO_2/kWh. (Motiva 2019). In electricity emission calculations monthly varying emission factors were used as the differences between summer and winter time electricity production are significant. Monthly emission factors for electricity production are presented in Table 5. Monthly emission factors are based on emission data of 2011-2015 where factors of imported electricity from other countries are neglected and emissions of bioproduction is assumed to be zero. (Finnish Energy 2018). Electricity amount used in calculations was amount of imported grid electricity i.e. the net consumption.

Table 5. Monthly CO_2 emission factors of electricity production.

Month	Electricity CO_2 emission factor (g/kWh)
January	173
February	174
March	156
April	132
May	125
June	85
July	81
August	115
September	148
October	143
November	131
December	131

In this study, only the amount of electricity that is needed to operate heating system which was partly from the grid and partly from the PV panels, was taken into account in electricity consumption calculations. Electricity that is generated using PV panels is CO_2 emission free and thus CO_2 emissions of on-site produced heating energy can be calculated dividing annual CO_2 emissions of imported electricity by amount of supplied on-site heating energy.

Every district heat plant that has heat production capacity more than 20 MW, must have emission allowances as well as smaller plants that are operating in the same distribution network. (Finlex 2011). The district heat energy amounts used in calculations were net values i.e. distribution losses from CHP plant to neighborhood area etc. was not taken into account. In electricity emission calculations amount of electricity from the grid was used. The cost of one emission allowance in EU auction has been deviating between 18.62 € and 27.46 € (Energy Authority 2019). Emission cost calculations of this hybrid energy system were computed using constant value 25.00 € per allowance. However, the cost of one emission allowance has been increasing significantly during past few years. It was roughly 5 € quite a long time but since end of the year 2017 the cost of emission allowances have been

increased. (Refinitiv 2018). As the aim of the emission allowances is to reduce carbon dioxide emissions, price of emission allowances may increase also in the future due to need of CO_2 emission reductions. For that reason it was compared, what would be the emission cost level of simulated local hybrid energy system if the price of emission allowance would be doubled or tripled in comparison to current situation.

3.7 Optimization

The idea of optimization process in general, is to find out the most suitable solution from among several alternatives. In building energy sector the aim of the optimization is usually to find out the best optimal solution where the system performance is as high as possible, but the system costs are as low as possible. Components of optimization problem are objective functions, constraints and decision variables. Objective functions define what is target of solution. Constraints can be either equality constraints or inequality constraints and their aim is to give limits for optimization. For example, maximum rooftop area that can be used for PV panels can be a constraint. By changing decision variables and seeing how they affect to the result of objective function, the optimal solution can be achieved.

In this study two objective functions was implemented so the optimization problem was multi-objective. Multi-objective optimization (MOO), also known as Pareto optimization, is required to find out the Pareto-optimal solutions and for that the genetic algorithm (GA) is used. Genetic algorithm is well-functioning tool in MOO and parallel calculations are simple to perform using GA. Moreover, discrete variables are simple to use with GA. Genetic algorithm is based on evolution theory, where the fittest individuals survive and transfer their genetic information to the following generations. In this study the genetic information consisted of decision variables that were specified before optimization. In Figure 25 is shown the main steps of genetic algorithm optimization process.

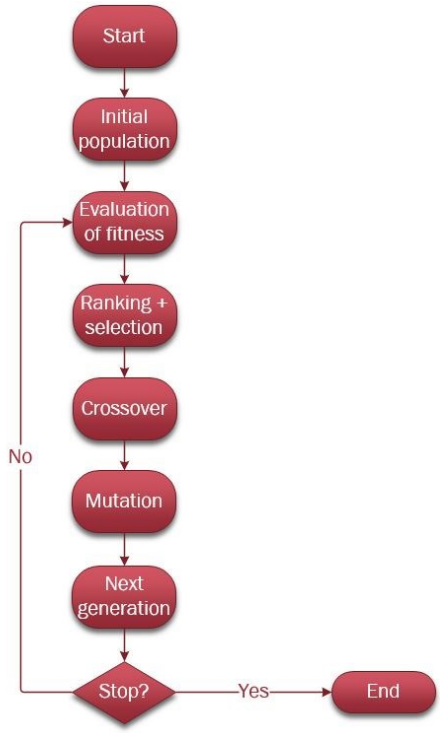

Figure 25. Genetic algorithm optimization process.

The algorithm starts from first generation that is selected randomly. Values of objective functions are calculated based on first generation variables and as a result the fitness of individuals are evaluated based on the values of objective functions. Then the individuals are ranked based on their fitness. If the non-dominated sorting i.e. NSGA is used, the non-dominated individuals are located and selected for the next generation. The other individuals that are not selected for the next generation, are used for crossover and mutation phases to keep up the diversity of population. In crossover phase, the crossover point is selected randomly or it is based on some pre-defined mechanism. On other side of crossover point the individuals are preserved for the next generation and on another side of the point decision variables will be changed. Then in mutation phase, some randomly selected decision variables are replaced with randomly selected individuals so that the diversity of population will be preserved. (Alanne 2018). After that the new generation has been formed and next generations are evaluated same way until the new generation does not deviate from previous generation based on pre-defined accuracy criteria. The criteria can be e.g. maximum number of generations, maximum elapsed time, acceptable value of objective function, convergence of objective function etc. Pareto front is a result of multi-objective optimization. Results forming the Pareto front are non-dominated i.e. they are mathematically equal when comparing to each other. In other words, it is not possible to improve one objective without worsening another at the same time. (Evins 2013). The decision makers have to select one or several solutions from Pareto front to be implemented or for further studies based on their preferences.

In this study the optimization was performed utilizing Multi-Objective Building Optimizer software (MOBO) developed by Aalto University and Technical Research Centre of Finland. It was combined with local hybrid energy model in TRNSYS using Matlab as a platform. Combined simulation and optimization process of this study is described in Figure 26. The optimization process was started so that MOBO selected randomly first decision variables based on pre-defined boundary conditions. Decision variables were entered to TRNSYS and then TRNSYS performed energy model simulation for four year time period. After the simulation was done, Matlab read the simulation results from the TRNSYS output file and computed the life cycle calculations of the local hybrid energy system. Then the results were printed to an output file that was read by MOBO which created mutations and crossovers to the population after that. Then MOBO selected the new decision variables based on results of previous generation and then the process started again from the beginning and continued similarly as long as the pre-defined amount of generations were calculated. Finally Pareto front was formed from the final generation results.

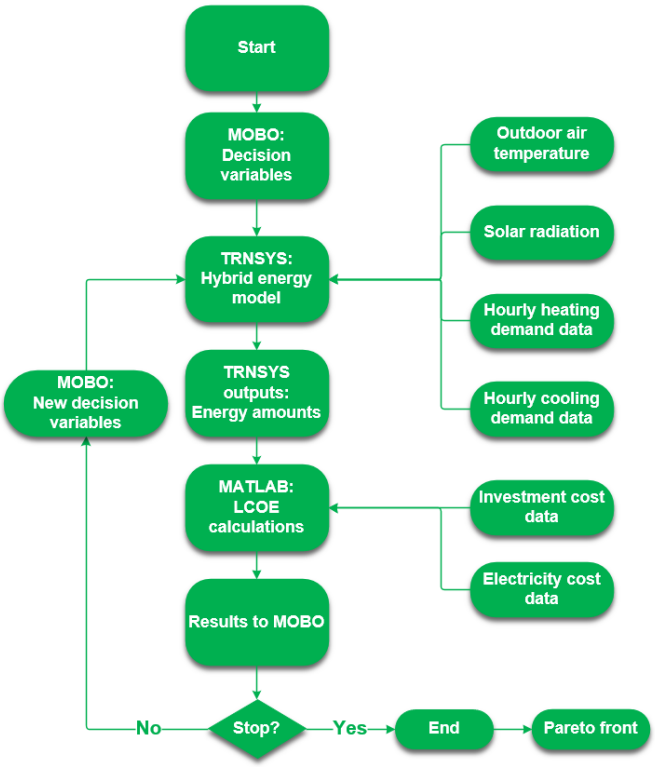

Figure 26. Combined simulation and optimization process implemented in this study.

3.8 Optimization parameters and optimization problem

Objective functions in this study were related to costs and system performance, as the aim of the study was to find out a cost-optimal and feasible local hybrid energy system. Objective function for system performance was amount of imported district heat and the aim of the optimization was to minimize it or in the other words, to maximize the on-site energy production as high as it was cost-efficient. Objective function for costs was levelized cost of energy and the aim was to minimize it.

Optimization problem was defined as

$$min\{f_1(x), f_2(x)\} \quad (20)$$
$$s.t.$$
$$H(x) = A_{PV} \leq 2100\ m^2$$
$$lb_i \leq x_i \leq ub_i, i \in \{1, \dots 10\}$$

where

$f_1(x)$	Amount of imported district heat (MWh)
$f_2(x)$	Levelized cost of energy (€/MWh)
$H(x)$	Limit for area that PV panels can be installed (m²)
lb_i	Lower bounds for decision variables
ub_i	Upper bounds for decision variables
x_i	Decision variables, introduced in Table 6.

In optimization, the population size was set to 30 and the number of generations was 150. Population size means the number of simulation cases that are calculated to form one generation of results. Number of generations means how many populations are calculated. In other words, totally 4500 different cases was simulated and final results i.e. the Pareto front was formed based on results of last generations. (Introduction to Genetic Algorithms 1998). Mutation probability was set 0.125 and crossover probability 0.09. Mutation probability denotes how large share of initial data i.e. data of previous generation before starting to calculate new generation, is changed randomly. It is important that mutation probability is low enough because if mutations happen too often, the optimization changes to random search. Crossover probability means, how large share of initial data i.e. data of previous generation is copied to next generation. If crossover does not exist at all, next generation is exactly the same as previous generation. (Introduction to Genetic Algorithms 1998). Decision variables are the variables that are affecting to the objective functions. Decision variables of optimization problem in this case were related to system components and they are shown in Table 6. Decision variables were selected so that all the factors that affect significantly to the system performance or operation of the system, were selected to optimize. Minimum and maximum limits were based on previous similar type of studies and test simulations. For fluent and reasonable optimization it was necessary to define feasible minimum and maximum values instead of setting them too wide.

Buffer tank volume values were based on test simulations. Maximum value of PV capacity was related to maximum amount of PV panels that were able to install on the rooftops as discussed in chapter 3.4.2 and minimum value is set to be low enough as it was already expected that optimal PV capacity might be quite high. Optimal tilt angle of PV panels may vary depending on in which time of the year PV electricity is needed the most so wide gap was set. Heat pump capacities were based on number of heat pumps that were used in modeling. BTES volume is the total volume of BTES and the boundaries were based on test simulations and previous studies. Shape of BTES, in other words the height-to-width ratio defines how deep boreholes are with respect to width of BTES, which depends on volume and borehole density. Borehole density describes how close the boreholes are drilled to each other. The lower the thermal conductivity of the ground is, the closer boreholes are drilled to achieve a proper heat transfer. In a study examined by Hirvonen and Sirén it was noticed that number of boreholes in series was relatively low in larger scale systems as discussed in chapter 2.5. Thus same result was expected also in this study and maximum number of boreholes in series was decided to be 4. Insulation thickness minimum value was set to be 0 m as in some cases it might be not feasible to insulate the BTES at all. Maximum value was set high enough to see if higher insulation thickness will be beneficial or not.

Table 6. Decision variables of optimization process.

Decision variable	Unit	Min	Max	Description
Buffer tank volume	m^3	20	200	Volume of warm buffer tank
PV capacity	kW	40	340	Nominal PV system total capacity
PV tilt angle	°	10	80	Tilt angle of PV panels
AW-HP capacity	kW	160	960	Total thermal power of air-to-water heat pumps
WW-HP capacity	kW	30	480	Total thermal power of water-to-water heat pumps
BTES volume	m^3	50000	200000	BTES total volume
BTES shape	-	0.25	4	Height-to-width ratio of BTES
Borehole density	borehole/m^2	0.05	0.2	Number of boreholes per m^2
Boreholes in series	-	1	4	Number of boreholes connected in series
BTES insulation thickness	m	0	4	BTES top insulation layer thickness

3.9 Optional control strategy for AW-HP

PV electricity is not available all the time, even there would be a potential to utilize AW-HPs and charge the BTES with optimal conditions. For example, a night time in summer, when there is no solar radiation but the air temperature is high enough to reach a high COP with AW-HP heat generation. For that purpose grid electricity can be utilized to increase the amount of energy charged to the BTES. For optimal cases that were selected to study more detailed, two different control strategies were developed in the simulation model to find out the feasibility and potential of this kind of solution. The four optimal cases were simulated again using those new control strategies. Different control algorithm of AW-HPs was the only change that was done in simulation model i.e. any other changes to the simulation model were not done. In every simulation, PV utilization was prioritized but if PV electricity was not available and there was heat need in the tank, AW-HPs were operated with grid electricity based on outdoor air temperature. Simulations with different control strategies are named so that simulation set A is the original optimal solutions i.e. no changes were done in that set. In simulation set B the AW-HPs were operated using grid electricity, if outdoor air temperature was more than 15 °C. As presented earlier in Figure 21 in chapter 3.4.3, at 15 °C outdoor air temperature it is possible to reach COP from 3.6 to 5.5, depending on load side outlet temperature. In simulation set C the AW-HPs were operated if outdoor air temperature were more than 5 °C. With that temperature, it is possible to reach COP from 3.0 to 4.5.

In one simulation case the results indicated that the seasonal storage was charged, but there was not enough heat demand to utilize that heat in discharge period i.e. the maximum share of heat demand was covered with on-site heat energy already. To increase the utilization of on-site heat energy, simulation D was implemented for that one case only. In that simulation, DHW control was changed so that DHW were pre-heated always with on-site energy instead of heating it totally with DH in summer time as it was done in other cases.

4 Results

The results of the combined simulation and optimization are presented in this chapter. In Figure 27 is shown all results of optimization and the Pareto front which consist of mathematically equal optimal results. That denotes that no one of the Pareto optimal solutions is dominating, and thus several optimal solutions are examined more precisely to find out the differences between them. In this study, the Pareto Front consists of 93 optimal results. The optimal result with highest LCOE is marked number one in figure, and the optimal result with lowest LCOE is marked number 93 in the figure.

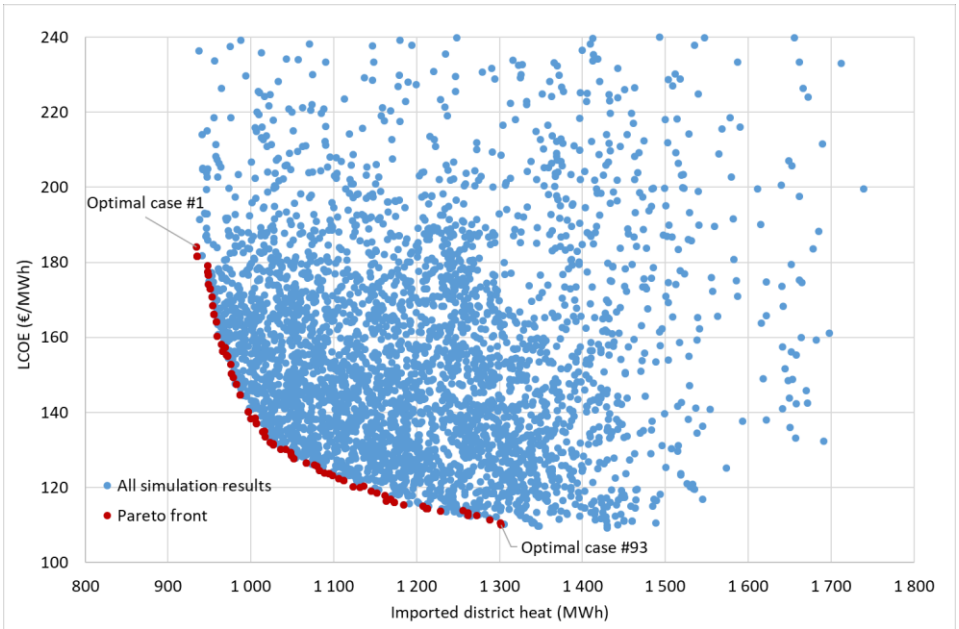

Figure 27. All optimization results (blue points) and optimal results aka. Pareto front (red points) in solution space.

4.1 Results of combined simulation and optimization

Life cycle costs and annual amount of imported district heat energy are presented in Figure 28. From the figure can be seen, that when the life cycle cost is increasing, the amount of imported district heat decreases. It indicates that with more expensive system it is possible to produce more on-site energy which decreases the need of purchased district heat. When considering on cost structure of different optimal systems, it can be noticed that price components affecting the most to the life cycle cost in most expensive solutions are AW-HP cost, seasonal storage cost and operation cost. The situation is a bit different with less expensive solutions as the PV system has more significant share of life cycle cost than cost of seasonal storage. PV system cost deviates not at all which indicates that PV capacity remains constant all the time. AW-HP cost is significantly higher than WW-HP cost in each optimal case and in general the WW-HP cost is the lowest price component in each case.

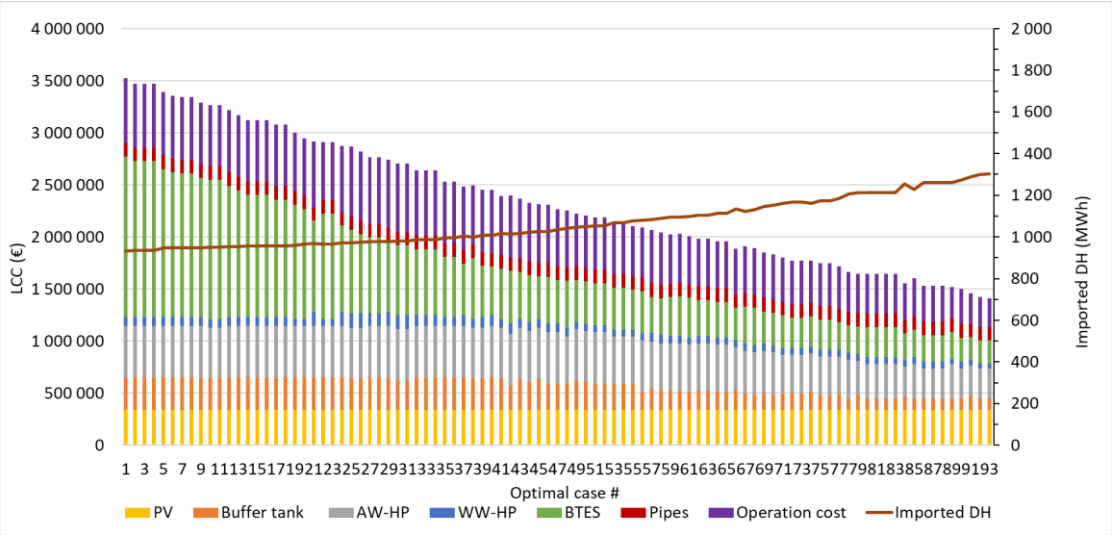

Figure 28. Life cycle costs and amount of imported district heat of all optimal solutions.

Cost structure of the seasonal storage in each optimal case is presented in Figure 29. Drilling of boreholes is the most expensive price component in most cases, but in most expensive cases the share of insulation cost is almost as high as drilling cost, or even higher in some cases. Piping and excavation of soil do not have significant impact to the total cost of seasonal storage. The difference in seasonal storage investment cost between highest and lowest cases is drastic, as the total cost in cheapest case is 217 500 € and in the most expensive case 1 543 500 €. The cheapest one costs only 14 % of the most expensive solution and the investment cost of the most expensive solution is 600 % higher than the cheapest one. Amount of imported DH is 1302 MWh in the cheapest case and 934 MWh in the most expensive case i.e. 368 MWh reduction of imported DH can be achieved which is 28 % of amount of imported DH of the cheapest case. In other words, investing 1 326 000 € more in seasonal storage, 368 MWh less imported DH is needed. When comparing to the reference case where all the heat energy demand (2 005 MWh) is covered with district heat, 35 % DH reduction is achieved in the cheapest case and 53 % DH reduction is achieved in the most expensive case. As a comparison in cheapest optimal case, with 217 500 € investment in seasonal storage it is possible to reduce amount of district heat 703 MWh when comparing to the reference case where all the heat energy is imported DH. Thus it can be stated that it is not feasible to invest in the most expensive case.

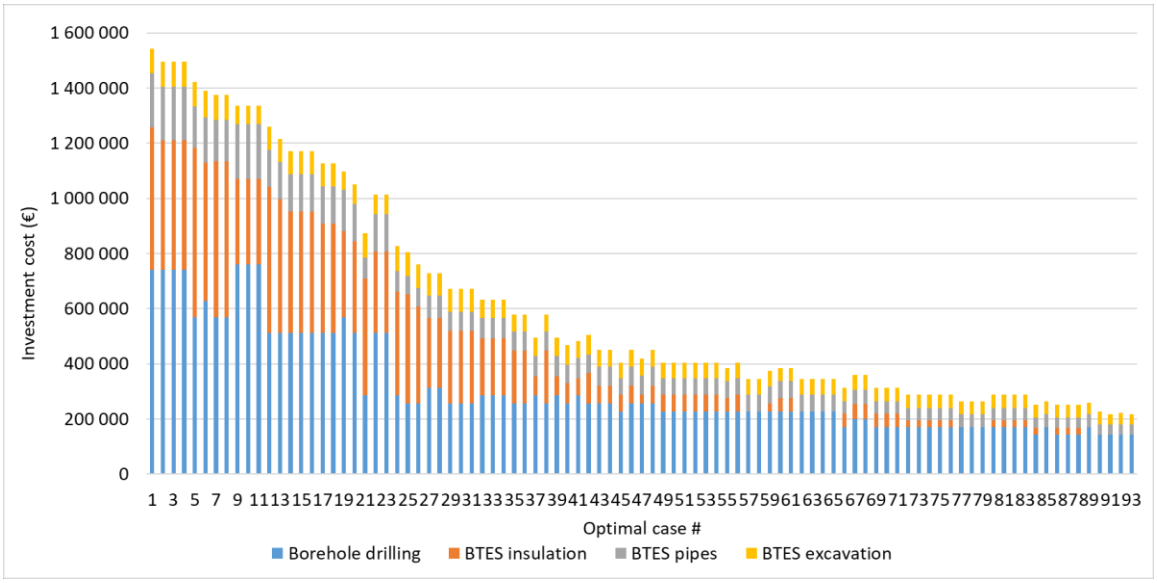

Figure 29. Cost structure of seasonal storage.

Annual heat energy distribution of all optimal solutions is presented in Figure 30. From the figure it can be noticed that increasing the share of on-site energy, also LCOE increases. To produce more on-site energy, the system size i.e. volume of BTES, number of heat pumps etc. are larger, and also operation costs are higher due to higher electricity consumption of heat pumps. This indicates that when increasing on-site heat production, the life cycle costs of the system increase that much that LCOE increases even the amount of on-site produced heat energy increases also. Another thing to notice is, that even with the most expensive and largest solution, only roughly half of the total heat energy demand can be produced on-site. Heat energy charged to the BTES consisted of AW-HP produced heat energy and condensate heat from the cooling energy production. Some share of heat energy was distributed to the buildings straight from the buffer tank i.e. not all energy was charged to the BTES. Thus exact shares of condensate and AW-HP heat energy amounts that were charged to the BTES are not available. However, the condensate from the cooling energy production transferred to the buffer tank was between 194 – 212 MWh depending on case, and heat energy produced by AW-HPs was varying between 940 – 1385 MWh. So the share of condensate was 15 – 21 % and AW-HP heat 79 – 85 % depending on case.

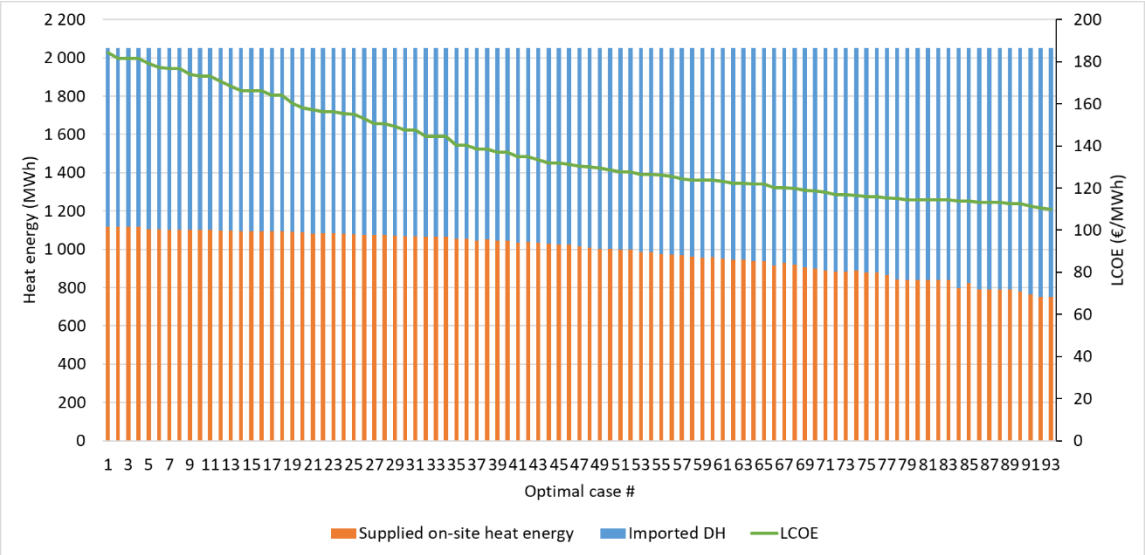

Figure 30. Annual supplied on-site heat energy, imported district heat and LCOE.

Annual PV electricity distribution of all optimal solutions is shown in Figure 31. In all cases, AW-HPs consume the largest share of PV electricity, which was the main purpose of the energy system. The interesting thing is, how small share WW-HPs get PV electricity. The reason for that is, that WW-HPs were operated mainly in winter time, when the PV electricity generation was very low due to low solar radiation. Amount of surplus electricity is higher in optimal results having lower LCOE because the size of energy system is smaller and there are not enough electricity demand (AW-HPs) to utilize all PV generated electricity. However, the optimal capacity of PV system is maximum also in those solutions as the surplus electricity was sold to the grid with market prices. This indicates that it is profitable to invest in maximum capacity of PV panels even if all electricity cannot be utilized on the site. Small differences in total PV electricity generation arise from different tilt angle (30°- 45°) of PV array as the size of PV system were largest possible in each optimal case.

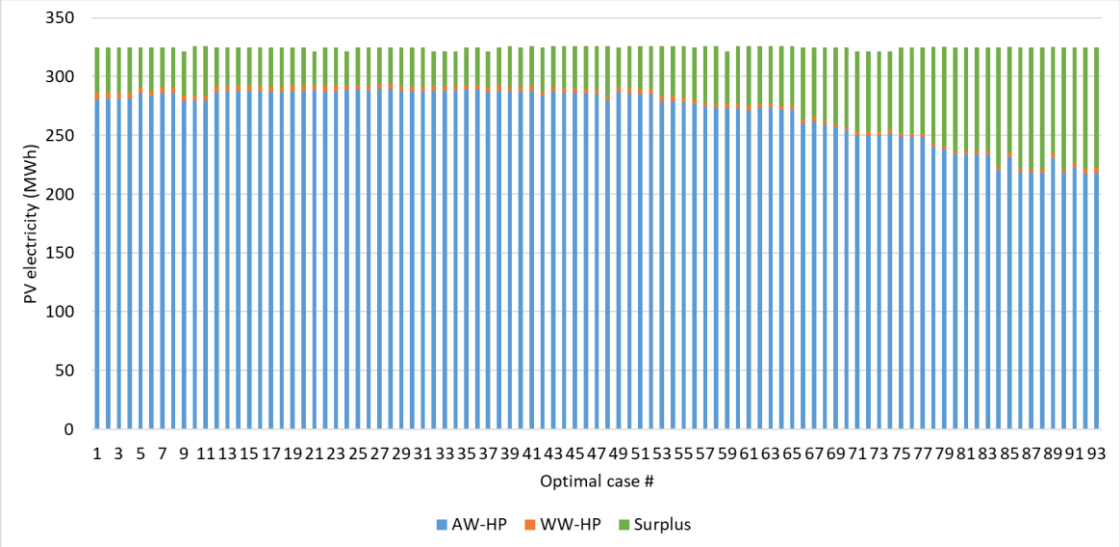

Figure 31. Annual distribution of PV electricity.

Annual efficiency of seasonal storage is presented in Figure 32. In general, the efficiencies are between 60 % and 70 %, but they are deviating depending on case. The deviation may occur due to changes in temperature level of BTES, surface-to-volume ratio as well as insulation thickness.

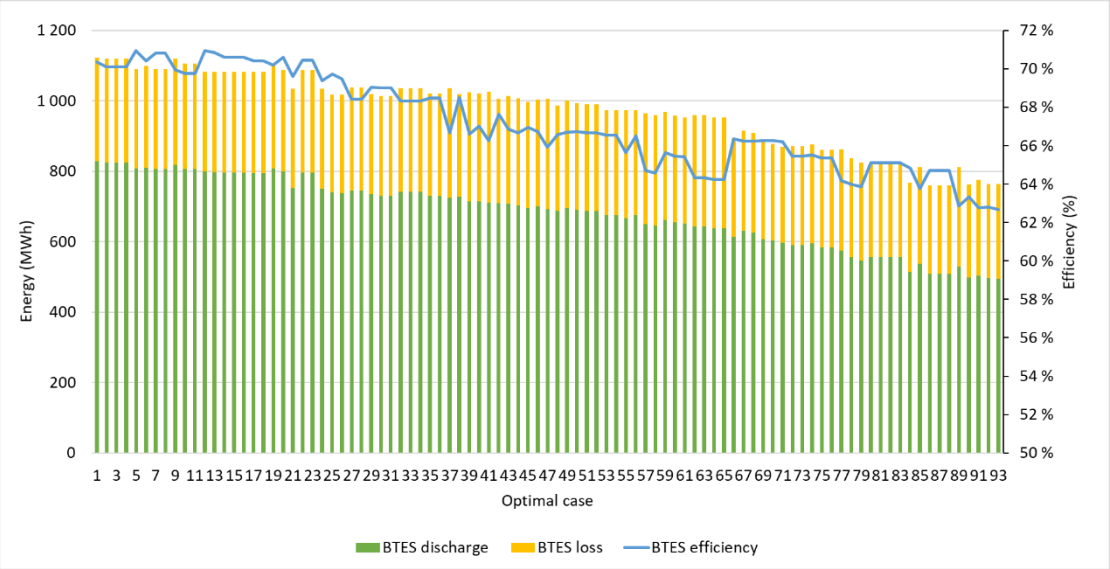

Figure 32. Efficiency of seasonal storage.

4.2 Selected optimal cases

From the group of 93 optimal solution, four different solutions were selected and analyzed in detail. The cases with highest and lowest LCOE were selected. Third selected case was one case where roughly half of total heating energy demand was covered with on-site heat energy. The fourth selected case was a case with LCOE below 120 €/MWh as the lowest LCOE of optimal solutions was 110 €/MWh. The cases were numbered so that case 1 is the case with highest LCOE. It is also the case where largest share of total heat demand was covered by on-site produced heat energy. Case number 2 is the case where half of total heat energy demand was covered with on-site energy. Case 3 is the case with LCOE below 120 €/MWh. Case 4 has a lowest LCOE and the amount of on-site produced heat energy was lowest of all optimal solutions. In Figure 33 selected optimal cases are marked into the Pareto front.

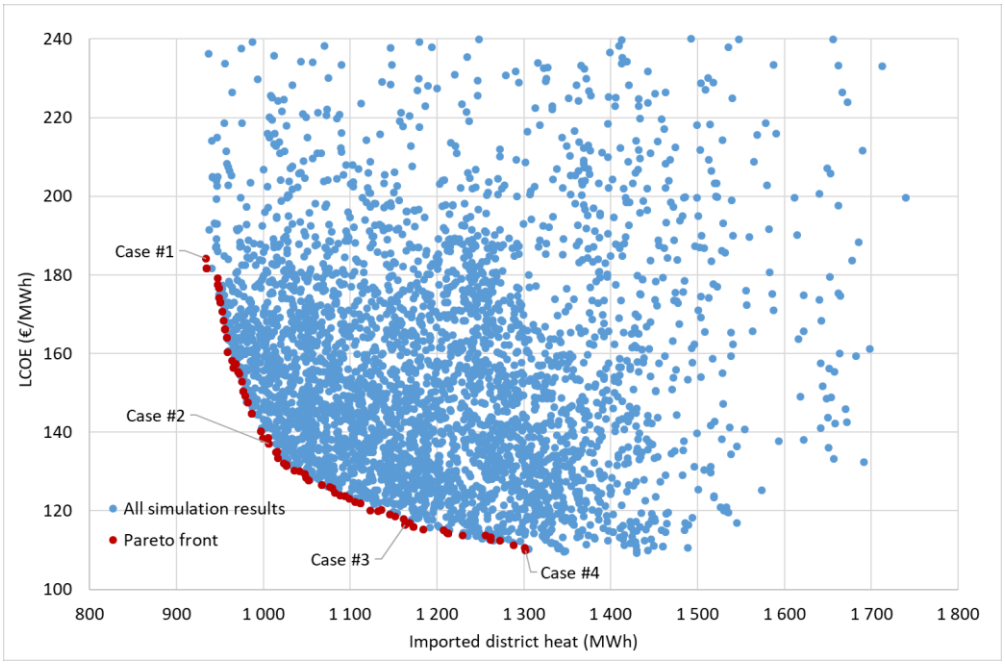

Figure 33. Pareto front and selected optimal cases.

In Figure 34 is presented life cycle costs and annual amount of imported district heat. From the cost structure of different cases it can be noticed that the changing price components are investment cost of seasonal storage, and system operation costs. The amount of imported district heat is decreasing when the life cycle cost is increasing. However, actually the difference in amount of imported DH between cases 1 and 4 is quite small, roughly 300 MWh as the life cycle costs are roughly 2 000 000 € higher in case 1 than in case 4. As a comparison, in case 4 with life cycle cost 1 500 000 € it is possible to produce almost 800 MWh energy when comparing to the reference case, where all heat energy would be imported from the district heat network. In other words, it is expensive and not feasible to increase on-site energy production using the largest optimal system.

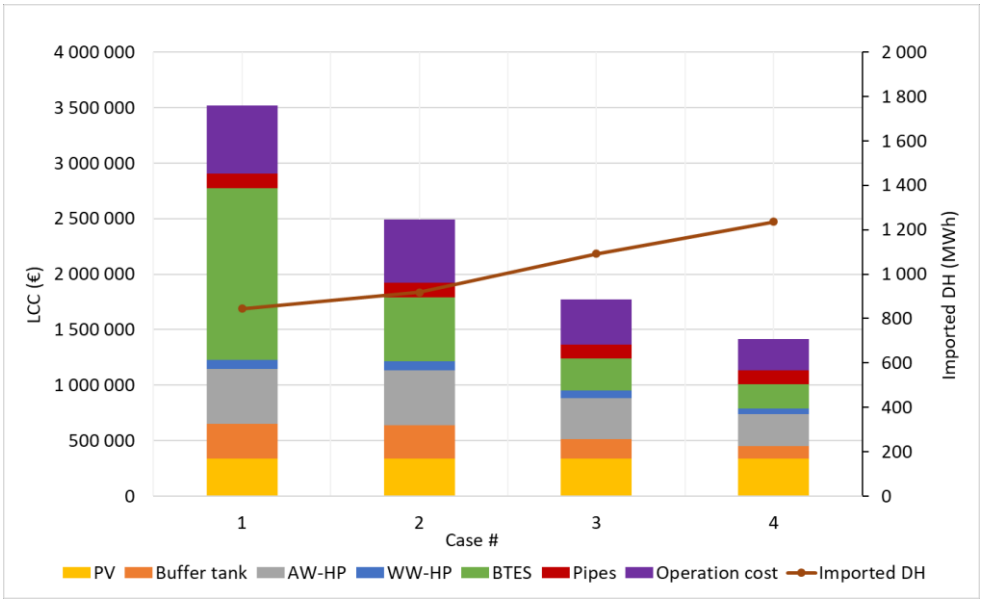

Figure 34. Life cycle costs and amount of imported district heat of selected optimal cases.

In Table 7 is shown key values of selected optimal cases. Sum of annual supplied on-site energy and annual imported district heat is the same in each case as the heating demand in the buildings remained constant on annual level. So when the amount of supplied on-site energy is increasing, amount of imported district heat is decreasing and vice versa. When comparing the share of on-site energy of total demand and renewable energy fraction (REF), it can be noticed that REF does not increase as rapidly as share of on-site energy. This is because in REF, the grid electricity needed for WW-HPs was taken into account and electricity consumption of WW-HPs increased when on-site energy production increased.

Table 7. Key values of selected optimal cases.

Parameter	Unit	1	2	3	4
LCOE	€/MWh	184	138	116	110
Annual supplied on-site energy	MWh	1 160	1 086	912	768
Annual imported district heat	MWh	844	918	1 092	1 236
On-site energy of total demand	%	54 %	51 %	43 %	37 %
Renewable Energy Fraction (REF)	%	41 %	38 %	33 %	29 %

Decision variables of selected optimal cases are shown in Table 8. In the same table is also presented properties of seasonal storage that are based on decision variables of optimization related to seasonal storage. Volumes of buffer tank and seasonal storage as well as capacity of both heat pump types are increasing when amount of supplied on-site heat energy is increasing. Thus it can be stated that the capacity of whole hybrid energy system increases when LCOE and share of on-site energy are increasing. PV capacity is maximum in all cases because the rooftop area was the limiting issue. Tilt angle of PV panels is quite low in all cases which denotes that PV electricity production was maximized in summer season. It is sensible as the aim was to maximize the charging potential of seasonal storage. The investment cost of seasonal storage was significantly higher in case 1 than in other cases, the reason for that can be seen when looking properties of seasonal storage. There are 355 boreholes in the seasonal storage of case 1 which increases the borehole drilling costs in comparison to other cases. In addition to that, the insulation layer is thick as there is 2.75 meters of insulation material.

Table 8. Properties of selected optimal cases.

Decision variable	**Unit**	**1**	**2**	**3**	**4**	**Description**
Buffer tank volume	m³	200	190	110	70	Volume of buffer tank
PV capacity	kW	340	340	340	340	Nominal PV system total capacity
PV tilt angle	°	35	35	30	35	Tilt angle of PV panels
AW-HP capacity	kW	960	960	720	560	Total thermal power of AW-HPs
Number of AW-HPs (à 16 kW)	-	60	60	45	35	Number of AW-HPs
WW-HP capacity	kW	300	300	240	180	Total thermal power of WW-HPs
Number of WW-HPs (à 60 kW)	-	5	5	4	3	Number of WW-HPs
BTES volume	m³	130 000	90 000	60 000	50 000	BTES total volume
BTES shape	-	1.0	1.25	1.25	1.5	Height-to-width ratio of BTES
Borehole density	borehole/m²	0.15	0.075	0.075	0.075	Number of boreholes per m²
Boreholes in series	-	3	1	1	1	Number of boreholes connected in series
BTES insulation thickness	m	2.75	1.5	0.25	0	BTES top insulation layer thickness
Other BTES properties	**Unit**	**1**	**2**	**3**	**4**	
Cross-sectional area	m²	2370	1600	1220	960	Cross-sectional area of BTES
Width	m	55	45	39	35	BTES width
Borehole length	m	55	56	49	52	BTES height
Number of boreholes	-	355	120	91	72	Total amount of boreholes
Total flow	kg/s	39.4	40.0	30.3	24.0	Total flow of heat transfer fluid

Detailed investment costs of selected cases are shown in Table 9.

Table 9. Investment costs of selected optimal cases.

Cost	**Unit**	**1**	**2**	**3**	**4**
Investment costs					
Buffer tank	€	314 000	298 300	172 700	109 900
PV system	€	340 200	340 200	340 200	340 200
AW-HP	€	492 000	492 000	369 000	287 000
WW-HP	€	84 000	84 000	67 200	50 400
BTES	€	1 543 500	578 900	287 700	217 600
Local heating network pipes	€	130 200	130 200	130 200	130 200
Pumps	€	10 000	10 000	10 000	10 000
Operation costs					
Imported electricity	€	539 700	521 500	398 100	299 600
Maintenance	€	101 500	67 300	48 000	39 900
Surplus PV electricity selling profit	€	22 800	18 600	38 900	61 300
Life cycle cost	**€**	**3 532 400**	**2 503 800**	**1 784 200**	**1 423 500**

Investment costs of seasonal storage are shown in Figure 35. The difference between cases 1 and 2 is significant, as only borehole drilling costs in case 1 are significantly higher than total cost of seasonal storage in case 2. The difference between cases 2-4 is more moderate.

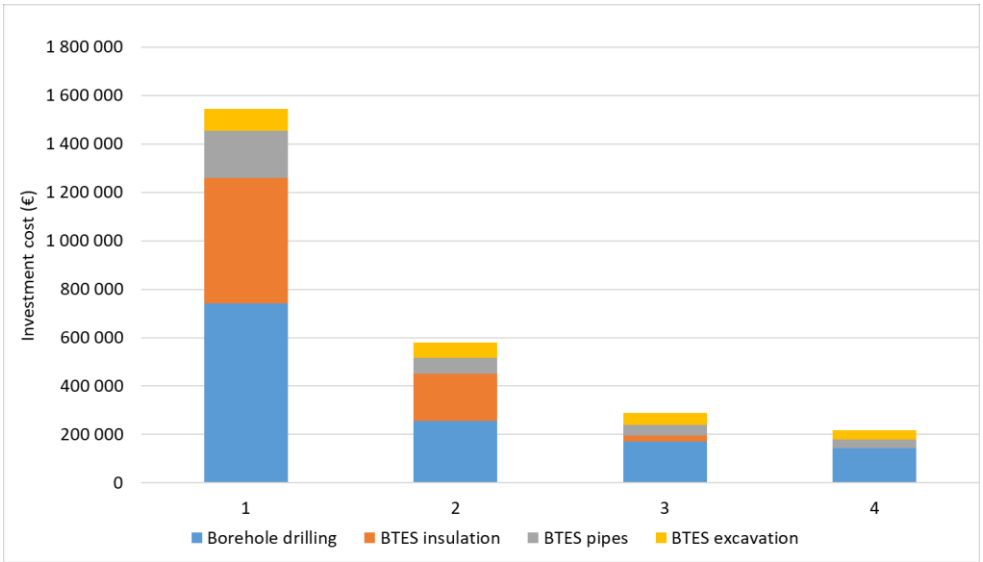

Figure 35. Seasonal storage investment costs of selected optimal cases.

In Figure 36 is presented annual heating energy distribution and LCOE of selected optimal cases. Space heating, ventilation heating and domestic hot water heating energies are separated to visualize energy distribution more detailed. Blue bars are expressing on-site energy, and green bars imported district heat. There are several notable details that can be considered. First, even the solution with lowest LCOE (4) can cover a significant share of SH demand. Secondly, even with the solution with highest LCOE (1) more than 50 % of DHW heat demand is still covered by district heat. Thirdly, the difference between case 1 and case 2 on-site energy amounts is very slight but the difference in LCOE is significant.

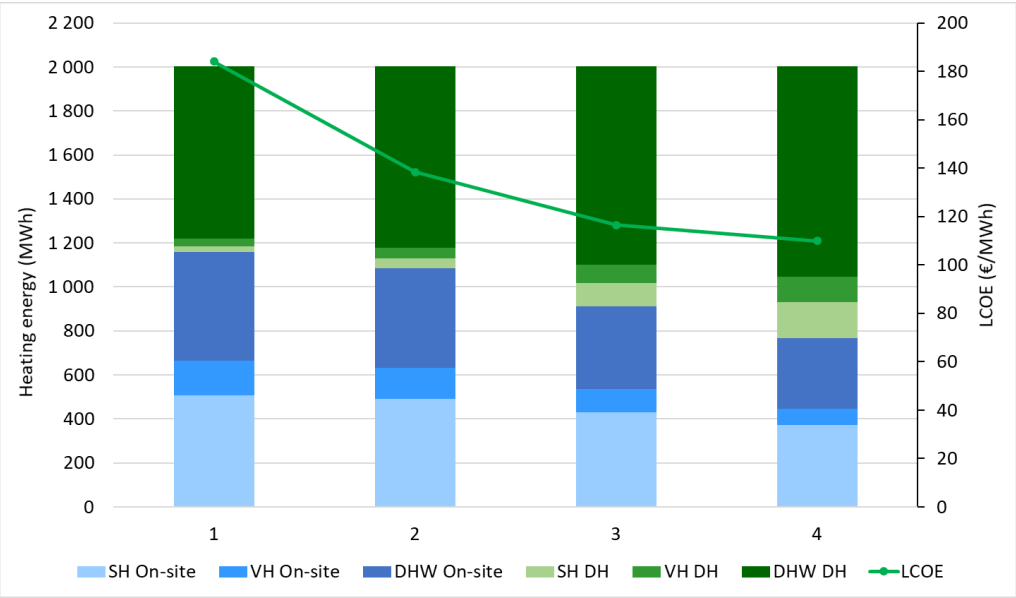

Figure 36. Life cycle heating energy distribution of selected optimal cases.

Heating energy demand and imported district heat duration curves on annual level are shown in Figure 37. The area between the heat demand duration curve and imported district heat curve defines the share of utilized on-site energy i.e. the amount decreased need of imported district heat. At the peak load hours, more than 200 kWh i.e. over 25 % of district heat consumption can be cut off utilizing on-site energy instead of district heat.

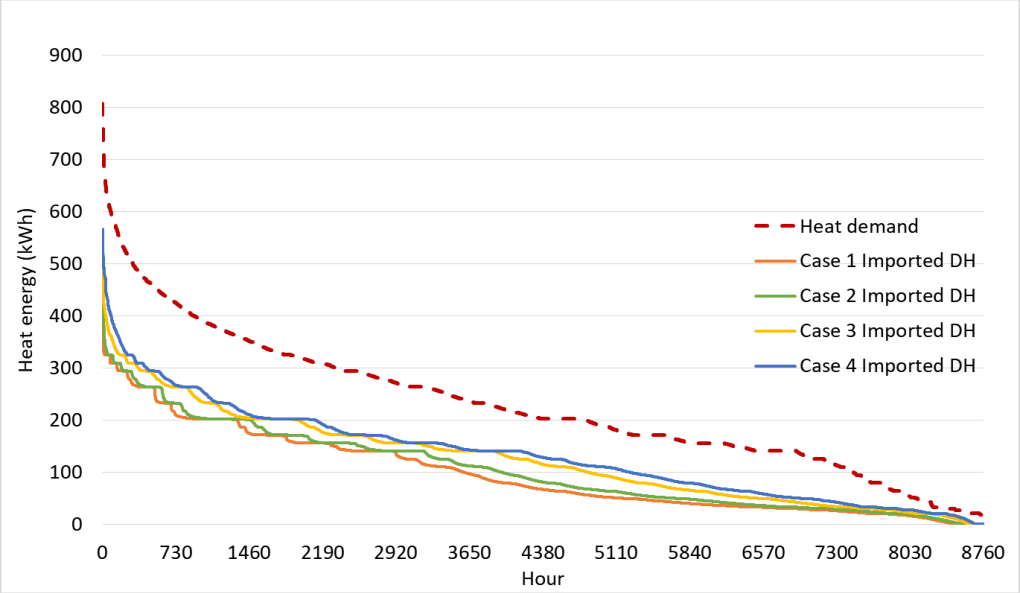

Figure 37. Heat demand and imported district heat annual duration curves of selected cases.

Efficiency of seasonal storage is presented in Figure 38. The amount of heat energy charged to the storage is sum of discharged energy and losses. As the storage capacity was the largest in case 1 and the smallest in case 4, it can be stated that efficiency of storage is increasing when the capacity of the storage is increasing which was related to decreasing surface-to-volume ratio.

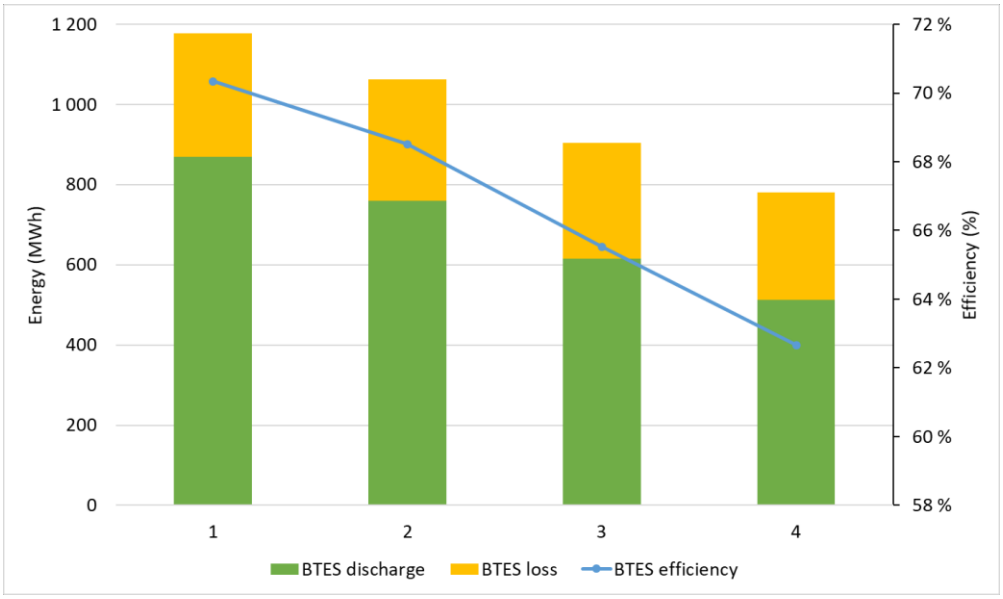

Figure 38. Seasonal storage efficiency of selected cases.

In Figure 39 is shown the temperature improvement of seasonal storage during simulation period i.e. the first four operation years. The different colored curves are presenting different selected optimal cases. First operation year differs from others the most, but there are also slight variations between second and third year. Third and fourth year are very similar to each other. In the first operation year, the seasonal storage was started to heat up from the initial temperature which was an average ground temperature 6.0 °C. For that reason, the maximum storage temperatures in first year are notably lower than later. As there were a temperature limit for discharging seasonal storage, the discharging was limited when the limit (12 °C) was reached. In the first operation year the limit was reached earlier as the maximum temperatures were lower. In addition to that, it has to be remembered that seasonal storage could not be discharged at the beginning of first year as there was not any heat energy to discharge. Thus the on-site energy production in first year differs significantly from later ones. When comparing the temperature curves of different cases, it can be stated that the larger the volume of seasonal storage is, the lower the maximum temperature is. Lower temperature level is one reason for better efficiency of larger storages in addition to better surface-to-volume ratio. Due to larger storage volume, more heat energy can be stored and thus share of on-site energy is higher with larger seasonal storage solution despite the lower temperature level.

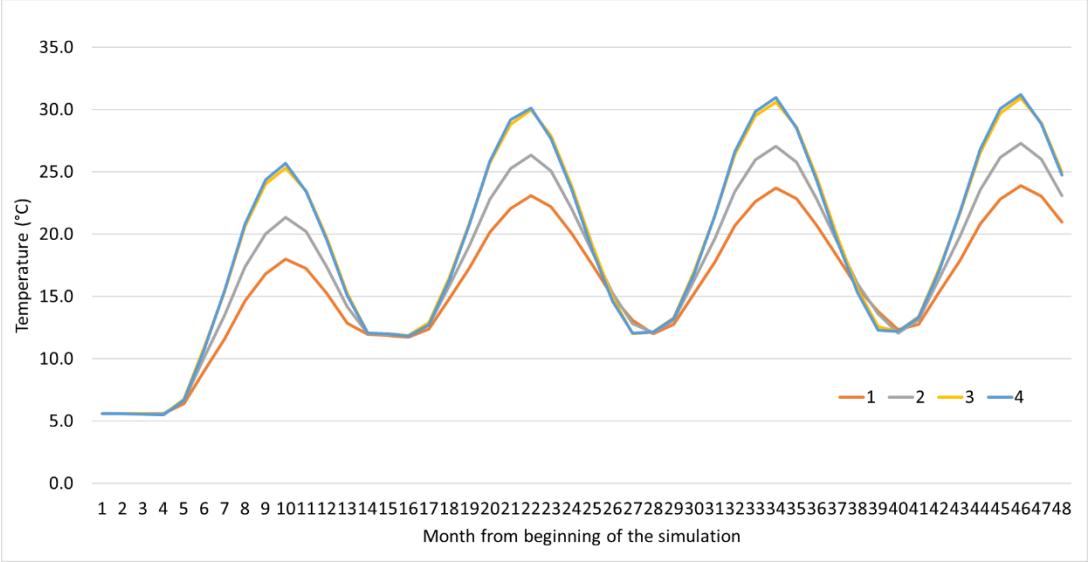

Figure 39. Development of seasonal storage temperatures in the first four operation years.

4.3 Optional control strategy for AW-HP

As an option, an alternative control strategy was developed for four selected optimal cases that were analyzed in earlier chapter. The aim was to increase the utilization rate of AW-HPs and thus increase the on-site heat energy production by using also grid electricity for AW-HPs in addition to utilize only PV electricity. To clarify the differences between different simulation cases, all simulated cases are shown in Table 10. Number 1-4 is the optimal case that were presented and analyzed in previous chapter. Letter A-D is the different simulation case which has different control strategy of AW-HP as discussed in chapter 3.9.

As the results of case 1B and 1C differed from others significantly, additional case 1D was developed. Due to large system size, almost the maximum possible share of on-site energy was reached in case 1A i.e. there were not enough demand in winter time to utilize the additional heat energy. This was mainly due to the control system, where DHW was heated up in summer time using district heat to maximize the charging potential of seasonal storage. Otherwise, the DHW heating would have been cut a large share of heat energy produced by AW-HPs and charged into buffer tank before charging it into the seasonal storage in systems that were based only on PV electricity. The difference in case 1D in comparison to all other simulation cases was that DHW was pre-heated in buffer tank year round.

Table 10. List of simulated cases

Case	Description
1A	Highest LCOE and on-site heat energy production
1B	Highest LCOE, AW-HP operated with grid electricity if PV is not available and outdoor air temperature exceeds 15 °C
1C	Lowest LCOE, AW-HP operated with grid electricity if PV is not available and outdoor air temperature exceeds 5 °C
1D	Highest LCOE, AW-HP operated with grid electricity if PV is not available and outdoor air temperature exceeds 5 °C, DHW pre-heated with on-site energy year round
2A	On-site energy covers half of the total heat demand
2B	On-site energy covers half of the total heat demand, AW-HP operated with grid electricity if PV is not available and outdoor air temperature exceeds 15 °C
2C	On-site energy covers half of the total heat demand, AW-HP operated with grid electricity if PV is not available and outdoor air temperature exceeds 5 °C
3A	LCOE below 120 €/MWh
3B	LCOE below 120 €/MWh, AW-HP operated with grid electricity if PV is not available and outdoor air temperature exceeds 15 °C
3C	LCOE below 120 €/MWh, AW-HP operated with grid electricity if PV is not available and outdoor air temperature exceeds 5 °C
4A	Lowest LCOE and on-site heat energy production
4B	Lowest LCOE, AW-HP operated with grid electricity if PV is not available and outdoor air temperature exceeds 15 °C
4C	Lowest LCOE, AW-HP operated with grid electricity if PV is not available and outdoor air temperature exceeds 5 °C

In Figure 40 is presented the life cycle costs and annual amount of imported district heat of simulated cases. It was assumed that different control logics do not need additional investments, so investment costs did not change. The only changing price component was operation cost as the grid electricity consumption increased. This was not only because AW-HPs were operated with grid electricity, but also due to increased operation of WW-HPs in winter time as there was more heat energy in the seasonal storage. In addition to that, the profit from surplus PV electricity that was sold to the grid was varying due to different control logics. It can be noticed from the figure, that each simulation B and C decreases the amount of imported district heat i.e. the share of on-site energy is increasing which was the purpose. The change is more significant with smaller scale systems (3 and 4). In case 2 the change is a bit lower than in 3 and 4, but the lowest the change is in case 1 which was also the largest scale system. When comparing increase of operation cost and decrease of imported DH, the correlation between them looks reasonable in cases 2, 3 and 4. In case 1, operation costs are

increasing significantly, but there is relatively small decrease in amount of imported district heat. Thus the additional simulation D was developed as explained earlier. As can be seen, the change in imported DH between 1C and 1D is drastic, even though the operation cost increases only a little.

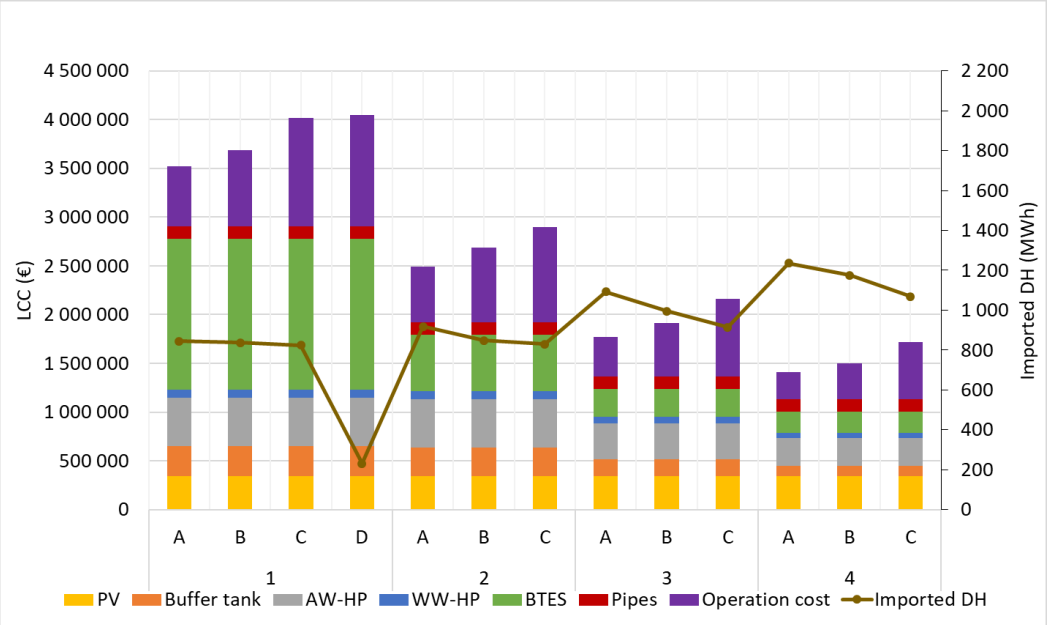

Figure 40. Life cycle costs and amount of imported district heat of simulated cases.

4.3.1 Annual energy distribution

Annual heat energy distribution and LCOE are shown in Figure 41. Common in cases 2, 3 and 4 is that when grid electricity is used for the AW-HPs, the share of on-site energy increases but there are not significant changes in LCOE. Cases 1A-1C differs from others notably as the share of on-site energy seems to be remaining the same though the grid electricity is used for additional charging of the seasonal storage. This is because all the demand that is possible to cover with on-site energy, is already covered in case 1A. In other words, there is no need to charge more energy to the seasonal storage as there is not any use for it. Thus the control system of DHW was modified so that in case 1D the DHW was pre-heated always instead of heating it totally with DH in summer time. From the figure it can be noticed that the change is significant. The share of on-site energy increases drastically and LCOE drops down in comparison to optimal case 1A.

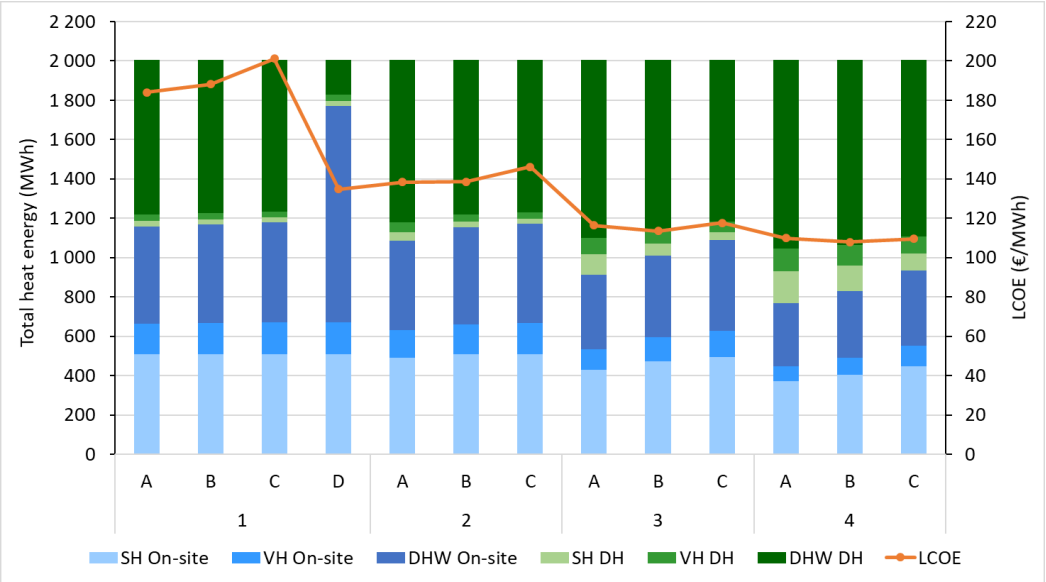

Figure 41. Annual heat energy distribution and LCOE.

Numerical values of annual supplied on-site energy, imported district heat, share of on-site energy of total demand and REF of simulated cases are presented in Table 11. As noticed earlier, the most significant change is in case 1D where the DHW was pre-heated year-round utilizing on-site energy. Notable thing is, that even though the share of on-site energy is increasing significantly and being near 90 % of total heat demand, REF does not increase that much as it is 57 %. This is because more grid electricity was used which increases the total amount of imported energy and thus slows the increase of REF. In cases 2B and 3B it is possible to slightly decrease the LCOE by utilizing grid electricity for additional charging of seasonal storage. The main reason for this LCOE decrease is the good effectiveness of AW-HPs as in simulation set B they were operated with grid electricity when outdoor air temperature was 15 °C or higher. At that high temperatures, the COP of AW-HP was on very effective level as explained in 3.4.3 and thus more heat energy was possible to generate with same amount of electricity.

Table 11. LCOE, supplied on-site energy, imported district heat and REF of simulated cases.

	LCOE €/MWh	Total supplied on-site energy MWh	Total imported district heat MWh	On-site energy of total demand %	Renewable Energy Fraction (REF) %
1A	184	1160	844	58 %	41 %
1B	188	1167	837	58 %	38 %
1C	201	1179	824	59 %	29 %
1D	135	1773	231	88 %	57 %
2A	138	1086	918	54 %	38 %
2B	139	1155	849	58 %	37 %
2C	146	1173	830	59 %	31 %
3A	116	912	1092	45 %	33 %
3B	114	1009	995	50 %	34 %
3C	118	1089	915	54 %	31 %
4A	110	768	1236	38 %	29 %
4B	108	829	1175	41 %	30 %
4C	110	935	1068	47 %	28 %

Annual distribution of PV electricity is presented in Figure 42. The main trend between different simulation sets A, B, C is that when grid electricity is used for AW-HPs, the utilization of PV electricity by AW-HPs is decreasing. The change is more slight when comparing A and B, and more significant when comparing A and C or B and C. The only exception is 1B, as the share of PV electricity utilized by AW-HPs is increasing slightly in comparison to 1A. The reason for decreasing PV electricity utilization is, that AW-HPs were using grid electricity always when there was a heat demand in the tank and outdoor air temperature was at suitable level. This may cause the situation where AW-HPs are operated and tank is charged using grid electricity, and after some time when there is PV electricity available, there is no need to operate AW-HPs as the tank temperature is high enough. The difference between simulations A and B is small as the grid electricity operation time is shorter due to higher outdoor air temperature limit, but the change is more significant between simulations B and C thus the grid electricity operation period is longer due to lower outdoor air temperature limit.

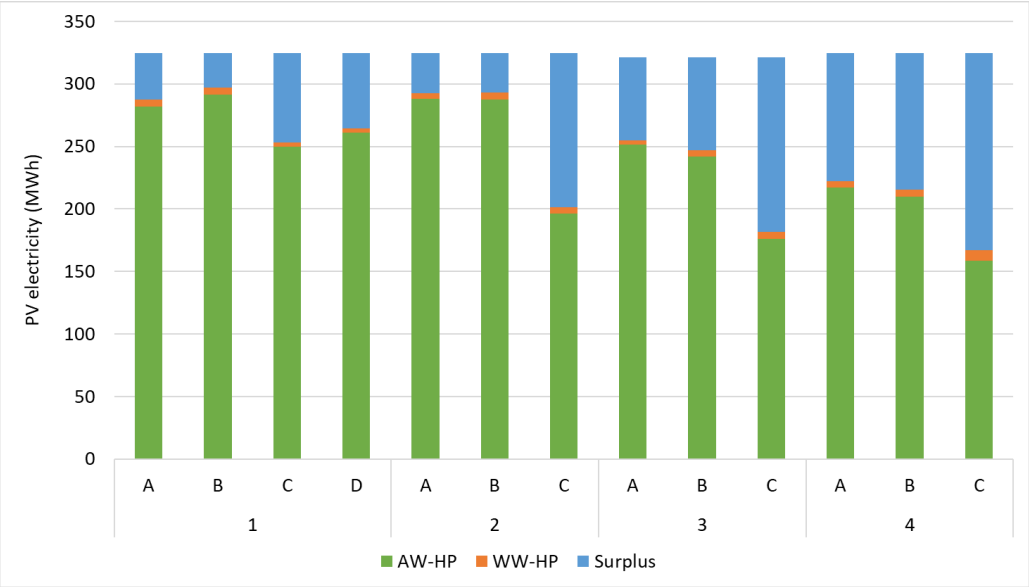

Figure 42. Annual PV electricity distribution.

Numerical values of annual PV and grid electricity consumption of heat pumps and amount of PV surplus electricity are presented in Table 12. Optimal cases i.e. the reference cases are marked with blue color, and case 1D differing from other optional simulation cases is marked yellow. The main observations that can be done are related to changes in grid electricity consumptions of AW-HP and also WW-HP. In all cases 1-4, AW-HP grid electricity consumption increases more between B and C than between A and B. The reason is that in C AW-HPs were operated more often than in B. The increase of grid electricity is also higher when the system is larger i.e. seasonal storage capacity is larger as well as the AW-HP capacity.

When considering on WW-HP grid electricity consumption, it is interesting to notice that it is actually decreasing between cases 1A, 1B and 1C. The reason for that is that maximum temperature of seasonal storage was higher due to larger amount of energy charged there. As there was no use for that charged energy, the temperature level stayed higher which increased the COP of WW-HP. However as noticed from previous figures, it was not feasible to charge seasonal storage only to increase the temperature level as the LCOE increased. So even the WW-HP grid electricity consumption decreased in those cases, AW-HP electricity consumption increased more and thus the LCOE was higher as there were not significant changes in amount of supplied on-site energy. When looking at cases 2-4 it can be noticed that WW-HP grid electricity consumption increases when AW-HPs are used more to charge BTES. This is reasonable as it indicates that WW-HPs are operated more as there is more heat energy in seasonal storage to utilize.

Table 12. Annual electricity consumption of heat pumps and PV surplus.

	AW-HP grid electricity	AW-HP PV electricity	WW-HP grid electricity	WW-HP PV electricity	PV surplus
	MWh	MWh	MWh	MWh	MWh
1A	0	282	290	6	37
1B	96	292	274	5	28
1C	332	250	223	3	72
1D	328	261	236	3	60
2A	0	288	277	5	32
2B	87	288	290	6	31
2C	254	196	259	5	123
3A	0	252	210	3	67
3B	49	242	242	5	75
3C	186	176	255	6	140
4A	0	217	158	5	102
4B	32	210	175	5	109
4C	147	159	198	9	157

4.3.2 Seasonal storage efficiency

Efficiency of the seasonal storage in different simulation cases is shown in Figure 43 and the annual temperature variation of the seasonal storage in Figure 44. In cases 3 and 4 there is no significant changes in efficiency even though more energy is charged to the seasonal storage. Cases 1 and 2 are different as the losses are increasing and therefore the efficiency decreases. This is due to the fact that temperature of the seasonal storage increases to a high level which increases losses to the environment of the storage. In addition to that, there is no enough heat demand in discharge period so the additional heat energy charged to the storage using grid electricity cannot fully utilized. For that reason, the different control strategy in case 1D was implemented, but as can be noticed from Figure 43, the amount of discharged heat energy does not significantly change from case 1A where only PV electricity was used for charging seasonal storage. This is related to the fact that after the control strategy of DHW pre-heating was changed, in summer time the DHW was actually pre-heated in buffer tank utilizing heat energy that was produced by PV and grid electricity run AW-HPs. If this is reasonable or not, depends on whether the utilization of district heat or electricity is more preferable.

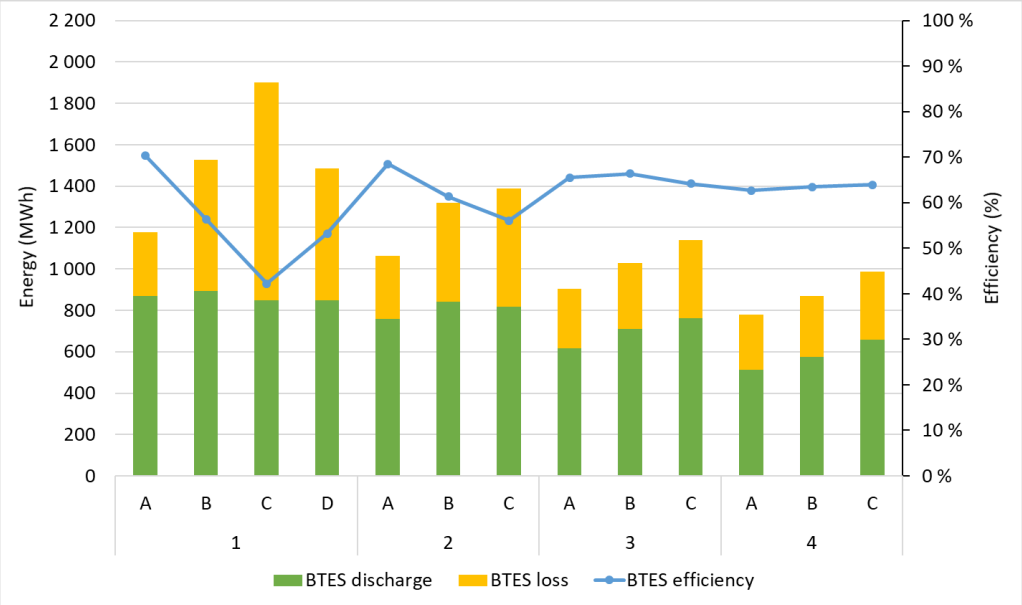

Figure 43. Annual efficiency of seasonal storage.

When looking seasonal storage temperatures in Figure 44, it can be noticed that in all optimal cases, 1A – 4A, the minimum temperature 12 °C was reached and thus discharging seasonal storage was restricted at some point of discharging period. It indicates that there is more demand to utilize on-site heat energy, but the amount of energy charged to the seasonal storage was not high enough due to limited capacity of PV system. Therefore the seasonal storage cannot be discharged more. When comparing the differences between simulation sets A and B it can be noticed that in cases 1 and 2 the limit temperature 12 °C was not reached anymore when the additional grid electricity was used to charge seasonal storage more. It indicates that the demand of on-site energy was fulfilled as there was discharging potential still left. In cases 3 and 4 the limit temperature was reached though extra charge of seasonal storage using grid electricity. It means that there was still potential to charge seasonal storage more to increase the on-site energy utilization. When considering on simulation set C of each case, it can be noticed that in case 4 the limit temperature was reached and thus all heat energy that was possible to discharge from the seasonal storage is discharged and utilized. In case 3 the limit temperature was quite close but it was not reached exactly which indicates that all demand that was possible to cover with on-site energy was covered. In cases 1 and 2 the minimum temperature was relatively high which denotes that the seasonal storage was charged unnecessarily much as there was not significant benefit of higher storage temperatures.

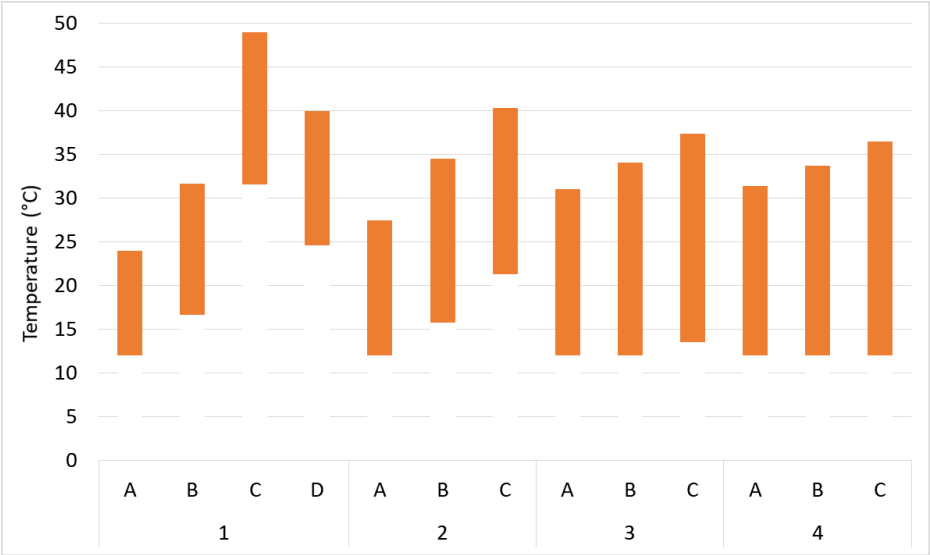

Figure 44. Annual temperature variation of seasonal storage.

4.3.3 Performance of heat pumps

Calculated COPs of AW-HPs based on annual heat production and electricity consumption are presented in Figure 45. In general, COP seems to be at feasible level in all cases which is important to achieve a desirable system performance. The COP curves of each case are decreasing when more grid electricity is used. This is due to the fact that AW-HP operation was based on outdoor air temperature in simulation sets B and C as well as simulation D. The higher the outdoor air temperature is, the higher the COP is. The reason why COP is the highest in optimal cases A where only PV electricity was utilized for AW-HPs is that solar radiation correlates with outdoor air temperature at least in summer time quite much. As the AW-HPs were operated only when solar radiation existed, COP is at high level. Even the minimum outdoor temperature to allow AW-HPs to operate in simulation set B was relatively high, 15 °C, COPs are lower when comparing to simulation set A.

When considering on differences between each case 1-4, it can be noticed that in case 1 the COP is significantly higher than in other cases. The reason for that is that volume of seasonal storage is notably higher than in other cases which denotes that it can be charged more and therefore the buffer tank temperature remains lower. Thus load side fluid outlet temperature of AW-HPs can be lower which improves the COP. The same affect can be seen in 1D where COP increases in comparison to simulation 1C. As DHW was pre-heated in buffer tank in summer time also, the tank temperature remains lower which improves the COP. In cases 2-4, COP is almost at same level in same simulation sets which indicates that AW-HPs operate similarly in those cases.

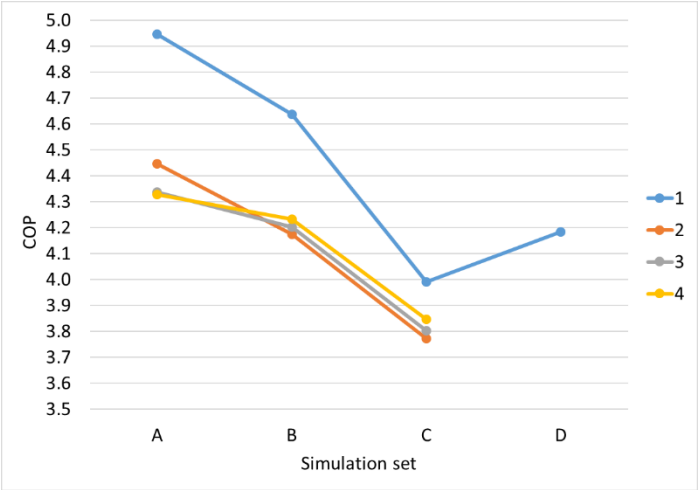

Figure 45. COPs of AW-HPs.

Calculated COPs of WW-HPs based on annual heat production and electricity consumption are presented in Figure 46. When comparing cases 1-4, it can be noticed that COP is varying in each case. When looking at different simulation sets of each case, it can be seen that in cases 3 and 4 there is a very small variation in COP as it stays nearly constant between different simulation sets. In cases 1 and 2 there is much more variation between different simulation sets and the changes are most significant in case 1. Changes in COPs of WW-HPs are related to temperatures of seasonal storage as WW-HPs used seasonal storage as a heat source. The higher the temperature of source side of WW-HP is, the better COP can be achieved as less electricity is needed to reach the same load side outlet temperature. As the temperature of seasonal storage was increasing notably in cases 1 and 2 when AW-HPs were operated also with grid electricity, COP of WW-HPs is increasing due to higher inlet temperature of source side of WW-HPs. In addition to that, the COP of WW-HPs depend also the load side temperature, and the lower the load side outlet fluid temperature is, the better COP can be achieved.

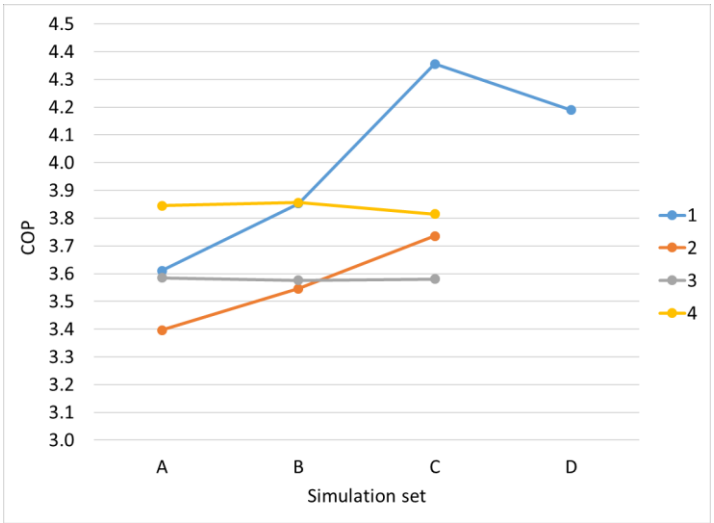

Figure 46. COPs of WW-HPs.

4.3.4 Heating duration curves

Annual duration curves of each optimal case 1-4 are presented in Figures 47 - 50. In each figure, red dashed curve is the total heat demand duration curve. Other duration curves marked with different colors are amounts of imported district heat. The area between the demand curve and other curves is the amount of supplied on-site heating energy which denotes the same as how large is the potential to decrease imported district heat. The area below imported DH curves is the amount of imported DH. From the figures it can be seen that there is a significant potential to decrease the imported DH in peak demand period. Depending on case, during the peak demand hours amount of imported DH energy can be reduced at least 200 kW (case 4) and almost 400 kW (case 1) even in base cases (A) where AW-HPs were operated only with PV electricity. The most radical decrease of consumption of imported DH was achieved in case 1D which can be seen also in Figure 47. At the peak load there is more than 600 kW decrease in need of imported DH and almost through the year the decrease potential is significant.

At base load period there is quite constant potential to decrease the consumption of imported DH, being roughly from 100 kW to 200 kW in base cases during most time of the year and from 100 kW to 300 kW in optional cases (B-D)

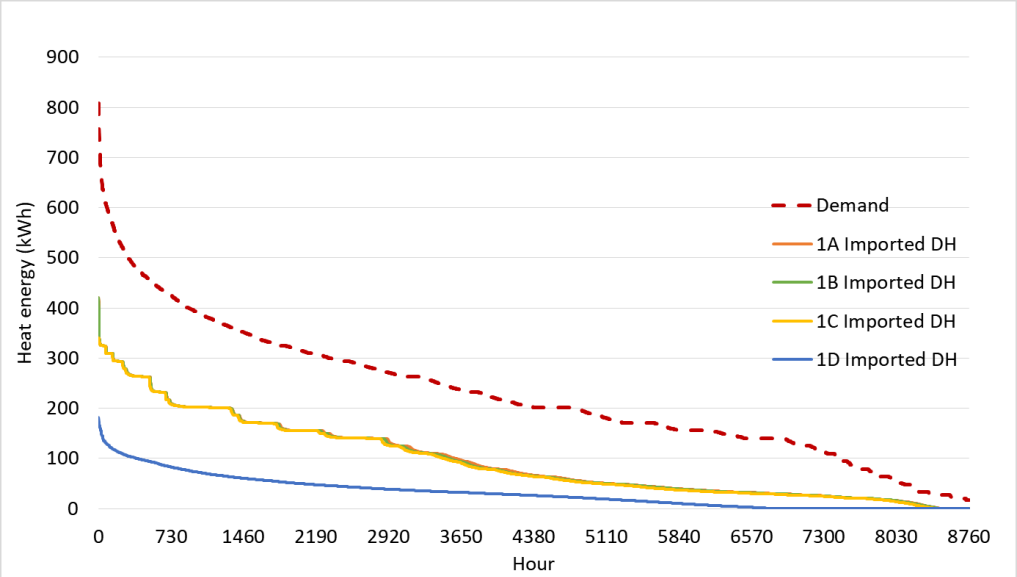

Figure 47. Duration curves of case 1

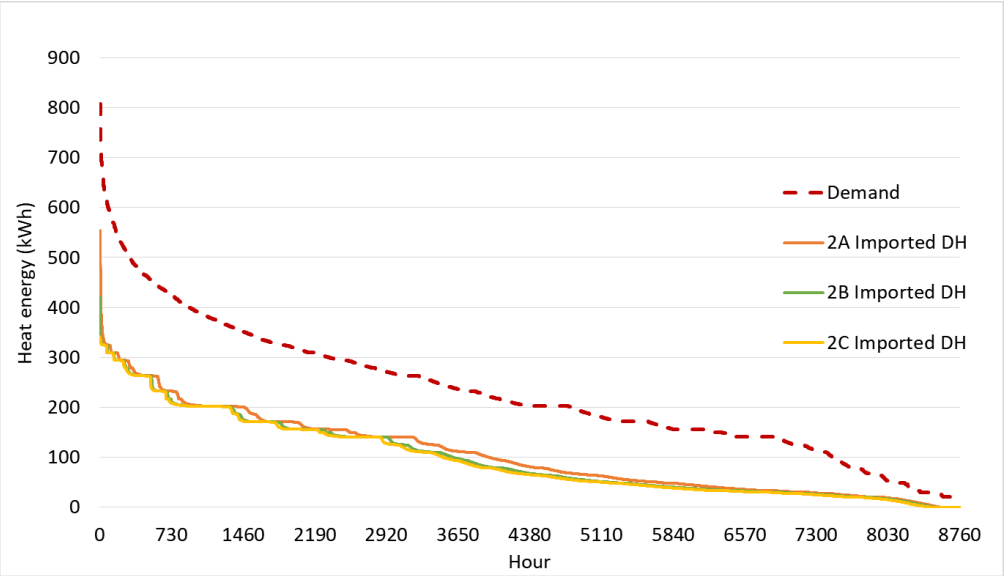

Figure 48. Duration curves of case 2.

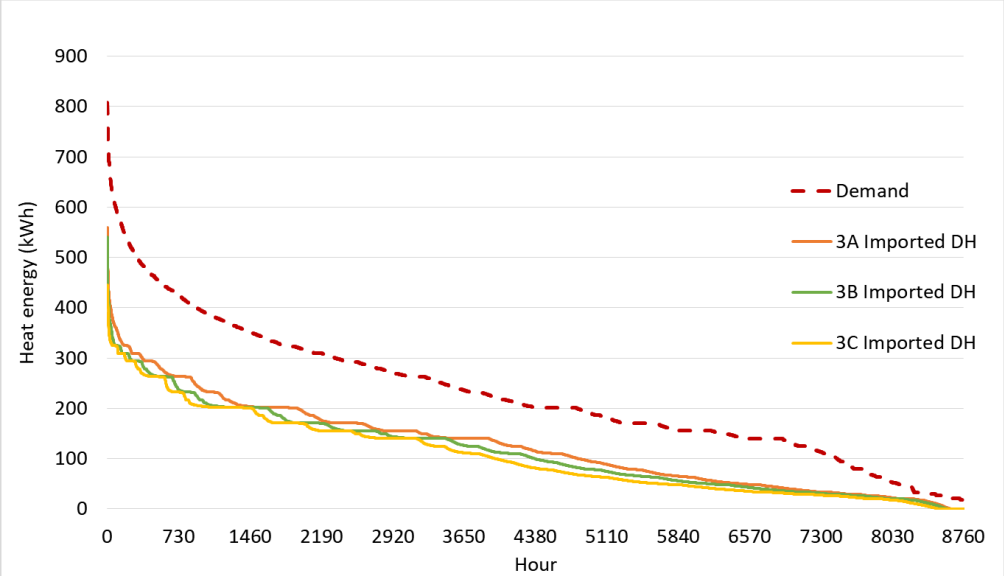

Figure 49. Duration curves of case 3.

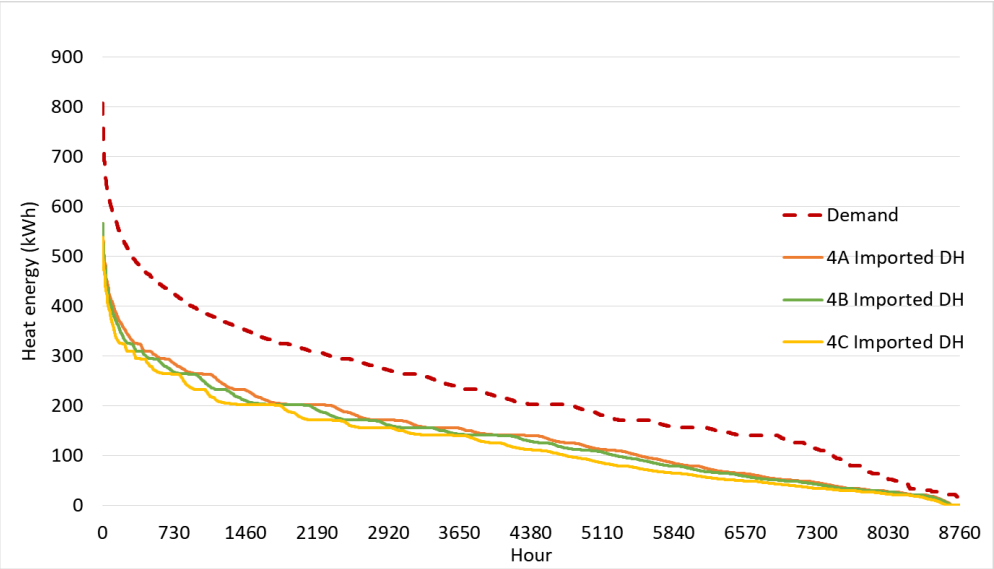

Figure 50. Duration curves of case 4.

4.3.5 Heating energy distribution in monthly level

Monthly heat energy distribution in cases 3A and 3C are presented in Figure 51 and Figure 52 and monthly level seasonal storage charge and discharge of cases 3A and 3C can be seen in Figure 53. All values are from 4th operation year which is also similar to further operation years. As the case 3 was feasible both in optimal case and also in the case where grid electricity was used for AW-HPs it is sensible to analyze that case on a monthly level. When looking at case 3A in Figure 51 it can be noticed that during the months that the heat demand is the highest, the share of on-site energy of total demand is higher than lower demand months. In other words, the on-site energy is utilized when heat demand is highest to cut off the need of imported DH which was the aim of the local hybrid energy system. The small shares of DH used for SH and VH might have been occured due to inlet temperature of SH and VH has not been high enough and for that reason the DH was needed as a backup.

However, in March the share of on-site energy seems to be lowering and when looking Figure 53, it can be noticed that amount of energy discharged from seasonal storage is very small. This is because the maximum amount of energy is discharged and temperature limit was reached and thus discharge of seasonal storage was not allowed anymore to conserve the energy balance. In April, seasonal storage is not discharged at all, but despite that on-site energy is utilized. This is because there were PV electricity available for AW-HPs and they were operating and producing heat energy which was transferred directly to the local network instead of charging it to the seasonal storage. From May to September the heat demand consists mainly of DHW heating demand. During these months DHW was heated using district heat to maximize charging potential of seasonal storage to utilize more on-site energy in winter time instead of summer.

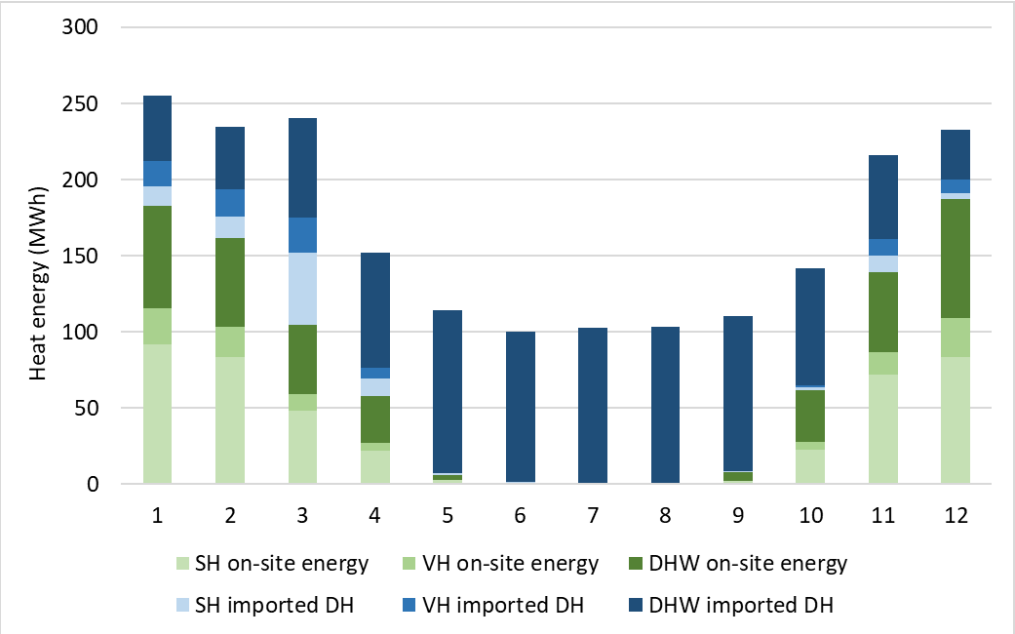

Figure 51. Monthly heat energy distribution in case 3A.

When considering case 3C presented in Figure 52 and comparing it to the case 3A, some observations can be done. The share of on-site energy is almost same from October to December and from January to February, even the share of on-site energy is slightly higher in those months too. The greatest difference can be seen in March and April as the share of on-site energy is significantly higher in 3C than in case 3A. When looking at seasonal storage discharge in March and April in case 3C it can be seen that much more heat energy is discharged at that time. So utilizing grid electricity to charge seasonal storage in addition to using only PV electricity, on-site energy can be also utilized at the end of heating season.

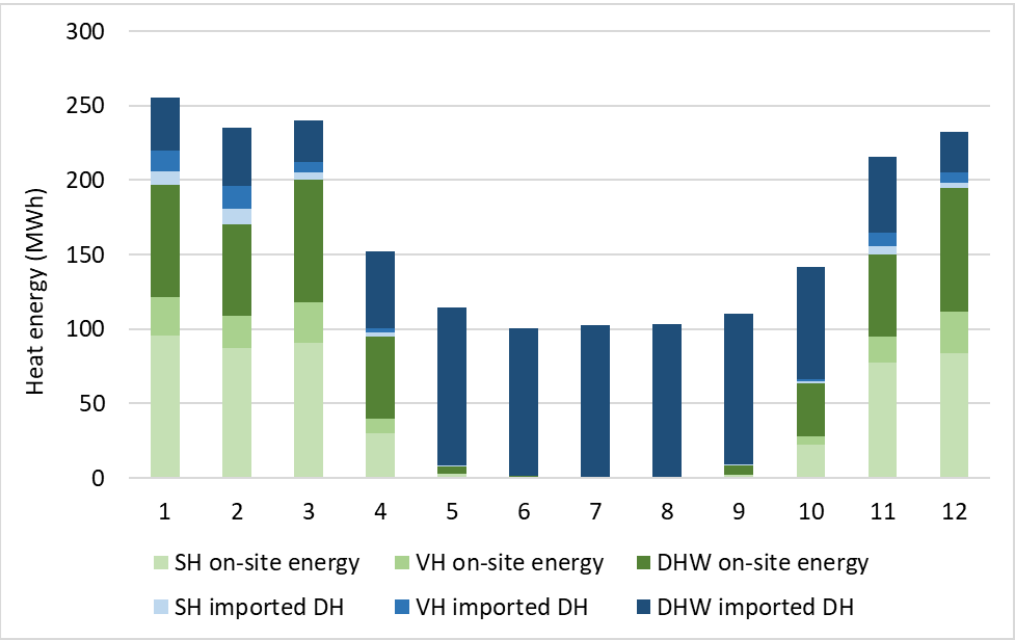

Figure 52. Monthly heat energy distribution in case 3C.

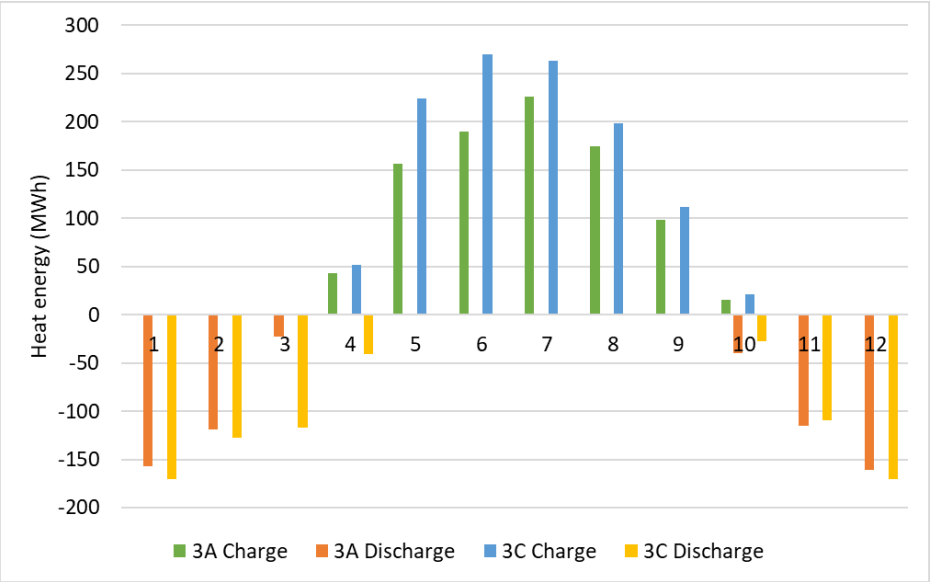

Figure 53. Monthly seasonal storage charge and discharge in cases 3A and 3C.

4.4 Possible changes in costs

Investment costs and operation costs of this kind of large hybrid energy system may vary depending on several issues, like type and manufacturer of heat pumps, borehole drilling technology, buffer tank type and form of installation. Improving technologies may also lower the costs as cutting-edge technology becomes more common. Also electricity price may change. Due to these reasons, it was reasonable to make a sensitivity analysis related to costs changes and see how changing costs affect to the feasibility of system i.e. LCOE. The selected price components to research were borehole drilling cost, AW-HP cost, PV system cost and tank cost. Borehole drilling cost was selected as it is significant part of BTES investment and if the drilling technology is developing, the costs may decrease. AW-HP cost was selected as it is significant part of total investment. AW-HPs used in this study were consumer products with relatively low heating capacity per appliance. If larger scale AW-HPs are utilized instead of consumer products, the investment cost may decrease. In past years PV system costs have been decreased as the PV panels have become more common and thus they were selected also to sensitivity analysis. As the tank cost was a bit rough and possibly overestimated because detailed cost structure of that kind of tank excavated to the ground was not found, it is necessary to see how lower tank cost affects to the LCOE.

In the modeled local hybrid energy system, grid electricity was used at least for WW-HPs, and also for AW-HPs in some cases. Therefore electricity is a vital component of the system and thus the electricity price changes are interesting to analyze. The important thing in electricity calculations is, that increasing electricity price increases the profit that is earned from selling surplus PV electricity to the grid. In electricity price sensitivity analysis only energy price was considered i.e. distribution cost and electricity tax remained the same. Also maintenance costs of system were difficult to estimate as this kind of hybrid energy system has not been implemented earlier. Therefore the higher maintenance costs and effect to the LCOE is important to see. All cost changes were decided to be drastic to find out what kind of effect they cause to the LCOE. Results of investment cost changes are shown in Table 13 and results of operation cost changes can be seen in Table 14.

In Table 13 is presented initial LCOE and LCOE after cost changes. Change of LCOE is also shown in percentage. Borehole drilling cost was the highest price component of BTES investment and on the other hand BTES investment was highest price component of total investment of hybrid energy system. Thus halved drilling cost affects to the LCOE significantly. The difference in LCOE is highest in case 1 as there were the largest BTES with highest amount of boreholes. 50 % decrease in AW-HP investment cost decreases LCOE from 6% to 10% depending on how large share AW-HP cost is of total investment. PV system was higher price component in solutions with lower total investment cost due to there was maximum PV capacity in each case. Thus LCOE is decreasing significantly more in cases 3 and 4 when comparing to cases 1 and 2. Tank cost change does not affect very much to LCOE but as seen in Figure 28 in chapter 4.1, tank is not so large price component as BTES or AW-HPs and on the other hand estimated cost reduction is smaller than others.

Table 13. Investment cost changes and affect to the LCOE.

	Initial LCOE	Borehole drilling cost decreases 50 %		AW-HP cost decreases 50 %		PV system cost decreases 50 %		Tank cost is 25 % lower	
	€	LCOE (€)	Difference	LCOE (€)	Difference	LCOE (€)	Difference	LCOE (€)	Difference
1A	184	165	-10 %	171	-7 %	175	-5 %	180	-2 %
1B	188	169	-10 %	176	-7 %	180	-5 %	184	-2 %
1C	201	183	-9 %	189	-6 %	193	-4 %	197	-2 %
1D	135	122	-9 %	127	-6 %	129	-4 %	132	-2 %
2A	138	131	-5 %	125	-10 %	129	-7 %	134	-3 %
2B	139	132	-5 %	126	-9 %	130	-6 %	135	-3 %
2C	146	140	-4 %	134	-8 %	138	-6 %	142	-3 %
3A	116	111	-5 %	104	-10 %	105	-10 %	114	-2 %
3B	114	109	-4 %	103	-10 %	104	-9 %	111	-2 %
3C	118	113	-4 %	108	-9 %	108	-8 %	115	-2 %
4A	110	104	-5 %	99	-10 %	97	-12 %	108	-2 %
4B	108	103	-5 %	98	-9 %	96	-11 %	106	-2 %
4C	110	105	-4 %	101	-8 %	99	-10 %	108	-2 %

In Table 14 is shown changes of operation costs and their affect to the LCOE. If electricity cost increases 50 %, the effect to the LCOE is not so significant in simulation set A where grid electricity was used only for WW-HPs. The effect is slightly higher in simulation sets B and C and simulation D where grid electricity was used for AW-HPs and thus the total electricity consumption was higher than in simulation set A. 100 % increase of electricity price is quite drastic and that kind of price increase is perhaps improbable in real life. 200 % increase of maintenance cost is increasing LCOE from 4% to 6% so it can be stated that the effect is quite moderate.

Table 14. Operation cost changes and affect to the LCOE.

	Initial LCOE	Electricity cost increases 50 %		Electricity cost increases 100 %		Maintenance cost is 200 % higher	
	€	LCOE (€)	Difference	LCOE (€)	Difference	LCOE (€)	Difference
1A	184	190	3 %	195	6 %	195	6 %
1B	188	195	4 %	203	8 %	199	5 %
1C	201	211	5 %	221	10 %	211	5 %
1D	135	142	5 %	148	10 %	142	5 %
2A	138	144	4 %	150	8 %	146	5 %
2B	139	146	5 %	154	11 %	145	5 %
2C	146	155	6 %	163	12 %	153	5 %
3A	116	121	4 %	125	8 %	123	5 %
3B	114	119	5 %	125	10 %	119	5 %
3C	118	125	6 %	133	13 %	123	4 %
4A	110	113	2 %	115	5 %	116	6 %
4B	108	112	3 %	115	7 %	114	5 %
4C	110	115	5 %	122	11 %	115	5 %

4.5 CO_2 emissions

Annual CO_2 emissions caused by district heat consumption and electricity consumption were calculated for each case as well as emission costs and the results are shown in Figure 54. As explained in chapter 3.6.4 it can be stated that total CO_2 emission of imported electricity is the same as total CO_2 emission of on-site produced energy. The first thing to notice from the figure is that each hybrid energy solution has lower CO_2 emission than the reference case where 100 % of heating demand was covered with district heat. This is mainly due to utilization of PV electricity and heat pumps. Even the WW-HPs were operated mainly in winter time when CO_2 emissions of electricity production are at highest level of the year, the emissions of on-site energy production are significantly lower than in district heat. This is mainly due to heat pump technology and particularly efficient COPs of WW-HPs. When comparing the results of simulation set A to results of simulation sets B and C it can be noticed that it is not reasonable in all cases to use grid electricity to operate AW-HPs from emission reduction point-of-view as the total emissions of hybrid energy system are decreasing only slightly. However the case 1D is an exception because in that case total CO_2 emissions are decreasing significantly mainly due to smaller amount of imported district heat, despite of using grid electricity to run AW-HPs.

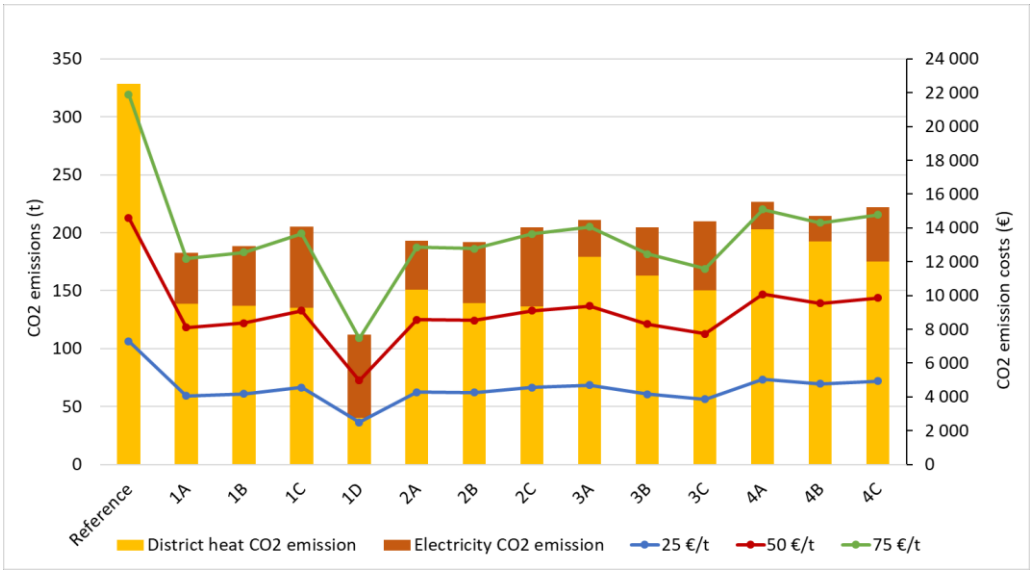

Figure 54. Annual CO_2 emissions and emission costs.

Numerical values of CO_2 emissions and calculated emission factors of on-site heat energy production are presented in Table 15. The emission factor of on-site produced heat energy is significantly lower than emission factors of district heat or electricity. This is mainly due to utilization PV electricity and heat pump technology. However the important thing to notice is that on-site energy is not totally CO_2 free because grid electricity is needed in each case for heat pumps. If imported grid electricity would be CO_2 free, the on-site produced energy would be also. This kind of situation can exist if used grid electricity is e.g. wind electricity or solar electricity. It is also important to understand, that calculated emission factor of on-site energy depends on emission factors of electricity CO_2 emissions. So it is only a theoretical value to compare different cases of this study.

Table 15. Numerical values of CO_2 emissions and calculated emission factor for on-site produced energy.

	CO_2 emissions of district heat	**CO_2 emissions of electricity**	**Total CO_2 emissions (t)**	**Difference to reference case**	**Emission factor of on-site produced energy (g/kWh)**
	t	**t**	**t**	**%**	**g/kWh**
Reference	329	0	329	-	-
1A	138	44	183	44 %	38
1B	137	51	188	43 %	44
1C	135	70	205	38 %	59
1D	40	72	112	66 %	41
2A	151	42	193	41 %	39
2B	139	53	192	42 %	45
2C	136	69	205	38 %	58
3A	179	32	211	36 %	35
3B	163	41	205	38 %	41
3C	150	60	210	36 %	55
4A	203	24	227	31 %	31
4B	193	22	215	35 %	26
4C	175	47	222	33 %	50

4.6 Waste heat option

As an option, costs of two optimal cases, 2 and 3 were modified so that investment cost of PV system and AW-HPs were assumed to be zero. The aim was to simulate a situation where the same amount of energy that was produced earlier with AW-HPs, would now imported as a waste heat e.g. from a datacenter. The purpose of this kind of variation was to find out how much the LCOE would decrease if free waste heat is utilized for charging BTES instead of investing in PV panels and AW-HPs as they were the most expensive components of the local hybrid energy system after seasonal storage. Any changes in simulation models were not done i.e. the energy amounts remained the same. The only variables in comparison to optimal cases were investment cost, maintenance cost as it was depending on investment cost, and profit from sold surplus PV electricity if assumed that there were no PV panels at all in this optional case. The results are shown in Table 16. Thus this study was initially considered on solar energy, this alternative waste heat case was not modeled or examined in more detail. The aim was only to see, how the LCOE would decrease if waste heat was utilized instead of solar energy. As can be seen from the table, the LCOE decreases significantly if waste heat is utilized instead of PV panels and AW-HPs. Of course there are practical limitations related to waste heat as the neighborhood should be located near waste heat source, and some kind of heat transfer network from waste heat source to the neighborhood is needed.

Table 16. Cost changes in waste heat option.

Cost	**Unit**	**Case 2**	**Case 3**
Initial LCOE	€/MWh	138	116
Initial LCC	€	2 503 800	1 784 200
PV investment reduction	€	-340 200	-340 200
AW-HP investment reduction	€	-492 000	-369 000
Maintenance cost reduction	€	-29 000	-24 700
Elec sell value profit reduction	€	18 700	38 900
New LCC	€	1 661 300	1 089 200
New LCOE	€/MWh	92	71
Difference to initial LCOE	%	-34 %	-39 %

5 Discussion

5.1 Analysis of local hybrid energy system

Key findings

Local hybrid energy system examined in this study seems to be a potential solution to provide heating energy to the residential district, decentralize heating energy production and to decrease CO_2 emissions from technical point-of-view. With smaller scale solutions, like cases 3 and 4, it is possible to cover 35 – 44 % of total heating demand of the neighborhood with renewable energy fraction 31 – 38 % and LCOE 110 – 132 €/MWh. On-site energy can meet 68 – 82 % of total space heating demand, 38 – 59 % of total ventilation heating demand and 24 – 29 % of total domestic hot water heating demand with smaller scale solutions (cases 3 and 4). With larger scale solutions, like cases 1 and 2, 45 – 53 % of total heating demand can be covered with on-site energy with renewable energy fraction 38 – 45 % and LCOE 122 – 184 €/MWh. 82 – 92 % of space heating demand, 59 – 78 % of ventilation heating demand and 29 – 36 % of domestic hot water heating demand can be covered with on-site energy if larger systems are implemented. A large share of space heating and ventilation heating demand can be covered even with smaller systems. However, as the DHW heating is the largest part of total heating energy consumption and there is a high temperature requirement for DHW, more district heat is needed in addition to on-site energy if smaller scale systems are implemented. On the other hand the costs of larger systems are relatively high in comparison to increase of on-site energy production. When comparing LCOEs of this study to the current district heat prices of Fortum which is the DH operator in Espoo, it can be concluded that the cost of on-site produced energy is significantly higher than conventional DH prices. Monthly consumer prices of DH including VAT are 31 – 73 €/MWh, and the lowest LCOE of studied energy system is 110 €/MWh.

At the peak load hours, 200 – 400 kWh of district heat demand can be decreased with optimal solutions, and if optional cases are implemented, the district heat demand decrease might be even 600 kWh. Annual CO_2 emissions can be lowered 100 – 150 tons in optimal solutions and even 215 tons with optional cases. However, CO_2 emission reduction potential depends strongly on emission factors. In emission costs the reduction is moderate, varying annually between 2 300 – 3 300 € in optimal solutions and even 4 800 € in optional cases but these estimations may vary depending on emission factors and emission allowance prices.

Using average values of COP of AW-HP and BTES efficiency, a rule of thumb for estimating this kind of local energy production can be defined based on PV capacity. PV system with nominal capacity of 100 kW_p can generate roughly 95 MWh electricity on annual level. AW-HP operating with COP 4.5 can produce 430 MWh heat energy that can be charged into the BTES. Assuming average efficiency of BTES to be 60 %, approximately 260 MWh of heat energy can be discharged from BTES to local heating network. Thus it can be stated that with 1 kW_p of PV capacity it is possible to produce 2.6 MWh heat energy on annual level. If using that thumb rule, to cover almost 100 % of heating demand (2 005 MWh) in residential area of this study, PV system with nominal capacity of 770 kW_p would have been needed. That is 126 % more than maximum nominal PV capacity was in this study.

BTES

Efficiency of BTES was high in all optimal cases, deviating between 63 % and 70 %. This was mainly due to relatively low temperature levels as the maximum temperature was 24 – 36 °C, depending on case. Borehole density was deviating from 0.075 to 0.2 boreholes/m² which means that there was one borehole in 5 – 13 m² area, depending on case. Thus, the distance between the boreholes was quite long, which indicates that heat transfer between boreholes and surrounding ground was high. In all optimal cases the borehole length was quite low as the length varied between 40 and 68 m. It indicates that high enough heat transfer between heat transfer fluid and surrounding ground was achieved even with lower height boreholes. Therefore there was no need to drill deeper boreholes. Cross-sectional area of BTES was 960 – 2570 m². Residential district of 14 apartment buildings needs notably larger land area than roughly 2600 m². Thus it can be concluded it might be possible to integrate even the largest borehole thermal energy storages of this study to the neighborhood. Investment costs of the BTES varied significantly between the smallest and largest solutions. However, at some point the gain achieved from higher investment in BTES was poor because it was not possible to charge BTES more due to limited PV capacity. In other words, increasing storage capacity and thus the on-site energy fraction was very expensive. For example, increasing on-site energy fraction from 35 % to 40 %, the investment cost of BTES was 70 000 € higher. When on-site energy fraction increased from 45 % to 50 %, 123 000 € higher investment for BTES was needed.

Grid electricity for AW-HPs

Feasibility of using grid electricity in addition to PV electricity to operate AW-HPs depends on how large a share of total energy demand is desired to cover with on-site energy. Investment costs of the local hybrid energy system are the greatest part of the life cycle cost. Thus from economical point-of-view it is more feasible to have smaller amount of AW-HPs that operate frequently instead of having a large amount of AW-HPs that operate not so often. However, grid electricity is needed to operate the AW-HPs when there is no solar radiation as there was no electrical storage in this study. Storing the surplus electricity on the site and utilizing it later for AW-HPs instead of selling to the grid is one solution to improve system performance without using grid electricity. Instead of physical batteries, future smart electricity grid might also be a possible storage media for electricity i.e. the same amount of surplus electricity that is transferred to the grid, can be imported from the grid later free of charge.

Utilization of surplus PV electricity

Instead of selling the surplus PV electricity to the grid, it is usually possible to utilize it on the neighborhood to cover electrical loads either in apartments or in public spaces of the buildings. However, it was difficult to define the economical value of surplus electricity if it was utilized in apartments. That was mainly due to the fact that distribution fee might be charged and taxes may be paid also in that kind of situation. Moreover, electricity demand profile for only public spaces was not available so it would have been challenging to estimate the load profile. Excess PV electricity would be also possible to utilize for cooling energy production. As the costs of cooling energy production was not considered in this study, it was not either reasonable to assume that excess PV electricity could be used for that purpose. However, it would be feasible because otherwise the electricity for cooling energy production has to be imported from the grid. All these observations are based on assumption that the operator of local hybrid energy system is an energy company, not the housing cooperative.

Practical issues

When considering practical issues, it should be noticed that local hybrid energy system may be more feasible in new neighborhood areas than in district heated existing neighborhoods. This is due to the fact that components of the energy system could be more challenging to integrate to the existing built environment. Moreover, the heat distribution networks in existing buildings may operate with higher temperatures than assumed underfloor heating in this study. Thus the efficiency of the local hybrid energy system may decrease if it is not possible to decrease the operating temperatures of the heat distribution networks in existing buildings. It can be also noticed that local hybrid energy system requires significantly more space for components than district heat system. In district heat system, the main components before building network are DH pipes and heat exchangers. Local hybrid energy system of this study consists of several components that need lots of installation space such as BTES, buffer tank and heat pumps. However all components of local hybrid energy system are suitable size to integrate to the site of this study with proper design. The largest single component is the BTES, which requires area from hundreds to thousands square meters. In four optimal solutions that were analyzed more closely, the cross-section area of BTES were deviating from 960 m² to 2370 m². As the site of this study was relatively large, even the largest optimal BTES can be implemented in practice. Another large size single component is the buffer tank. In four optimal solutions with volume from 70 m³ to 200 m³ and height deviating from 5.8 meters to 8.3 meters. As this large tanks are difficult to integrate inside the buildings, the one solution is to excavate the tank into the ground. The power and therefore the size of the heat pumps is high, and some kind of energy center is necessary to locate them in the same place.

If this kind of local hybrid energy solution would be implemented, lots of pre-designing related to layout of the site is required. Main things to solve are e.g. how to locate the apartment buildings, BTES, buffer tank and energy center to the site in a suitable way. This challenging pre-design may add investment costs of the system. On the other hand, the tank cost was assumed relatively high in calculations of this study. So the excessive tank price may cover a share of designing and construction costs of the system. In general, usually the investment costs of first implemented cases are higher due to more designing, adjusting and testing is needed. When the system becomes more common, the investment costs may decrease.

Bi-directional network possibilities

Operating temperatures of the modeled local heating network are between 30 – 55 °C. They are significantly lower than conventional district heat network temperatures, which are typically 65 – 115 °C. Thus bi-directional operation i.e. selling heat energy to conventional district heat network is not possible with the hybrid energy system examined in this study. Additional heat pump would be needed to increase the temperature level of the local heating network to supply heat energy to the DH network. That kind of investment and operation is not feasible as the costs would be too high. In addition to that, as the amount of on-site energy did not cover even the heat demand of the buildings, it might not be feasible to transfer on-site produced energy to larger scale DH network as all on-site produced energy can be utilized on site. If the larger scale DH network would be 4th generation network with lower operating temperatures and on the other hand if the local heating network would operate a higher temperature levels, there it would be possible to transfer heat energy to the

larger scale network. But there is still the question if it is feasible or not as all on-site produced heat energy can be utilized in the neighborhood so there is no actually surplus heat energy to sell to the larger scale network.

Comparison to previous study

As previous study by Hirvonen and Sirén considered detached house neighborhood, it is interesting to compare results of this study to that earlier study. However, the heating demand of detached house differs from heating demand of apartment block. Due to that it is not feasible to compare the results based on heated floor area. Thus the more feasible method is to compare the results based on heating demand. Results of both one optimal solution introduced in article as well as results of four selected optimal cases of this study were scaled based on heating demand. PV capacity, BTES volume and total length of boreholes are compared.

The most drastic difference is in PV capacity. In Hirvonen and Sirén's study the PV capacity was 1.9 kW_p/MWh and in this study it was 0.45 kW_p/MWh which was maximum PV capacity in each case. The PV capacity of this study is 24 % of PV capacity of Hirvonen and Siren's study. Even though PV electricity was not used to cover appliance load at all in this study as it was done in Hirvonen and Sirén's study, the difference is significant. It is also the most important reason why the renewable energy fraction is lower than in Hirvonen and Siren's study. Wall-mounted PV panels, in addition to PV panels installed to the rooftop, might be one method to increase the share of solar electricity because rooftop area was a limiting issue in apartment buildings. However in apartment buildings there is usually a large area of walls covered by windows and balconies so area for PV panels is restricted also on walls. In addition to that, buildings may locate quite near each other and therefore one building may shade another and thus affect significantly to PV electricity generation.

BTES volume per heating demand was 88 m³/MWh in previous study and in this study it varied between 70 m³/MWh (case 4) and 181 m³/MWh (case 1). In case 2 it was 126 m³/MWh and in case 3 84 m³/MWh. So the BTES volume per heating demand is quite same in some cases, and slightly or notably higher in some other cases. This might be due to low borehole density in this study because more area and therefore more volume was needed for same amount of boreholes than in earlier study. Total length of boreholes was 20 m/MWh in previous study. In this study it varied between 5 m/MWh (case 4) and 27 m/MWh (case 1). In case 2 it was 9 m/MWh and in case 3 6 m/MWh. Total length of boreholes is lower in most of the cases of this study. It indicates that heat transfer rate between heat transfer fluid and ground is higher in BTES of this study because lower length of boreholes was needed.

Feasible cases for further studies

From among the analyzed optimal cases, cases 2, 3 and 4 are most reasonable to research and develop further. The final decision which one of the cases is the most feasible depends on two main factors. First affecting issue is that how large share of heating energy is desired to produce on-site i.e. how self-sufficient the system should be. The second important issue is that what size of system can be integrated to the site. Case 1 is not feasible to research further because the LCOE is significantly higher, but there is not notable increase in on-site energy fraction or notable decrease in CO_2 emissions when comparing to cases 2, 3 and 4.

5.2 Reliability of the results

One important data affecting to the dimensioning of local hybrid energy system and thus to the optimal solution was hourly energy demand profile as it defined the energy demand. Energy demand profile of this study was based on IDA ICE simulated apartment building that was fulfilling current requirements of Finnish Building Code. However, actual energy consumption in buildings deviates usually from simulations as the energy consumption may depend on many different components such as is there water metering in each apartment or not, how many people are living in one apartment and so on. Thus implementing this kind of system in real life, more validation to energy consumption profile has to be done to avoid oversizing or undersizing the energy system. Technical specifications of heat pumps used in the simulation model of this study were based on heat pumps for domestic use that are in the market. If larger scale, e.g. industrial heat pumps are utilized instead of those in this study, the heating and cooling capacities, temperature levels as well as the investment costs may vary significantly. In heat pumps that are designed for domestic use, the maximum COP can be achieved with source side temperatures between 25 – 30 °C. In industrial heat pumps, higher source side temperatures, like 30 – 50 °C can be utilized which increases the load side temperature and COP. With that kind of heat pumps it would be possible to achieve more gain from higher BTES temperatures.

Charging of seasonal storage depends strongly on utilization of PV electricity. If actual PV electricity generation deviates from modeled generation, it may significantly influence the system performance and feasibility. Even though the degradation of PV panels was taken into account in calculations, there might be other issues that decrease the PV generation. For example if the vertical installation angle of PV panels is not directly to the south as assumed in model, PV electricity generation can be lower than in the model. Therefore the heat generation of AW-HPs might decrease which also decreases charge potential of seasonal storage.

The operation and heat transfer efficiency of BTES depends on soil and bedrock materials. In this study the average thermal conductivity of rock types in Finland was used as a thermal conductivity of bedrock of BTES. If this kind of energy system is implemented, it is necessary to model the BTES using site-specific soil and bedrock values to find out the behavior and heat transfer and storing capacity of BTES.

5.3 Future research topics

To develop the local hybrid energy system of this study further, some useful research topics are mentioned. The optimal use of on-site energy versus district heat was not considered in this study in much detail. However, there is a potential to optimize operation of local hybrid energy system in such a way that on-site energy could be utilized when the prices of district heat are higher, usually in winter time. Respectively district heat could be utilized when the DH prices are lower, usually in summer time. In this study that kind of optimization was done in large scale as the seasonal storage was discharged in winter time and charged in summer time. Better value for on-site energy might be achieved, if discharging of BTES could be controlled based on hourly district heat prices. Thus it would be reasonable to develop a control algorithm to control the hybrid energy system based on district heat prices. Another alternative method would be weather forecast based control algorithm.

Utilizing grid electricity to produce more heating energy with AW-HPs decreased utilization of PV electricity in many cases. This was mainly due to lack of prediction of solar radiation availability. Thus grid electricity was used to charge the tank, and after few hours when there was PV electricity available, there was no heat need in the tank. For that reason the AW-HPs were not operated even there was PV electricity available. As it was in some cases feasible to use grid electricity for that purpose, it would be reasonable and interesting to optimize the grid electricity usage for AW-HPs based on weather forecasts. If it would be possible to forecast that there will be enough solar radiation to operate AW-HPs within few hours, the grid electricity would not be used to drive AW-HPs.

Cooling system and cost structure of on-site produced cooling energy is an interesting topic to research more as there is possibility to lower the cost structure of on-site heat energy production also. Seasonal storage was not discharged in summer time and thus WW-HPs were useless during summer. Because the need for space cooling in apartment buildings is in summer time, it is reasonable to use the same WW-HPs for producing cooling energy for space cooling. As the WW-HPs exist already, the investment cost of cooling system is lower in comparison to situation where WW-HPs or other appliances to produce cooling energy has to be included in the investment. On the other hand, in this study the condensate of cooling energy production was utilized free of charge which already decreased the price of on-site energy. Therefore it would be important to find out the cost structure and pricing of on-site produced cooling energy.

Utilization of waste heat has also potential but the waste heat source should be located near to the neighborhood which may be a difficult combination. But if that kind of situation exists, the modeling and feasibility analysis would be sensible to perform.
The purpose of this study was pre-feasibility analysis of local hybrid energy system for neighborhood area consisting of apartment blocks. Thus it can be stated that to implement this kind of system in practice, more research, modeling and feasibility analysis are needed to find out the more precise operation of system and cost structure.

6 Conclusions

Reduction of CO_2 emissions is absolutely necessary to restrict the climate change. Building sector covers significant share of total energy consumption particularly in high latitude areas due to cold climate and heating need of buildings. Thus solutions and actions that decrease CO_2 emissions of building sector are needed. In addition to improve energy efficiency of the buildings and decrease the heat energy consumption and therefore lower CO_2 emissions, heat energy production has also to be considered. Using renewable energy sources for heating energy production, there is a significant potential to reduce CO_2 emissions in building sector. Solar energy is a significant renewable energy source and thus well utilizable also to heating energy production. The main challenge in utilizing solar energy for heating is the seasonal mismatch of solar radiation and heating demand. Neighborhood-level decentralized heating energy production allows the utilization of seasonal thermal energy storage, where heat energy can be charged in summer when solar radiation is at highest level and discharged in winter when the heating demand is at highest level. In this study a solar energy based local hybrid energy system was investigated. The idea of system was to cover part of heating energy demand of neighborhood area consisting of 14 apartment buildings. The optimal design of the system was determined using simulations and genetic algorithm based optimization. Based on optimization results the feasibility of system was evaluated.

Depending on system size, 35 - 53 % of heating energy of the neighborhood area can be produced on-site with LCOE 110 – 184 €/MWh. If grid electricity is used to drive air-to-water heat pumps in addition to PV electricity, 41 – 88 % of total heating demand of the neighborhood can be covered with on-site energy with LCOE 108 – 201 €/MWh. At the peak demand hours, 200 – 600 kWh decrease of district heat demand can be achieved with the studied system. Depending on case, CO_2 emissions can be lowered annually 100 - 215 tons in comparison to the situation where all the heating demand of the neighborhood would be covered with district heat. Borehole thermal energy storage seems to be a potential seasonal storage for residential district due to moderate heat losses and flexible implementation. It would be also possible to integrate it to the site of the neighborhood examined in this study. The most important things of planning implementation of BTES are precise predesign and detailed ground area investigations.

Available rooftop area of apartment buildings is the main limiting factor for the high performance of the system, as the on-site energy production is dependent on PV electricity generation. Because the rooftop area was limited in this study, PV electricity generation was maximized by optimizing the tilt angle of PV panels and charging BTES in summer time as much as possible. However, that was not enough because the nominal power production and heating demand ratio was low when compared to more feasible results of study where detached house neighborhood was examined. By increasing the PV panel area somehow, the feasibility of the system could be increased. The main challenge is, that the ratio of rooftop area and heating demand is significantly higher in apartment building than in detached house, so there is no enough space for PV panels. As the neighborhood areas are typically tightly constructed due to high land prices, additional land space for PV panels do not usually exist. Using wall-mounted PV panels, on-site energy production could be increased but on the other hand, the investment cost of wall-mounted panels is higher and efficiency can be lower which may affect to the feasibility.

When considering the operation of the system, there would be a good potential to decrease the peak demands of district heat by utilizing more on-site energy during peak demand. To evaluate the profitability of that kind of operating principle of the system, a control algorithm has to be developed. That might improve the value of on-site energy and thus increase the feasibility of the system.

Larger investments do not always increase the self-sufficiency of the hybrid energy system significantly. The most feasible solution for further development depends on how large share of district heat is desired to replace with on-site energy and what is the maximum allowed LCOE. To decrease the LCOE, investment costs of the main components has to be decreased as they have the most significant effect to the LCOE. The most expensive component of the local hybrid energy system was the BTES and largest share of BTES investment was due to borehole drilling. However, if the borehole drilling cost would be halved and thus LCOE would be 6 – 19 €/MWh lower, the cost of produced energy is still higher than DH prices. So notably cost reductions of main components would be needed to decrease LCOE more. However, if the aim is to decentralize heat energy production and to lower CO_2 emissions, such a system alternative should be researched and developed further. If PV electricity generated somewhere else e.g. in larger PV power stations can be utilized on site to produce heat energy, the renewable energy fraction would increase and the system would be more feasible.

References

Alanne, Kari. 2018. Course material: Introduction to optimization. Espoo, Finland: Aalto University.

Alva, G., Lin, Y. and Fang, G. 2018. An overview of thermal energy storage systems. Energy. Vol. 144, pp. 341-378. //doi.org/10.1016/j.energy.2017.12.037.

Axitec. 2018. AXIpower 207-275 Wp. Retrieved 4.2.2019, from: https://www.axitecsolar.com/data/solarpanels_documents/DB_60zlg_poly_power_MiA_US_neo.pdf.

Cao, S., Hasan, A. and Sirén, K. 2013. On-site energy matching indices for buildings with energy conversion, storage and hybrid grid connections. Energy and Buildings. Vol. 64, pp. 423-438. //doi.org/10.1016/j.enbuild.2013.05.030.

Caruna Espoo Oy. 2018. Verkkopalveluhinnasto (In Finnish). Retrieved 6.5.2019, from: https://caruna-cms-prod.s3-eu-west-1.amazonaws.com/web_30693845_caruna_ces_verkkopalveluhin_espoo_6s_2018_fi.pdf?xv7kYW..81MvcW_w5uKyPfXBdMRvS1QD.

City of Espoo. 2019. Map service. Retrieved 29.1.2019, from: https://kartat.espoo.fi/IMS/en/Map.

Dalenbäck, J., Dahm, J., Lundin, S., Hellström, G. and Nordell, B. 2000. Solar heated residential area Anneberg. Retrieved 27.6.2019, from: http://ptp.irb.hr/upload/mape/kuca/09_Jan-Olof_Dalenback_SOLAR_HEATED_RESIDENTIAL_AREA_ANNEBERG.pdf.

Drake Landing Solar Community. 2019a. Borehole Thermal Energy Storage. Retrieved 12.2.2019, from: https://www.dlsc.ca/borehole.htm.

Drake Landing Solar Community. 2019b. How it Works. Retrieved 27.6.2019, from: https://www.dlsc.ca/how.htm.

E-hub. 2018. The Energy Hub Challenge. Retrieved 29.5.2019, from: https://www.e-hub.org/energy-hub-challenge.html.

Energiateollisuus ry. 2019. Lämmitysmarkkinat asiakkaiden ehdoilla. Retrieved 26.2.2019, from: https://energia.fi/energiateollisuuden_edunvalvonta/energiapolitiikka/toimivat_markkinat/lammitysmarkkinat.

Energy Authority. 2019. Auctioning of emission allowances 2013 - 2020. Retrieved 28.5.2019, from: https://energiavirasto.fi/documents/11120570/12749404/P%C3%A4%C3%A4st%C3%B6oikeuksien-huutokaupat-2013-2020.xlsx/aed6b127-b98d-2585-13ab-948e9fdcb95c.

Engineering Toolbox. 2019. Ethylene Glycol Heat Transfer Fluid. Retrieved 26.2.2019, from: https://www.engineeringtoolbox.com/ethylene-glycol-d_146.html.

Engineering Toolbox. 2018. Thermal Conductivity of common Materials and Gases. Retrieved 26.2.2019, from: https://www.engineeringtoolbox.com/thermal-conductivity-d_429.html.

Erat, B., 2008. Solar energy guide - Solar energy for buildings (In Finnish). Porvoo, Finland: Solar Engineering Association . ISBN 978-952-92-2721-1.

European Commission. 2012a. Commission Delegated Regulation C(2011). Retrieved 20.4.2019, from: http://ec.europa.eu/transparency/regdoc/rep/3/2011/EN/3-2011-10050-EN-F1-1.Pdf.

European Commission. 2012b. Geographical Assessment of Solar Resource and Performance of Photovoltaic Technology. Retrieved 25.6.2019, from: http://re.jrc.ec.europa.eu/pvgis/.

Evins, R. 2013. A review of computational optimisation methods applied to sustainable building design. Renewable and Sustainable Energy Reviews. Vol. 22, pp. 230-245. //doi.org/10.1016/j.rser.2013.02.004.

Finlex. 2011. Emission trading law (In Finnish). Retrieved 28.5.2019, from: https://www.finlex.fi/fi/laki/ajantasa/2011/20110311.

Finnish Energy. 2019. Energy Year 2018 - District Heating. Retrieved 21.2.2019, from: https://energia.fi/files/3321/Energy_Year_2018_DistrictHeating.pptx.

Finnish Energy. 2018. Monthly CO2 emission factors of electricity production - Email from Finnish Energy.

Finnish Energy. 2014. District Heating of Buildings - Regulations and guidelines (In Finnish). Retrieved 13.2.2019, from: https://energia.fi/files/502/JulkaisuK1_2013_20140509.pdf.

Finnish ground source heat wholesale. 2019a. NIBE F1345 60 kW (In Finnish). Retrieved 23.4.2019, from: https://www.maalampotukku.fi/product/402/nibe-f1345-60kw-maalampopumppu.

Finnish ground source heat wholesale. 2019b. NIBE F2120-20 (In Finnish). Retrieved 23.4.2019, from: https://www.maalampotukku.fi/product/2595/nibe-f2120-20-kw.

Flynn, C. and Sirén, K. 2015. Influence of location and design on the performance of a solar district heating system equipped with borehole seasonal storage. Renewable Energy. Vol. 81, pp. 377-388. //doi.org/10.1016/j.renene.2015.03.036.

Fortum. 2019a. Lähisähkö (In Finnish). Retrieved 6.5.2019, from: https://www.fortum.fi/kotiasiakkaille/sahkoa-kotiin/oman-tuotannon-myynti-lahisahko.

Fortum. 2019b. Open district heat. Retrieved 26.2.2019, from: https://www.fortum.fi/yrityksille-ja-yhteisoille/lammitys/kaukolampo-0/avoin-kaukolampo/avoin-kaukolampo-ostohinnat.

Fortum. 2019c. Tarkka Pörssisähkö (In Finnish). Retrieved 6.5.2019, from: https://www.fortum.fi/kotiasiakkaille/sahkoa-kotiin/sahkosopimukset/tarkka-porssisahko.

Geofoorumi. 2018. Kaurapellossa varastoidaan hukkalämpöä (In Finnish). Retrieved 27.6.2019, from: http://verkkolehti.geofoorumi.fi/fi/2018/05/25/kaurapellossa-varastoidaan-hukkalampoa/.

Geological Survey of Finland. 2019. Geoenergy (In Finnish). Retrieved 20.3.2019, from: http://www.gtk.fi/geologia/luonnonvarat/geoenergia/.

Hakala, P., Huusko, A., Leppäharju, N. and Martinkauppi, I., 2015. Geoenergy of new building (In Finnish). Espoo, Finland: Geological Survey of Finland.

Hirvonen, J., Heljo, J., Jokisalo, J. and Kosonen, R. 2018. Towards the EU emissions targets of 2050: optimal energy renovation measures of Finnish apartment buildings. International Journal of Sustainable Energy. Vol. 38, no. 7, pp. 649-672. https://doi.org/10.1080/14786451.2018.1559164.

Hirvonen, J. and Sirén, K. 2018. A novel fully electrified solar heating system with a high renewable fraction - Optimal designs for a high latitude community. Renewable Energy. Vol. 127, pp. 298-309. //doi.org/10.1016/j.renene.2018.04.028.

Hirvonen, J., ur Rehman, H. and Sirén, K. 2018. Techno-economic optimization and analysis of a high latitude solar district heating system with seasonal storage, considering different community sizes. Solar Energy. Vol. 162, pp. 472-488. //doi.org/10.1016/j.solener.2018.01.052.

International Energy Agency. 2019. Energy Efficiency: Buildings. Retrieved 12.02.2019, from: https://www.iea.org/topics/energyefficiency/buildings/.

International Energy Agency. 2016. Technology and demonstrators - Technical Report Subtask C – Part C1: Classification and benchmarking of solar thermal systems in urban environments. Retrieved 23.4.2019, from: http://task52.iea-shc.org/data/sites/1/publications/IEA-SHC-Task52-STC1-Classification-and-benchmarking-Report-2016-03-31.pdf.

Introduction to Genetic Algorithms. 1998. Parameters of GA. Retrieved 27.6.2019, from: https://www.obitko.com/tutorials/genetic-algorithms/parameters.php.

Jensen, M.V. 2014. Seasonal pit heat storages - Guidelines for materials & construction. Retrieved 20.3.2019, from: http://task45.iea-shc.org/data/sites/1/publications/IEA-SHC%20T45.B.3.2%20TECH%20Seasonal%20storages%20-%20Water%20Pit%20Guidelines.pdf.

Jordan, D.C. and Kurtz, S.R. 2012. Photovoltaic Degradation Rates — An Analytical Review. Retrieved 5.4.2019, from: https://www.nrel.gov/docs/fy12osti/51664.pdf.

Juvonen, J. and Lapinlampi, T., 2013. Energy well (In Finnish). Helsinki, Finland: Ministry of the Environment. ISSN 1796-167X. Retrieved 24.3.2019, from: https://helda.helsinki.fi/handle/10138/40953.

Keskipohjanmaa. 2018. Finn Springin tehdasalueelle Toholammille rakentuu 15000 kuution aurinkoenergialla lämpenevä maavarasto (In Finnish). Retrieved 27.6.2019, from: https://www.keskipohjanmaa.fi/uutiset/536056/finn-springin-tehdasalueelle-toholammille-rakentuu-15000-kuution-aurinkoenergialla-lampeneva-maavara.

K-rauta. 2019. Thermisol insulation panel (In Finnish). Retrieved 23.4.2019, from: https://www.k-rauta.fi/rautakauppa/eristyslevy-thermisol-eps-120-routa-50x1000x1200mm-12m2.

Laihian Nuuka Lämpö Oy. 2015. Esimerkkikytkennät (In Finnish). Retrieved 19.2.2019, from: http://www.laihiannuukalampo.fi/downloadable/PDF/Esimerkkikytkennat.pdf.

Lanahan, M. and Tabares-Velasco, P.C. 2017. Seasonal Thermal-Energy Storage: A Critical Review on BTES Systems, Modeling, and System Design for Higher System Efficiency. Energies. Vol. 10, no. 6. https://doi.org/10.3390/en10060743.

Lund, H., Werner, S., Wiltshire, R., Svendsen, S., Thorsen, J.E., Hvelplund, F. and Mathiesen, B.V. 2014. 4th Generation District Heating (4GDH): Integrating smart thermal grids into future sustainable energy systems. Energy. Vol. 68, pp. 1-11. //doi.org/10.1016/j.energy.2014.02.089.

Lundh, M. and Dalenbäck, J.-. 2008. Swedish solar heated residential area with seasonal storage in rock: Initial evaluation. Renewable Energy. Vol. 33, no. 4, pp. 703-711. //doi.org/10.1016/j.renene.2007.03.024.

Mäkelä, V. and Tuunanen, J., 2015. Finnish district heating. Mikkeli, Finland: Mikkelin ammattikorkeakoulu . ISBN 978-951-588-507-4.

Ministry of the Environment. 2019. The National Building Code of Finland. Retrieved 8.4.2019, from: https://www.ym.fi/en-US/Land_use_and_building/Legislation_and_instructions/The_National_Building_Code_of_Finland.

Ministry of the Environment. 2017. 1010/2017 Decree of the Ministry of the Environment on the Energy Performance of New Buildings. Retrieved 15.2.2019, from: https://www.ym.fi/download/noname/%7BE12CDE2C-9C2B-4B84-8C81-851349E2880B%7D/140297.

Ministry of the Environment. 2011. Rakennusten energianlaskennan testivuodet (In Finnish). Retrieved 4.4.2019, from: https://www.ym.fi/download/noname/%7B8D997677-9ECB-49DC-9D73-9DD93C1C875E%7D/31275.

Motiva. 2019. CO2 emission factors (In Finnish). Retrieved 23.5.2019, from: https://www.motiva.fi/ratkaisut/energiankaytto_suomessa/co2-laskentaohje_energiankulutuksen_hiilidioksidipaastojen_laskentaan/co2-paastokertoimet.

Motiva. 2018. Auringonsäteilyn määrä Suomessa (In Finnish). Retrieved 5.2.2019, from: https://www.motiva.fi/ratkaisut/uusiutuva_energia/aurinkosahko/aurinkosahkon_perusteet/auringonsateilyn_maara_suomessa.

NIBE. 2018a. Asentajan käsikirja NIBE F2120. Retrieved 20.02.2019, from: https://www.nibe.fi/nibedocuments/24652/331387-4.pdf.

NIBE. 2018b. NIBE F1345-60 Properties.

NIBE. 2018c. NIBE F1345-60 Technical information.

Ouman Oy. 2017. EH-800 Temperature Control Unit (In Finnish). Retrieved 26.2.2019, from: http://ouman.fi/documentbank/EH-800__manual__fi.pdf.

Pearsall, N.M. 2017. 1 - Introduction to photovoltaic system performance. The Performance of Photovoltaic (PV) Systems, pp. 1-19. //doi.org/10.1016/B978-1-78242-336-2.00001-X.

Photovoltaic electricity home. 2019. Offerings (In Finnish). Retrieved 23.4.2019, from: https://aurinkosahkoakotiin.fi/tarjoukset/.

PVeducation. 2019. Solar Radiation on a Tilted Surface. Retrieved 28.2.2019, from: https://www.pveducation.org/pvcdrom/properties-of-sunlight/solar-radiation-on-a-tilted-surface.

Rad, F.M. and Fung, A.S. 2016. Solar community heating and cooling system with borehole thermal energy storage – Review of systems. Renewable and Sustainable Energy Reviews. Vol. 60, pp. 1550-1561. //doi.org/10.1016/j.rser.2016.03.025.

Rauheat. 2019. PexFlex Plus local heating pipe. Retrieved 23.4.2019, from: https://www.rauheat.fi/weboost.php?sivu=tiedosto&t=119&url=rauheat_esite_hinnasto_2019_lowres&type=pdf.

Refinitiv. 2018. Will high European carbon prices last? Retrieved 25.6.2019, from: https://www.refinitiv.com/perspectives/market-insights/will-high-european-carbon-prices-last/.

Reuss, M. 2015. 6 - The use of borehole thermal energy storage (BTES) systems. Advances in Thermal Energy Storage Systems, pp. 117-147. //doi.org/10.1533/9781782420965.1.117.

Rohde, D., Andresen, T. and Nord, N. 2018. Analysis of an integrated heating and cooling system for a building complex with focus on long–term thermal storage. Applied Thermal Engineering. Vol. 145, pp. 791-803. //doi.org/10.1016/j.applthermaleng.2018.09.044.

Schmidt, T. and Miedaner, O. 2012. Solar district heating guidelines - Storage. Retrieved 25.3.2019, from: https://www.solar-district-heating.eu/en/knowledge-database/.

Smoltczyk, U., 2003. Geotechnical Engineering Handbook Volume 2: Procedures. ISBN 978-3433014509.

SPECIAL Project. 2015. Knowledge Pool. Retrieved 27.6.2019, from: http://www.special-eu.org/knowledge-pool/module-4-implementation-of-sustainable-planning/storage/.

Statistics Finland. 2019a. Final energy consumption by sector 2018. Retrieved 31.3.2019, from: https://www.tilastokeskus.fi/til/ehk/2018/04/ehk_2018_04_2019-03-28_kuv_014_en.html.

Statistics Finland. 2019b. Share of renewables of total primary energy 2018. Retrieved 31.3.2019, from: https://www.tilastokeskus.fi/til/ehk/2018/04/ehk_2018_04_2019-03-28_kuv_013_en.html.

SULPU - Finnish heat pump association. 2019. Heat pumps (In Finnish). Retrieved 14.5.2019, from: https://www.sulpu.fi/lampopumput.

Sunstore 3 Project., 2015. Final report. Retrieved 27.6.2019, from: https://energiteknologi.dk/sites/energiteknologi.dk/files/slutrapporter/sunstore_3_-_final_report_1_23102015_1501.pdf.

Syri, Sanna. 2018. Course material: LCOE calculations. Espoo, Finland: Aalto University.

Techeat. 2018. Energy well - Frequently asked questions (In Finnish). Retrieved 23.4.2019, from: http://www.techeat.fi/porakaivo-yleisimmat-kysymykset/.

Underground Energy. 2018a. ATES – Aquifer Thermal Energy Storage. Retrieved 20.3.2019, from: http://underground-energy.com/our-technology/ates/#what-is-ates.

Underground Energy. 2018b. BTES - Borehole Thermal Energy Storage. Retrieved 19.2.2019, from: http://underground-energy.com/our-technology/btes/.

Xu, J., Wang, R.Z. and Li, Y. 2014. A review of available technologies for seasonal thermal energy storage. Solar Energy. Vol. 103, pp. 610-638. //doi.org/10.1016/j.solener.2013.06.006.

Xu, R., Ni, K., Hu, Y., Si, J., Wen, H. and Yu, D. 2017. Analysis of the optimum tilt angle for a soiled PV panel. Energy Conversion and Management. Vol. 148, pp. 100-109. //doi.org/10.1016/j.enconman.2017.05.058.

Yle. 2018. Aurinkoenergiaa säilötään maavarastoon talvea varten Toholammilla – ympärivuotinen hyödyntäminen ottaa isoja askelia pilottihankkeessa. Retrieved 27.6.2019, from: https://yle.fi/uutiset/3-10368936.

Appendix 1. Annual energy flows of simulation cases

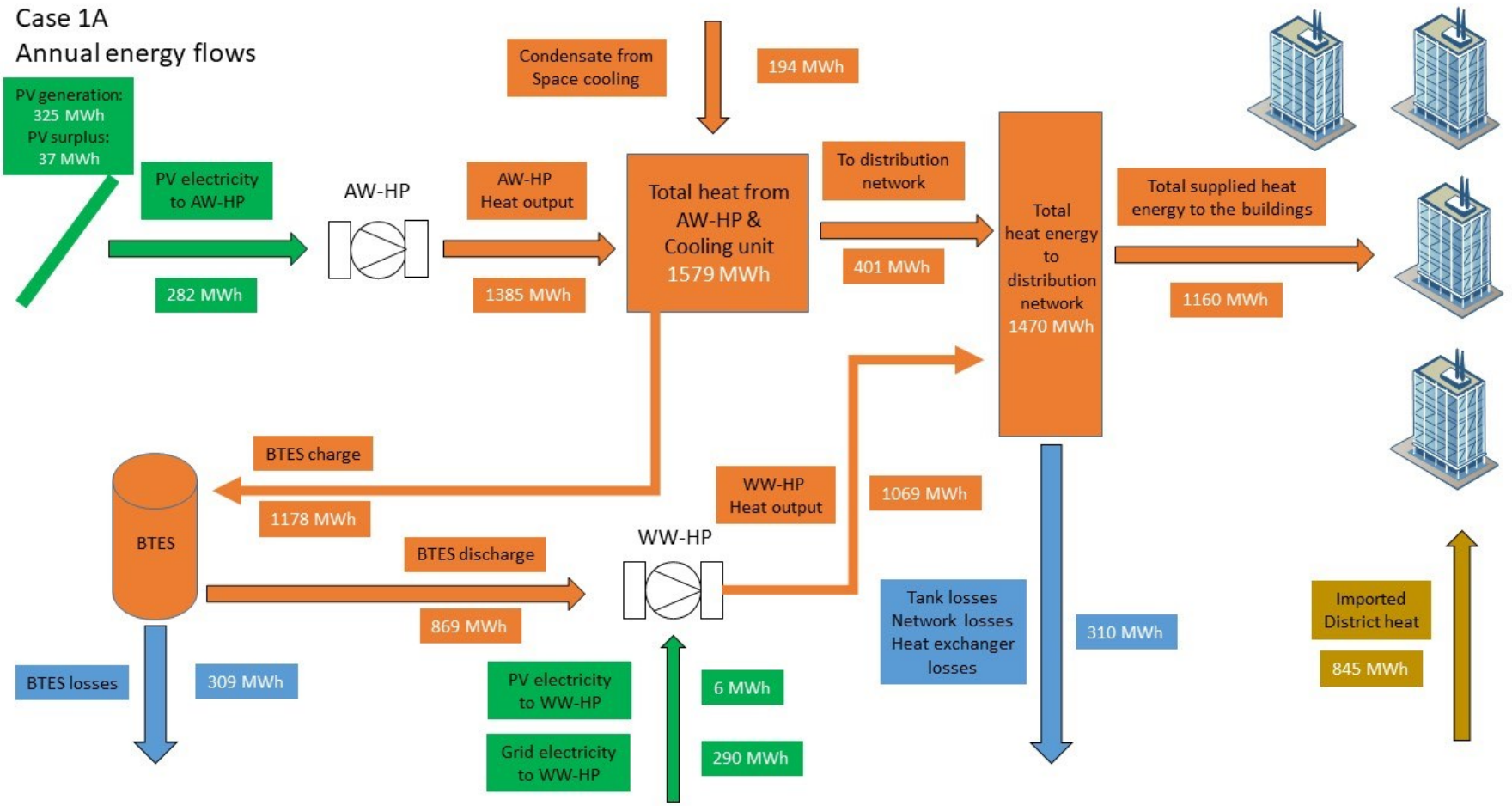

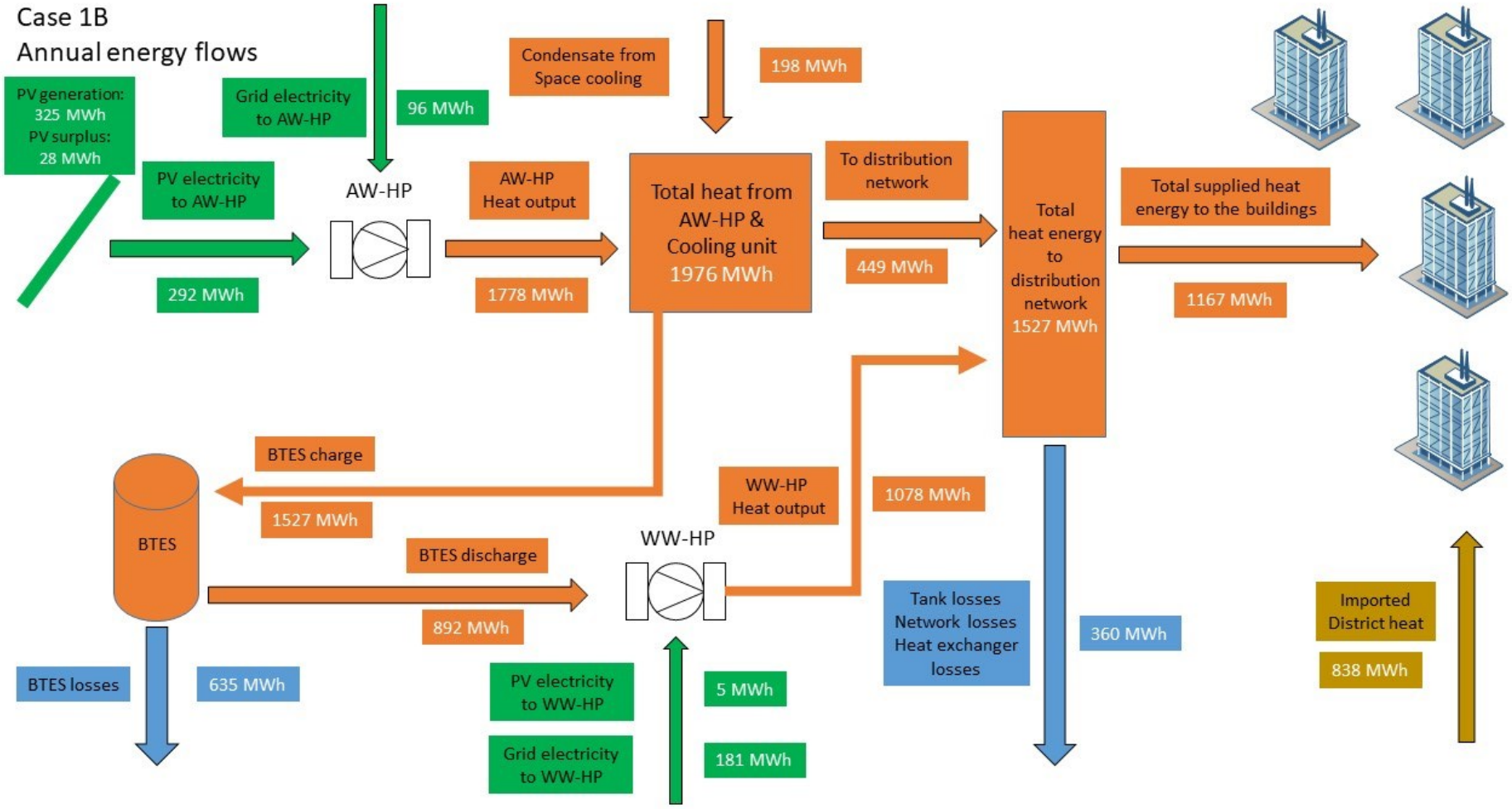
Case 1B
Annual energy flows
PV generation:
325 MWh
PV surplus:
28 MWh
Grid electricity
to AW-HP
96 MWh
Condensate from
Space cooling
198 MWh
PV electricity
to AW-HP
AW-HP
AW-HP
Heat output
Total heat from
AW-HP &
Cooling unit
1976 MWh
To distribution
network
Total
heat energy
to
distribution
network
1527 MWh
Total supplied heat
energy to the buildings
292 MWh
1778 MWh
449 MWh
1167 MWh
BTES charge
1527 MWh
BTES
WW-HP
Heat output
1078 MWh
BTES discharge
WW-HP
892 MWh
Tank losses
Network losses
Heat exchanger
losses
360 MWh
Imported
District heat
838 MWh
BTES losses
635 MWh
PV electricity
to WW-HP
5 MWh
Grid electricity
to WW-HP
181 MWh

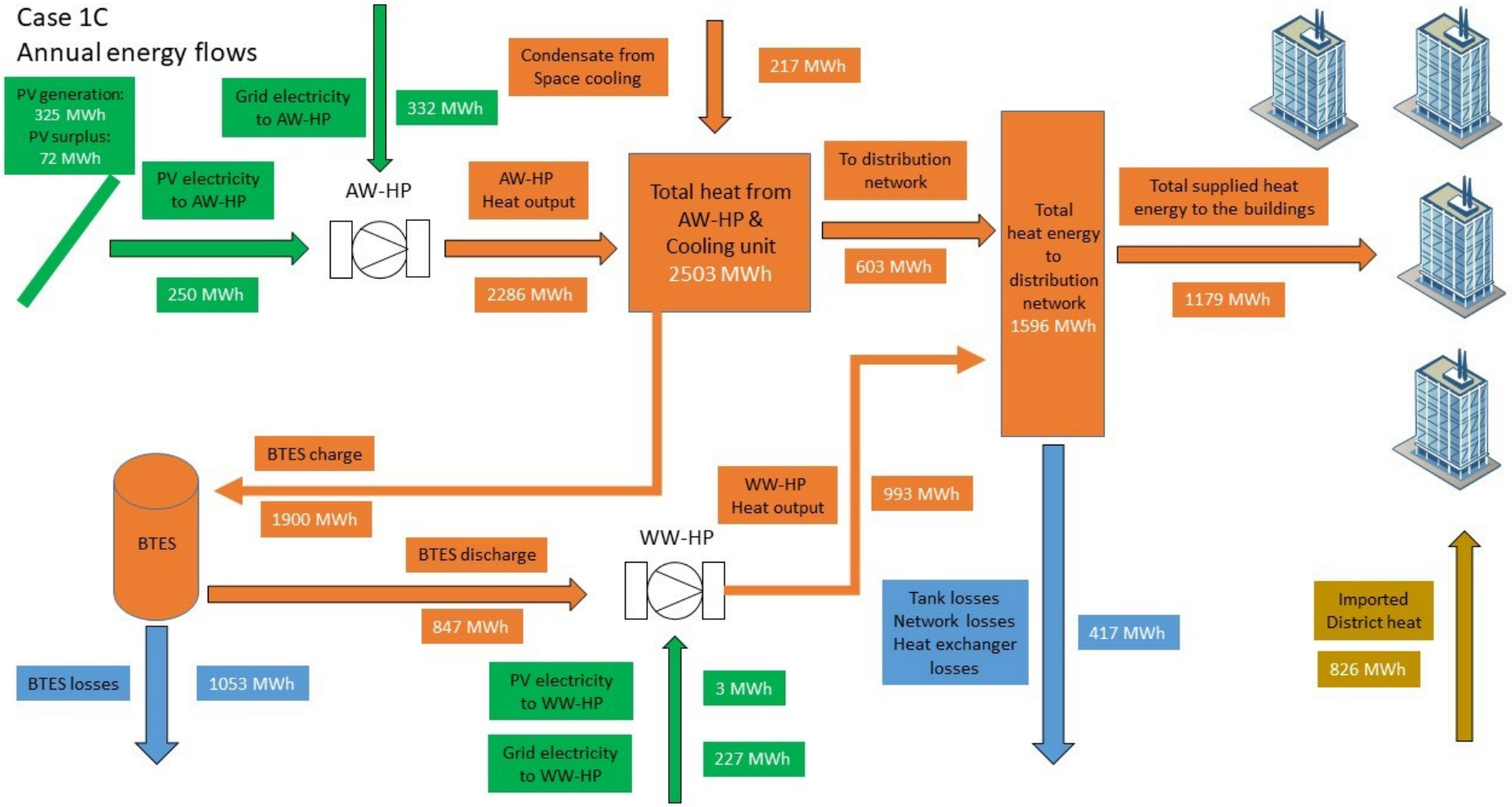
Case 1C
Annual energy flows
PV generation:
325 MWh
PV surplus:
72 MWh
Grid electricity
to AW-HP
332 MWh
Condensate from
Space cooling
217 MWh
PV electricity
to AW-HP
250 MWh
AW-HP
AW-HP
Heat output
2286 MWh
Total heat from
AW-HP &
Cooling unit
2503 MWh
To distribution
network
603 MWh
Total
heat energy
to
distribution
network
1596 MWh
Total supplied heat
energy to the buildings
1179 MWh
BTES charge
1900 MWh
BTES
BTES discharge
847 MWh
WW-HP
WW-HP
Heat output
993 MWh
Tank losses
Network losses
Heat exchanger
losses
417 MWh
BTES losses
1053 MWh
PV electricity
to WW-HP
Grid electricity
to WW-HP
3 MWh
227 MWh
Imported
District heat
826 MWh

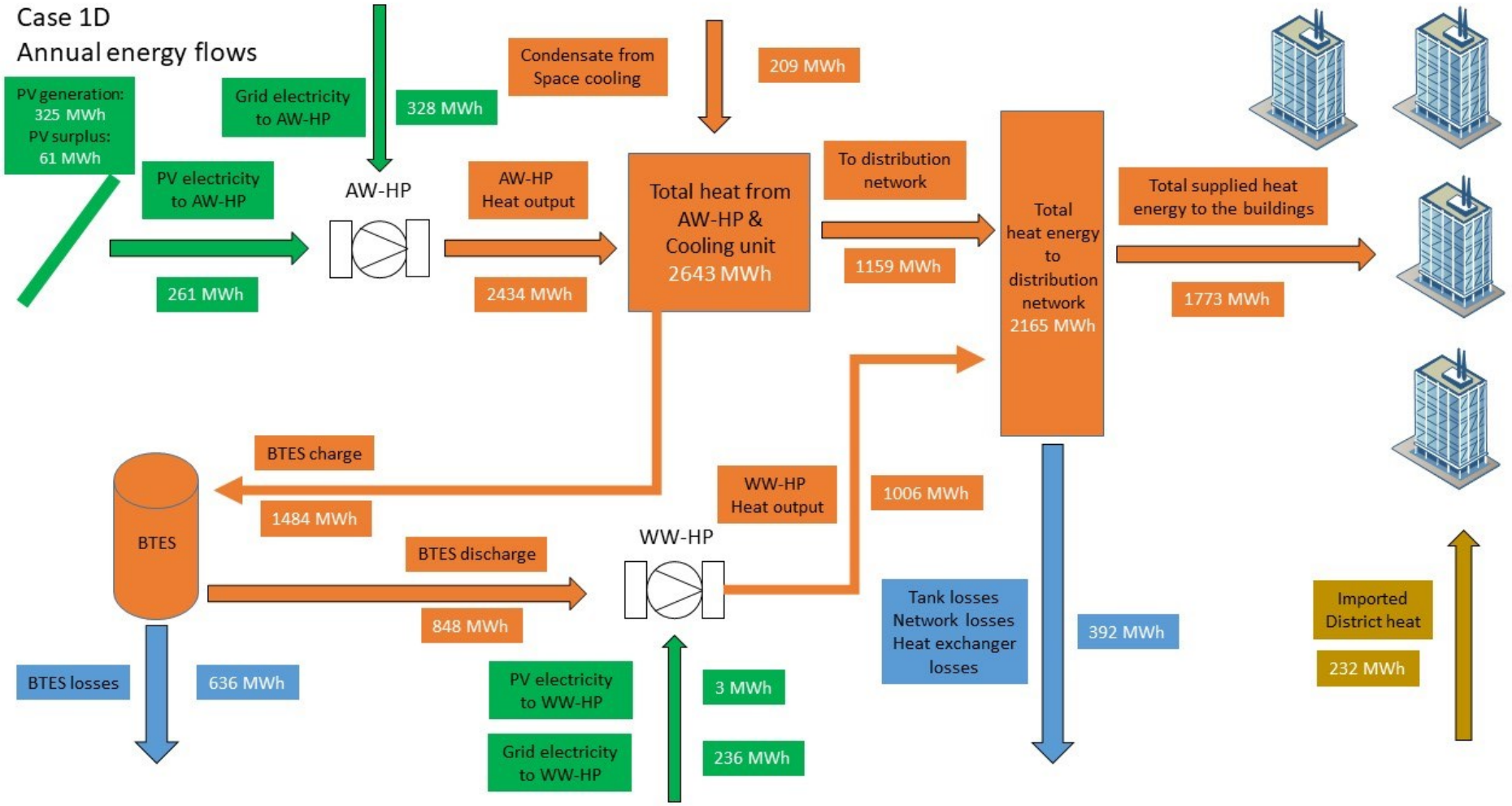
Case 1D
Annual energy flows
PV generation:
325 MWh
PV surplus:
61 MWh
Grid electricity
to AW-HP
328 MWh
Condensate from
Space cooling
209 MWh
PV electricity
to AW-HP
261 MWh
AW-HP
AW-HP
Heat output
2434 MWh
Total heat from
AW-HP &
Cooling unit
2643 MWh
To distribution
network
1159 MWh
Total
heat energy
to
distribution
network
2165 MWh
Total supplied heat
energy to the buildings
1773 MWh
BTES charge
1484 MWh
BTES
BTES discharge
848 MWh
WW-HP
WW-HP
Heat output
1006 MWh
Tank losses
Network losses
Heat exchanger
losses
392 MWh
BTES losses
636 MWh
PV electricity
to WW-HP
Grid electricity
to WW-HP
3 MWh
236 MWh
Imported
District heat
232 MWh

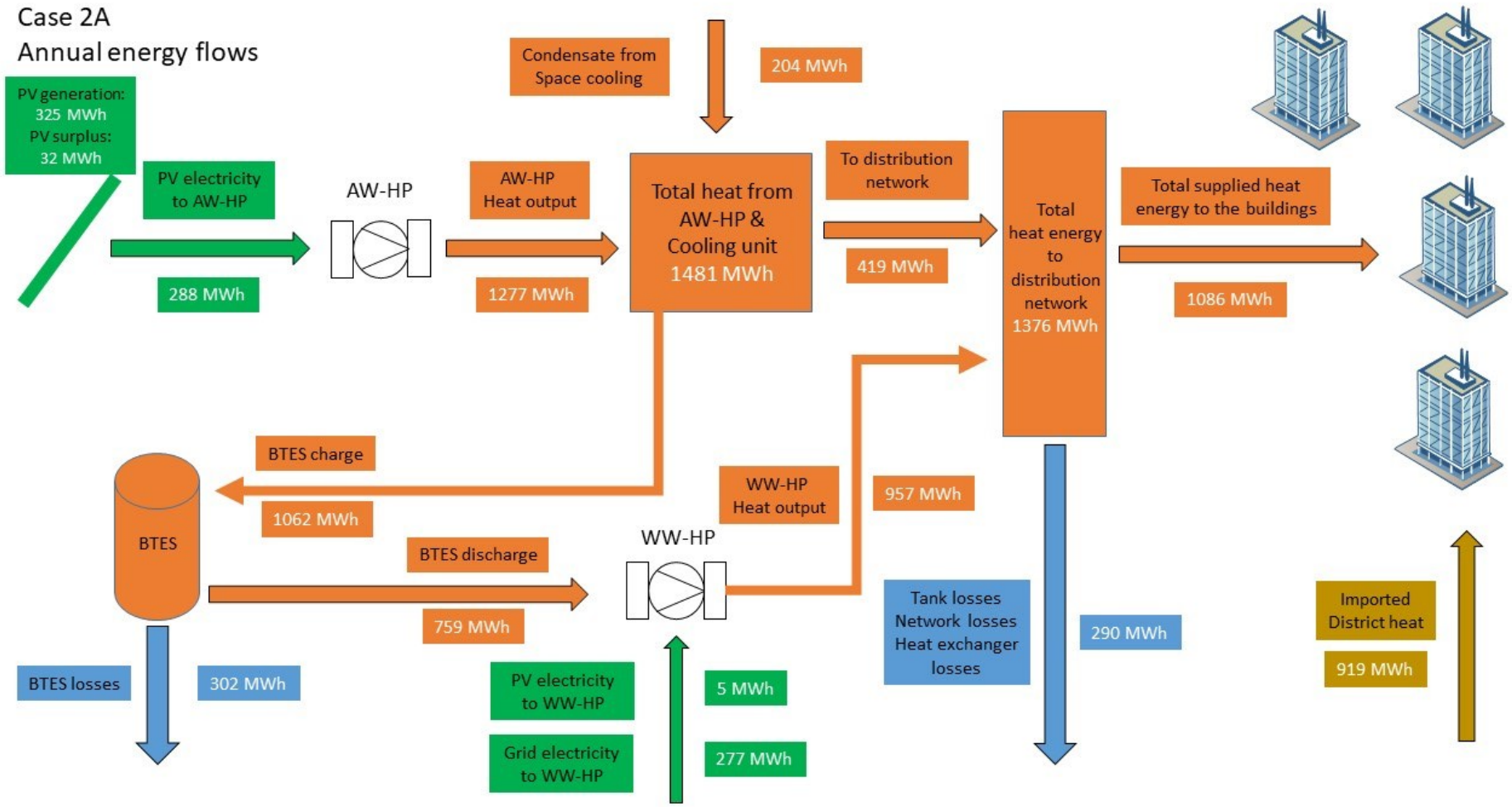
Case 2A
Annual energy flows
PV generation:
325 MWh
PV surplus:
32 MWh
PV electricity
to AW-HP
288 MWh
AW-HP
AW-HP
Heat output
1277 MWh
Condensate from
Space cooling
204 MWh
Total heat from
AW-HP &
Cooling unit
1481 MWh
To distribution
network
419 MWh
Total
heat energy
to
distribution
network
1376 MWh
Total supplied heat
energy to the buildings
1086 MWh
BTES charge
1062 MWh
BTES
BTES discharge
759 MWh
BTES losses
302 MWh
WW-HP
WW-HP
Heat output
957 MWh
PV electricity
to WW-HP
Grid electricity
to WW-HP
5 MWh
277 MWh
Tank losses
Network losses
Heat exchanger
losses
290 MWh
Imported
District heat
919 MWh

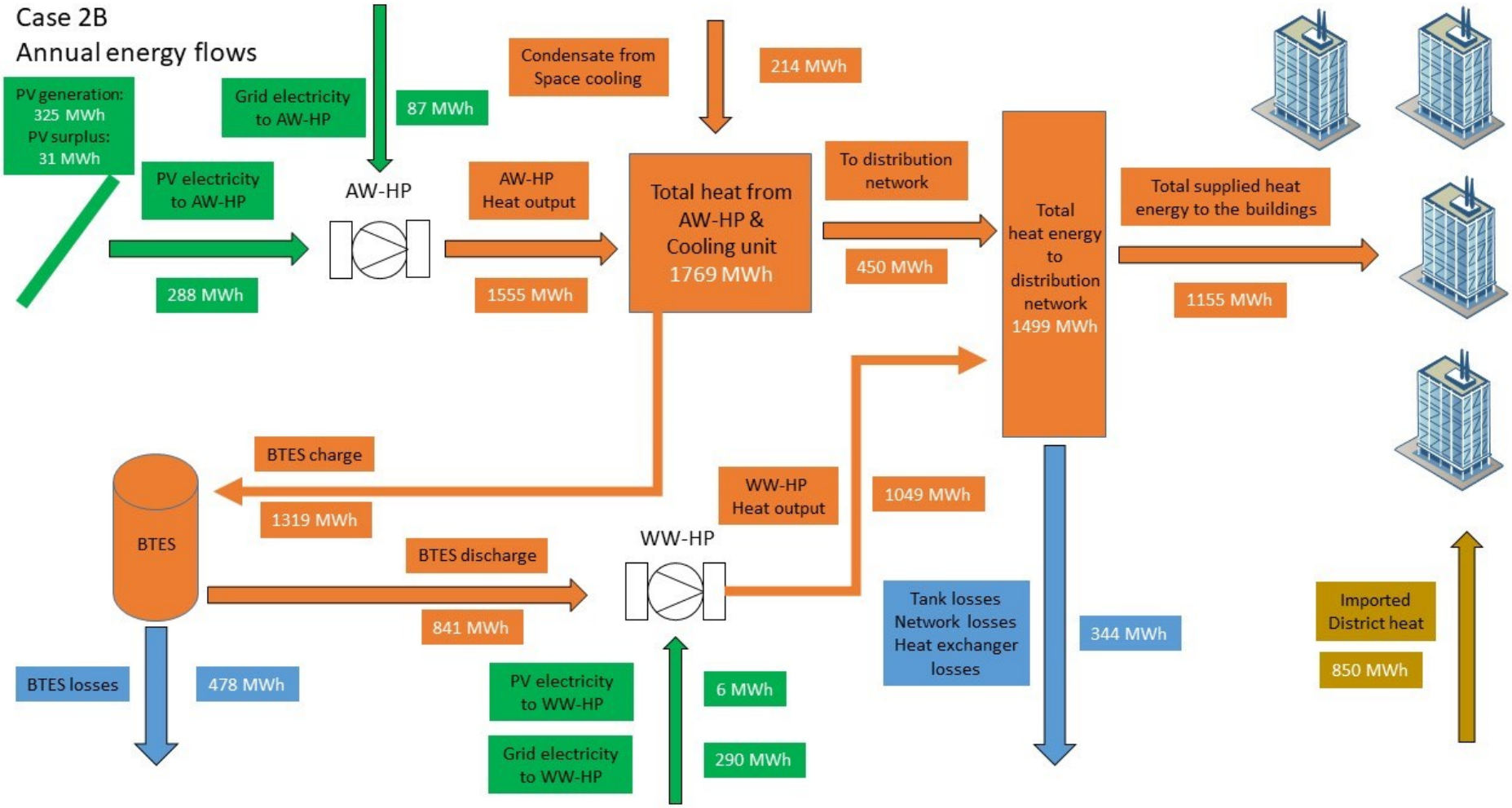
Case 2B
Annual energy flows
PV generation:
325 MWh
PV surplus:
31 MWh
Grid electricity
to AW-HP
87 MWh
Condensate from
Space cooling
214 MWh
PV electricity
to AW-HP
AW-HP
AW-HP
Heat output
Total heat from
AW-HP &
Cooling unit
1769 MWh
To distribution
network
Total
heat energy
to
distribution
network
1499 MWh
Total supplied heat
energy to the buildings
288 MWh
1555 MWh
450 MWh
1155 MWh
BTES charge
1319 MWh
BTES
BTES discharge
841 MWh
WW-HP
WW-HP
Heat output
1049 MWh
Tank losses
Network losses
Heat exchanger
losses
344 MWh
Imported
District heat
850 MWh
BTES losses
478 MWh
PV electricity
to WW-HP
Grid electricity
to WW-HP
6 MWh
290 MWh

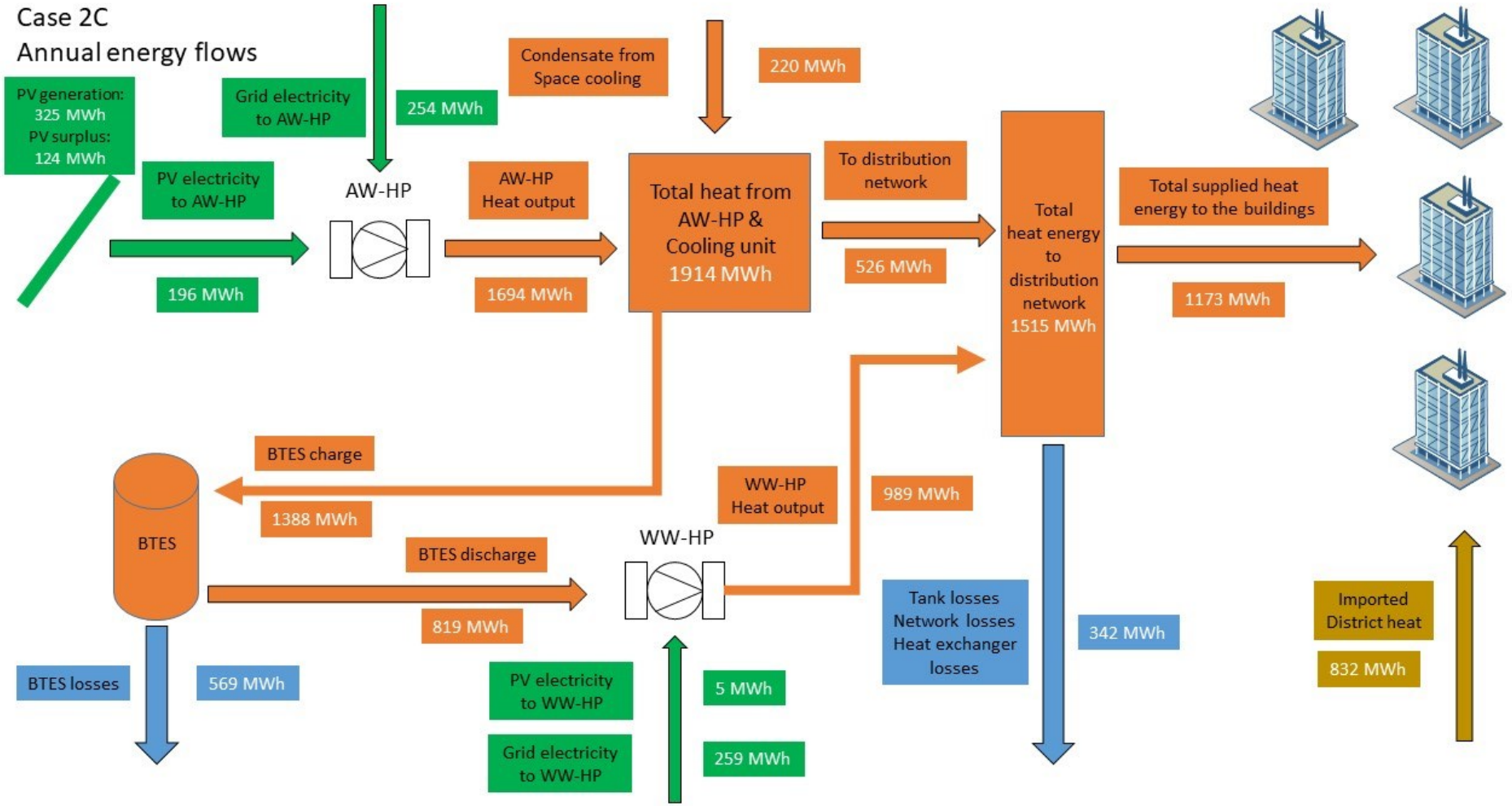
Case 2C
Annual energy flows
PV generation:
325 MWh
PV surplus:
124 MWh
Grid electricity
to AW-HP
254 MWh
Condensate from
Space cooling
220 MWh
PV electricity
to AW-HP
196 MWh
AW-HP
AW-HP
Heat output
1694 MWh
Total heat from
AW-HP &
Cooling unit
1914 MWh
To distribution
network
526 MWh
Total
heat energy
to
distribution
network
1515 MWh
Total supplied heat
energy to the buildings
1173 MWh
BTES charge
1388 MWh
BTES
BTES discharge
819 MWh
WW-HP
WW-HP
Heat output
989 MWh
Tank losses
Network losses
Heat exchanger
losses
342 MWh
BTES losses
569 MWh
PV electricity
to WW-HP
Grid electricity
to WW-HP
5 MWh
259 MWh
Imported
District heat
832 MWh

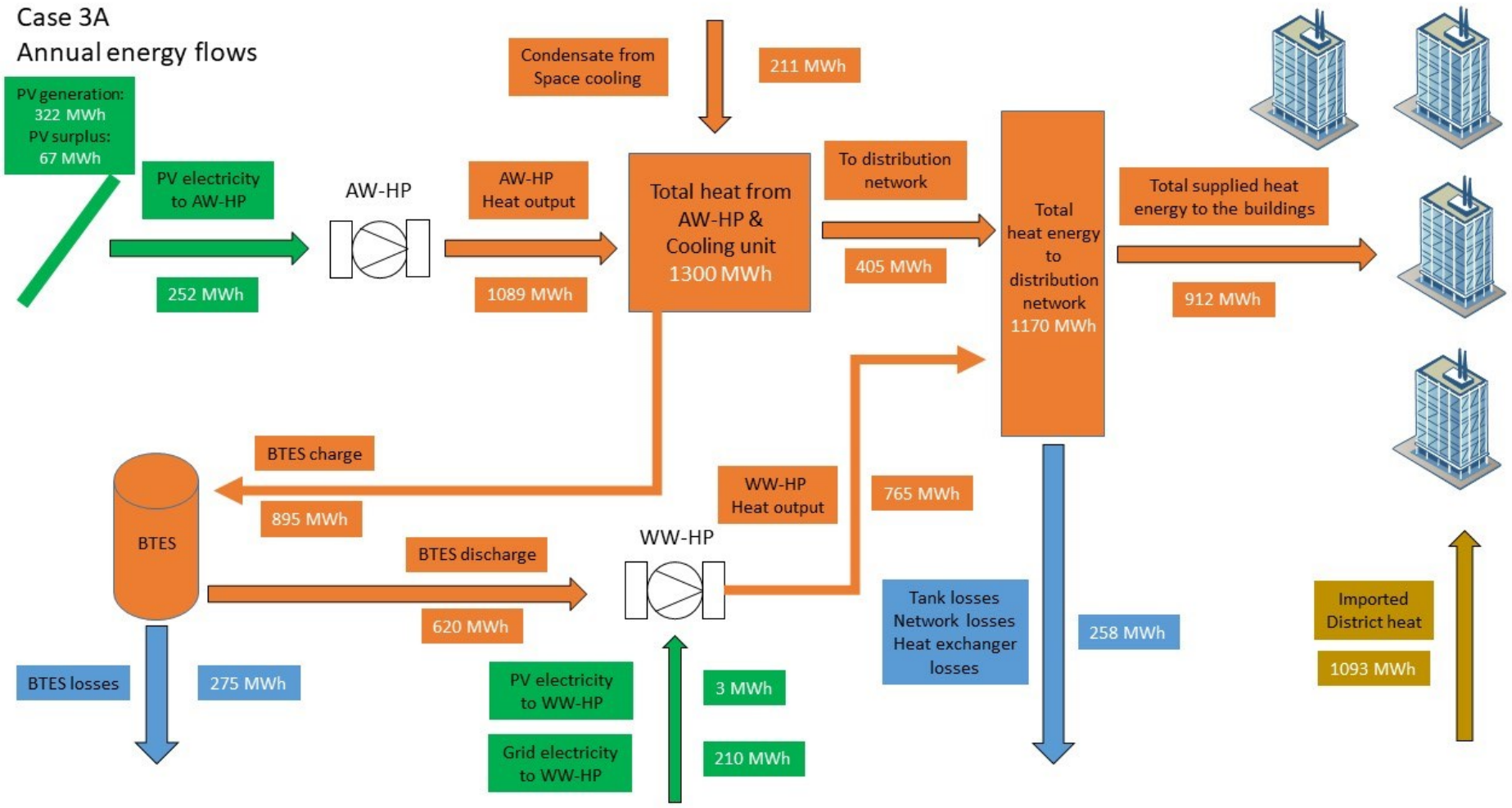
Case 3A
Annual energy flows
PV generation:
322 MWh
PV surplus:
67 MWh
PV electricity
to AW-HP
252 MWh
AW-HP
AW-HP
Heat output
1089 MWh
Condensate from
Space cooling
211 MWh
Total heat from
AW-HP &
Cooling unit
1300 MWh
To distribution
network
405 MWh
Total
heat energy
to
distribution
network
1170 MWh
Total supplied heat
energy to the buildings
912 MWh
BTES charge
895 MWh
BTES
BTES discharge
620 MWh
BTES losses
275 MWh
WW-HP
WW-HP
Heat output
765 MWh
PV electricity
to WW-HP
Grid electricity
to WW-HP
3 MWh
210 MWh
Tank losses
Network losses
Heat exchanger
losses
258 MWh
Imported
District heat
1093 MWh

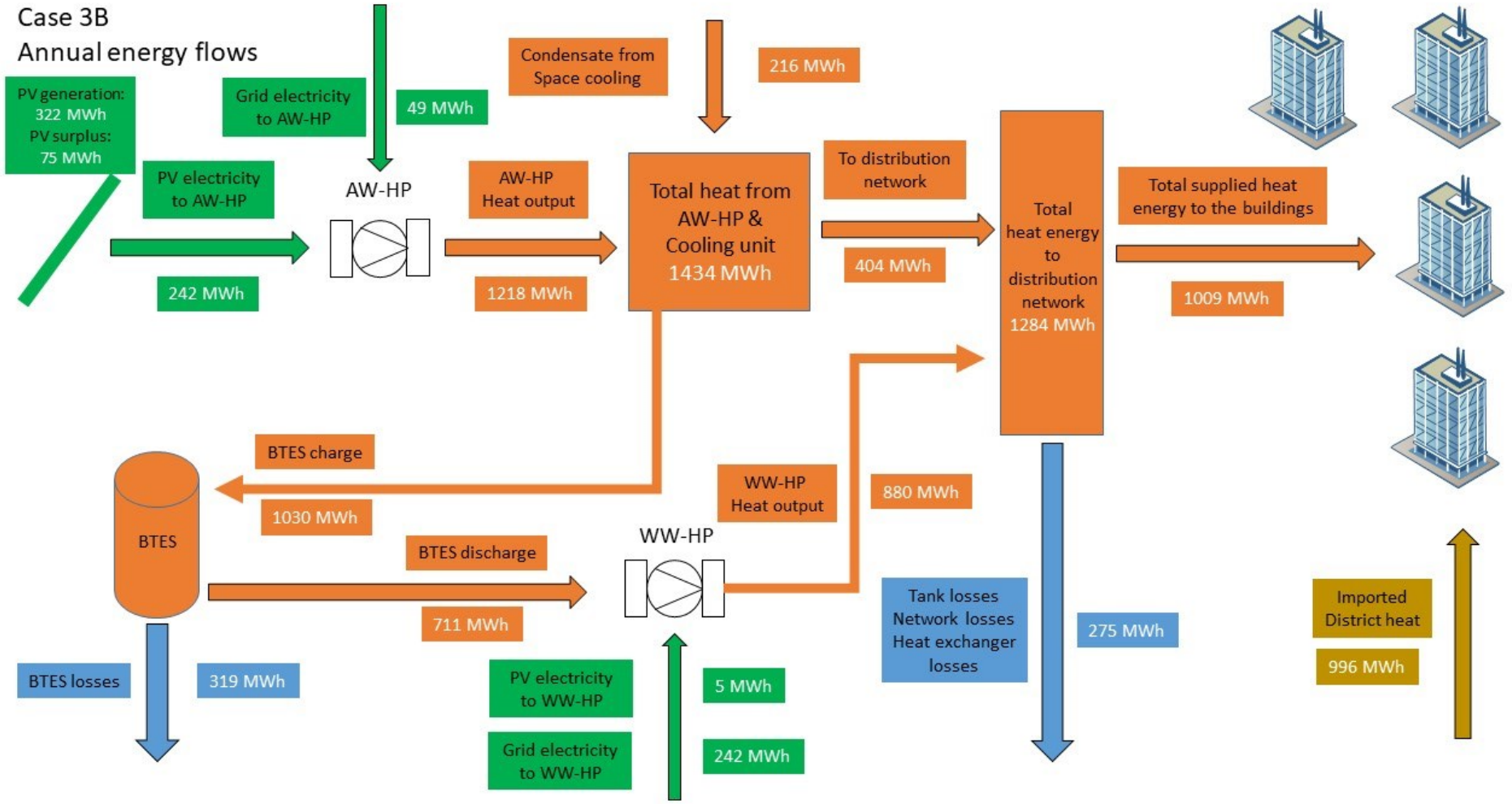
Case 3B
Annual energy flows
PV generation:
322 MWh
PV surplus:
75 MWh
Grid electricity
to AW-HP
49 MWh
Condensate from
Space cooling
216 MWh
PV electricity
to AW-HP
242 MWh
AW-HP
AW-HP
Heat output
1218 MWh
Total heat from
AW-HP &
Cooling unit
1434 MWh
To distribution
network
404 MWh
Total
heat energy
to
distribution
network
1284 MWh
Total supplied heat
energy to the buildings
1009 MWh
BTES charge
1030 MWh
BTES
BTES discharge
711 MWh
WW-HP
WW-HP
Heat output
880 MWh
BTES losses
319 MWh
PV electricity
to WW-HP
Grid electricity
to WW-HP
5 MWh
242 MWh
Tank losses
Network losses
Heat exchanger
losses
275 MWh
Imported
District heat
996 MWh

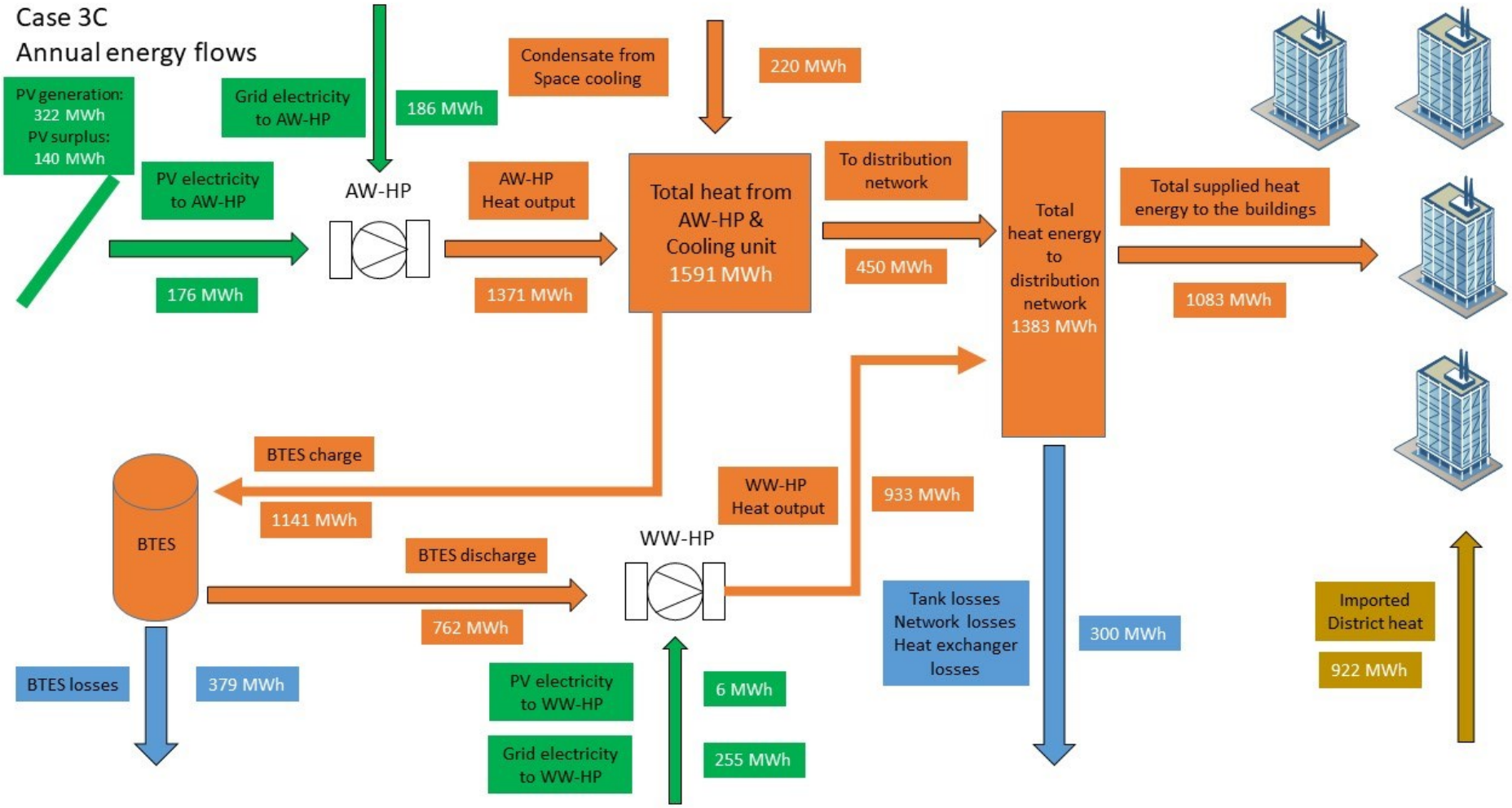
Case 3C
Annual energy flows
PV generation:
322 MWh
PV surplus:
140 MWh
Grid electricity
to AW-HP
186 MWh
Condensate from
Space cooling
220 MWh
PV electricity
to AW-HP
176 MWh
AW-HP
AW-HP
Heat output
1371 MWh
Total heat from
AW-HP &
Cooling unit
1591 MWh
To distribution
network
450 MWh
Total
heat energy
to
distribution
network
1383 MWh
Total supplied heat
energy to the buildings
1083 MWh
BTES charge
1141 MWh
BTES
BTES discharge
762 MWh
WW-HP
WW-HP
Heat output
933 MWh
Tank losses
Network losses
Heat exchanger
losses
300 MWh
BTES losses
379 MWh
PV electricity
to WW-HP
Grid electricity
to WW-HP
6 MWh
255 MWh
Imported
District heat
922 MWh

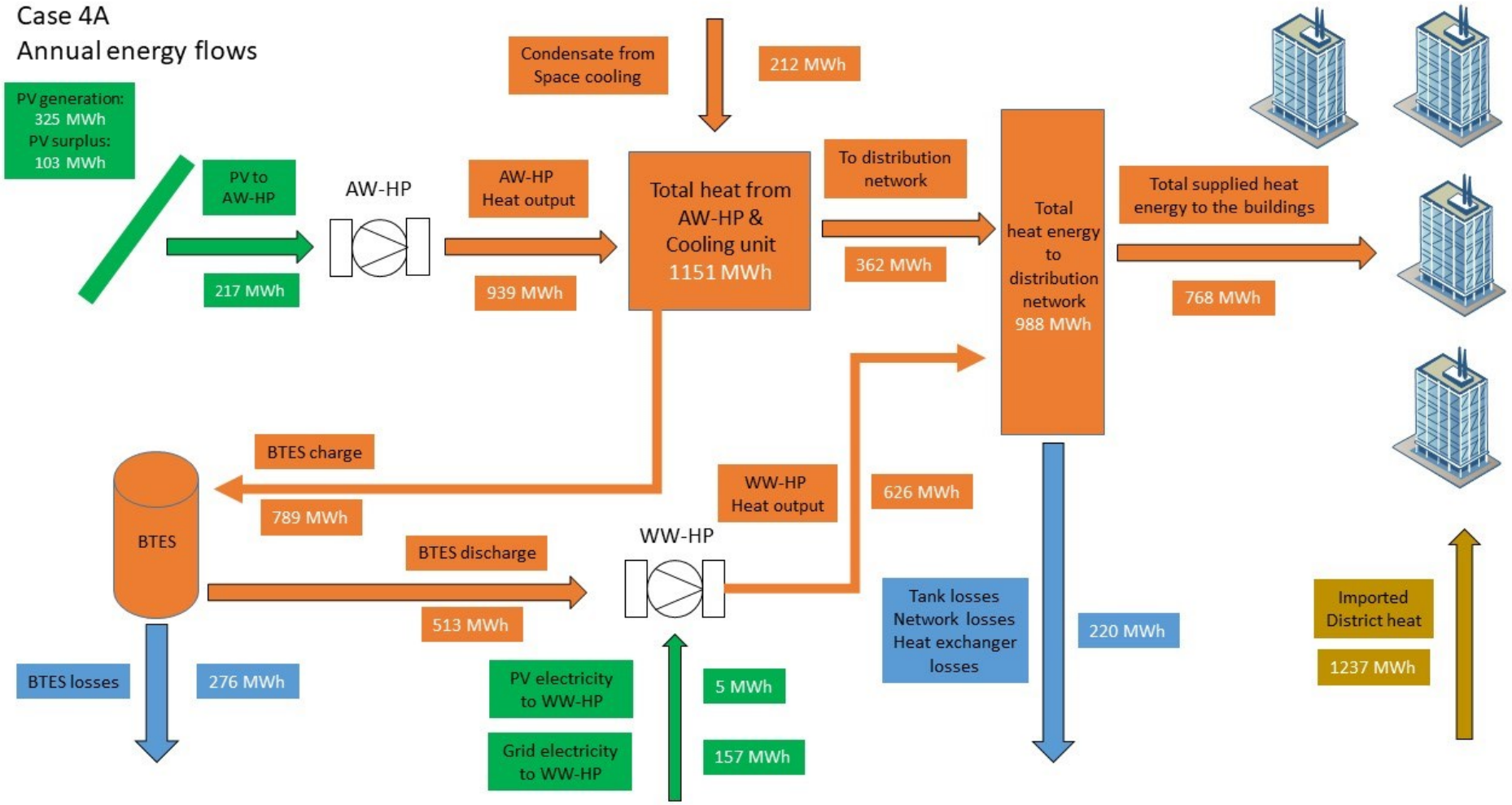
Case 4A
Annual energy flows
PV generation:
325 MWh
PV surplus:
103 MWh
PV to
AW-HP
217 MWh
AW-HP
AW-HP
Heat output
939 MWh
Condensate from
Space cooling
212 MWh
Total heat from
AW-HP &
Cooling unit
1151 MWh
To distribution
network
362 MWh
Total
heat energy
to
distribution
network
988 MWh
Total supplied heat
energy to the buildings
768 MWh
BTES charge
789 MWh
BTES
BTES losses
276 MWh
BTES discharge
513 MWh
WW-HP
WW-HP
Heat output
626 MWh
PV electricity
to WW-HP
Grid electricity
to WW-HP
5 MWh
157 MWh
Tank losses
Network losses
Heat exchanger
losses
220 MWh
Imported
District heat
1237 MWh

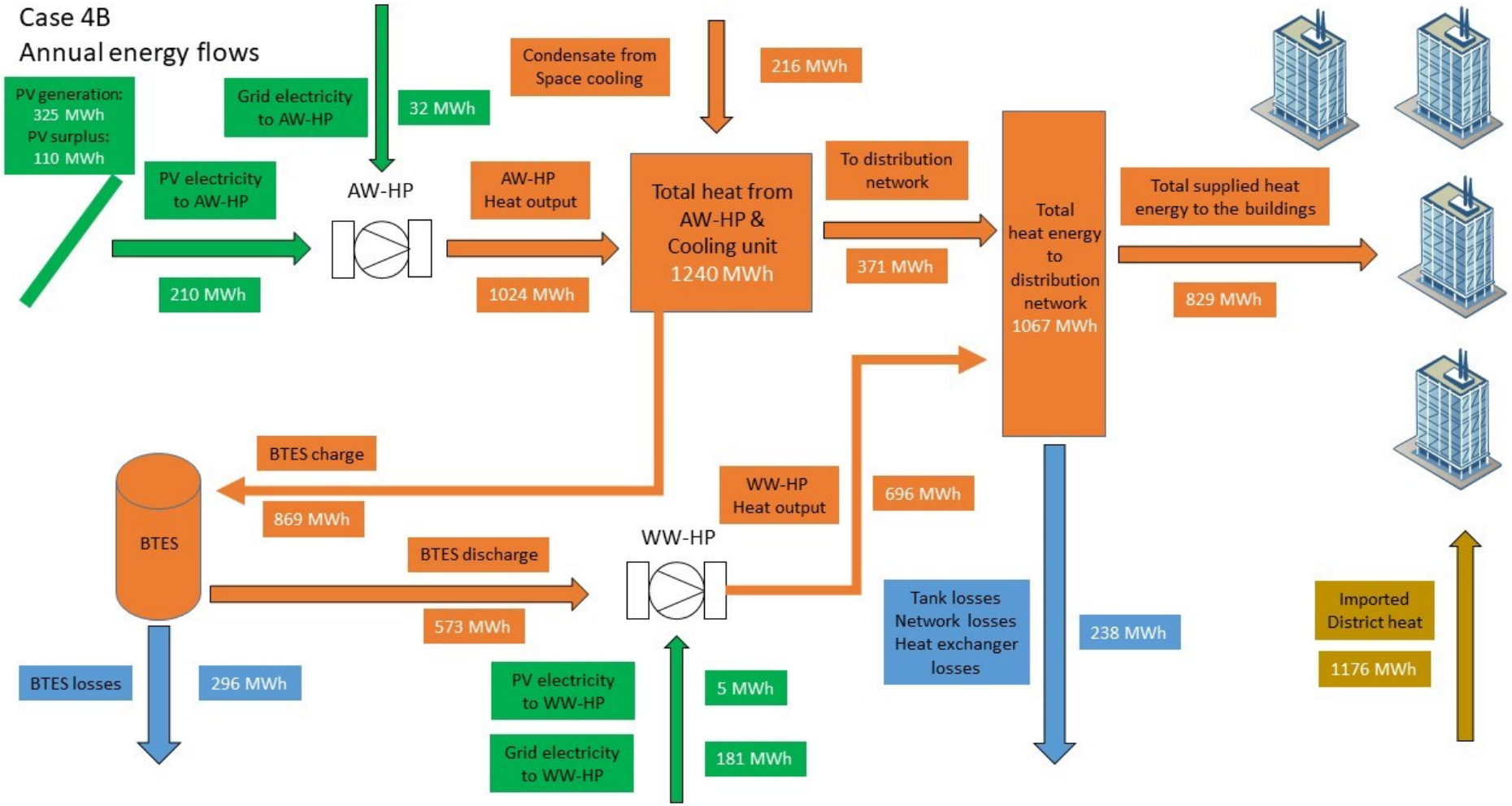
Case 4B
Annual energy flows
PV generation:
325 MWh
PV surplus:
110 MWh
Grid electricity
to AW-HP
32 MWh
Condensate from
Space cooling
216 MWh
PV electricity
to AW-HP
210 MWh
AW-HP
AW-HP
Heat output
1024 MWh
Total heat from
AW-HP &
Cooling unit
1240 MWh
To distribution
network
371 MWh
Total
heat energy
to
distribution
network
1067 MWh
Total supplied heat
energy to the buildings
829 MWh
BTES charge
869 MWh
BTES
BTES discharge
573 MWh
WW-HP
WW-HP
Heat output
696 MWh
Tank losses
Network losses
Heat exchanger
losses
238 MWh
BTES losses
296 MWh
PV electricity
to WW-HP
Grid electricity
to WW-HP
5 MWh
181 MWh
Imported
District heat
1176 MWh

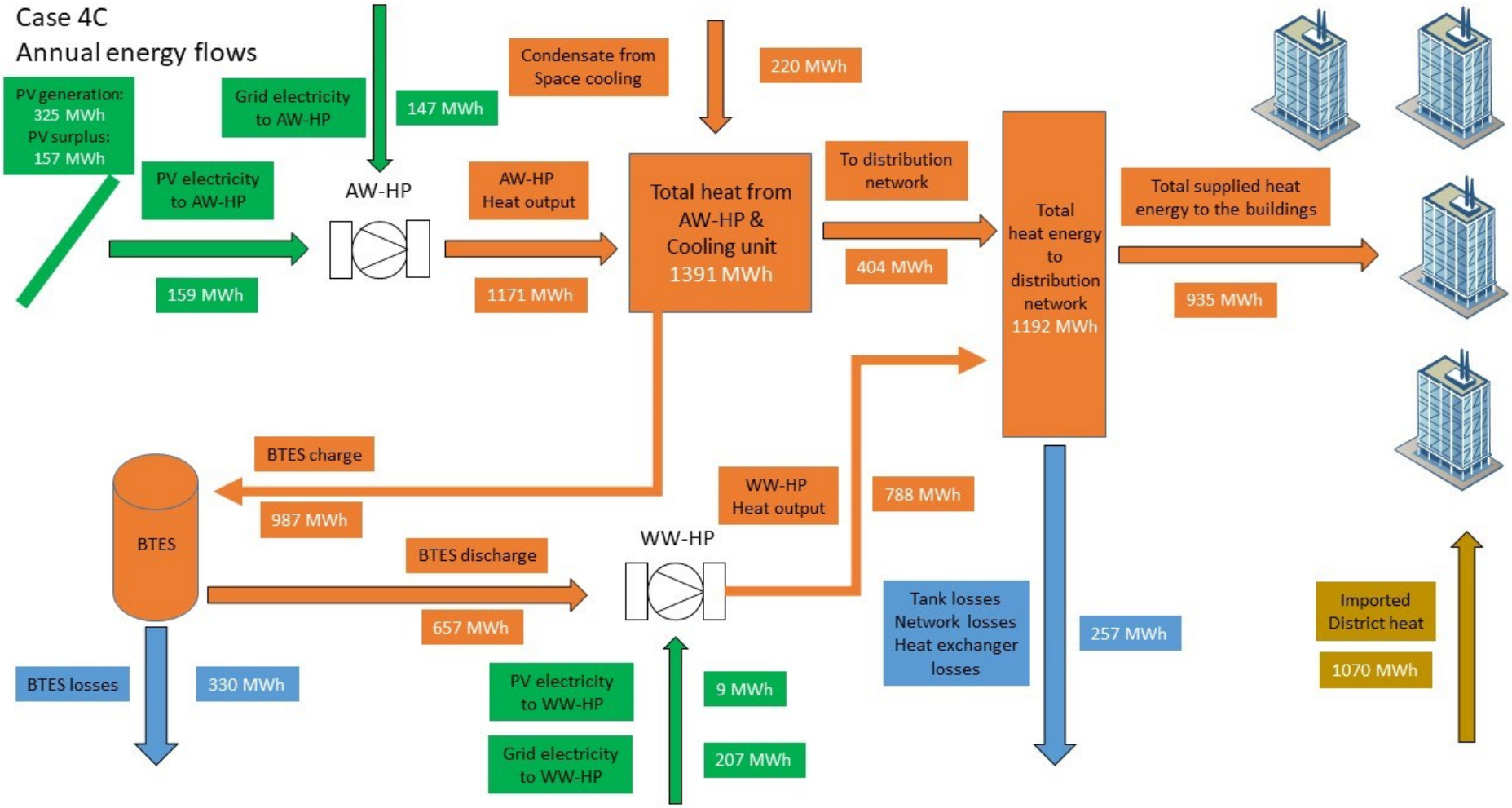
Case 4C
Annual energy flows
PV generation:
325 MWh
PV surplus:
157 MWh
Grid electricity
to AW-HP
147 MWh
Condensate from
Space cooling
220 MWh
PV electricity
to AW-HP
159 MWh
AW-HP
AW-HP
Heat output
1171 MWh
Total heat from
AW-HP &
Cooling unit
1391 MWh
To distribution
network
404 MWh
Total
heat energy
to
distribution
network
1192 MWh
Total supplied heat
energy to the buildings
935 MWh
BTES charge
987 MWh
BTES
BTES discharge
657 MWh
WW-HP
WW-HP
Heat output
788 MWh
Tank losses
Network losses
Heat exchanger
losses
257 MWh
BTES losses
330 MWh
PV electricity
to WW-HP
Grid electricity
to WW-HP
9 MWh
207 MWh
Imported
District heat
1070 MWh